Mechanisms and Kinetics of Exocytosis and Endocytosis in Plant and in Yeast Cells

TECHNISCHE UNIVERSITÄT DARMSTADT

Vom Fachbereich Biologie der Technischen Universität Darmstadt
zur Erlangung des akademischen Grades
eines Doctor rerum naturalium
genehmigte Dissertation von

Dipl. Biol. Vera Bandmann
aus Groß-Umstadt

Berichterstatter PD Dr. Ulrike Homann
Mitberichterstatter Prof. Dr. Gerhard Thiel

Tag der Einreichung: 15.09.2011
Tag der mündlichen Prüfung: 11.11.2011
Darmstadt 2011
D 17

Table of Contents

Chapter 1

1 General Introduction

1.1 The Secretory and the Endocytotic Pathway in Plants

Exocytosis reflects the final step in the secretory pathway which typically starts at the endoplasmic reticulum (ER), passes the Golgi, the trans-Golgi network (TGN) and ends with vesicle docking to and fusion with the plasma membrane. Exocytosis serves for the delivery of cargo from the insight of the cell to the extracellular space and also for the delivery of proteins or lipids to the plasma membrane. Proteins which are appointed for the vacuole are recognized in the TGN and transported via the prevacuolar compartment (PVC) to the vacuole. In Figure 1 the secretory pathway is indicated by red arrows.

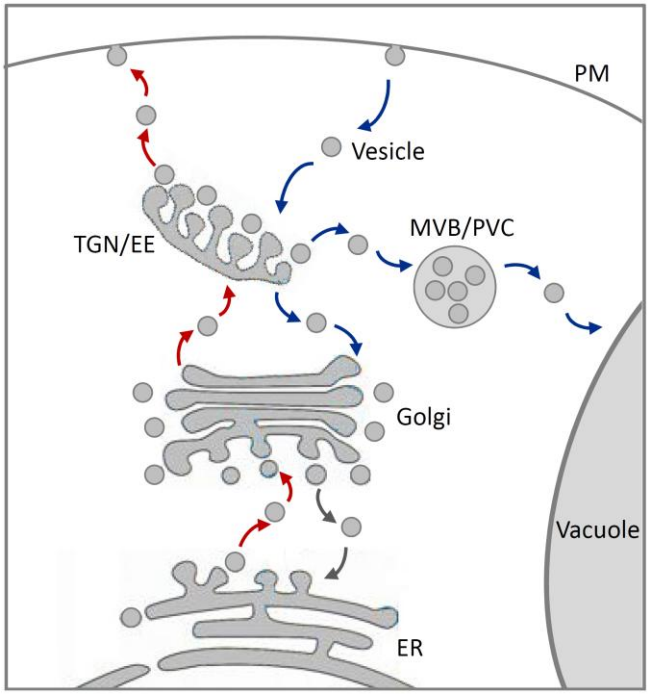

Figure 1: The secretory and the endocytic pathway in plants. ER: endoplasmic reticulum, TGN: trans-Golgi network, EE: early endosome, MVB: multivesicular body, PVC: prevacuolar compartment and PM: plasma membrane. The way of an exocytic vesicle is marked with red arrows. The endocytic pathway is indicated by blue arrows.

Endocytosis describes the fission of vesicles from the plasma membrane and the further transport along the endocytic pathway to the early endosome (EE). In plants it could be shown that the TGN serves as an EE and plays the role of a central sorting station in vesicle trafficking (Lam et al., 2007). From the TGN vesicles can be directed to the vacuole via PVC or to the Golgi apparatus. In tobacco BY-2 cells multivesicular bodies were identified as prevacuolar compartments (Tse et al., 2004). At the same time MVB/PVC serves as a late endosome (LE). In Figure 1 the endosomal compartments are illustrated and the way of an endocytic vesicle is marked with blue arrows.
The important organelles of vesicle trafficking are shown in a TEM picture (Figure 2) of a tobacco BY-2 cell.

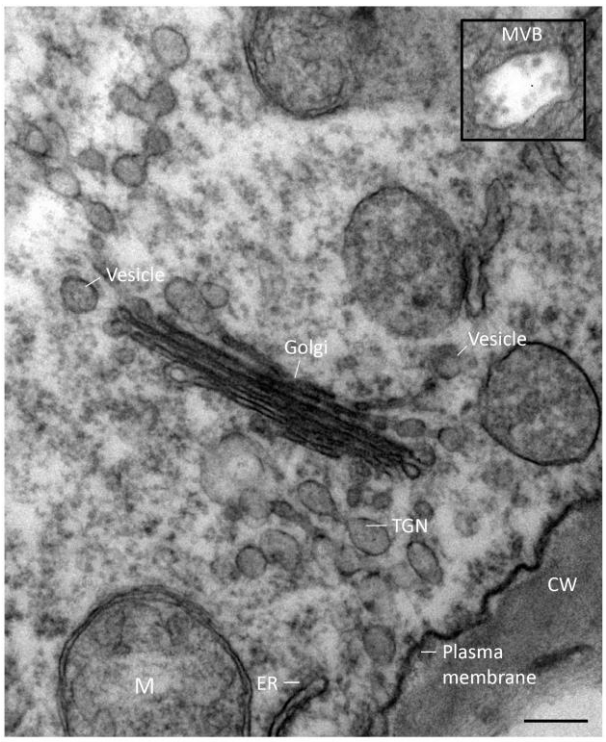

Figure 2: TEM picture of a tobacco BY-2 cell. Endoplasmic reticulum (ER), trans-Golgi-network (TGN) Golgi, plasma membrane, mitochondria (M), cell wall (CW) and cytosolic vesicles are indicated. The inlay shows a multivesicular body (MVB). Scale bar 200 nm.

The very last part of the secretory pathway involves the fusion of an exocytic vesicle with the plasma membrane which includes the release of the vesicular cargo and the incorporation of membrane proteins and lipids into the membrane. In plant cells different stimuli of exocytosis have been discovered. It has been shown that the raising of cytosolic Ca^{2+} concentration induces exocytosis which can be described by two distinct kinetic phases (Sutter et al., 2000).

A fast initial increase of vesicle fusion is followed by a slower but continuous rise. This pattern most likely reflects the existence of two different vesicle pools: a ready-to-fuse vesicle pool with a strong Ca^{2+} dependency and a reserve vesicle pool from which the ready-to-fuse vesicle pool can be refilled. This second process also seems to be regulated by Ca^{2+} but with a weaker dependency (Sutter et al., 2000). Another stimulus which induces exocytosis in plant cells is represented by the application of hypoosmotic stress (Homan 1998, Homann and Thiel 1999). This increase in vesicle fusion caused by presssure is Ca^{2+} independent and the rise in surface area progressed linearly over time. This may reflect a very fast replenishment of the ready-to-fuse vesicle pool or point to a different mechanism.

Which plant endomembrane compartment produces exocytotic vesicles is not completely understood but is seems likely that the targeting of vesicles occur according to their cargo. In cell-wall forming plant cells, cell wall precursor like polysaccharides and pectins are transported into the lumen of exocytotic Golgi vesicles which contain cellulose synthase in their membrane. After the fusion of the vesicles the cellulose synthase is incorporated into the plasma membrane and the cell wall matrix precursors are deposited into the existing cell wall (Lindeboom et al., 2008). The exocytosis in growing cells therefore represents a process which accounts for both secretion and assembly of proteins in the plasma membrane. These two processes probably also function separately. The secretion of enzymes (Denecke et al., 1990) and the cycling of the auxin efflux carrier PIN1 between the plasma membrane and the EE (Geldner et al., 2003) are two examples.

1.1.1 Mechanisms of Vesicle Targeting and Fusion

The fusion process can be divided in several steps: Docking of the vesicle to the plasma membrane, initial fusion to the membrane which involves the coalescence of vesicle and plasma membrane and the formation of the fusion pore, release of vesicular cargo and fusion with the plasma membrane. Fusion can either be permanent or transient. The later mechanism corresponds to the so-called kiss-and-run vesicle fusion or transient vesicle fusion. In this case the vesicular matrix can be re-used for another round of exocytosis and material from the inside of the cell can be secreted without subsequent surface area increase.

The initial step of vesicle fusion to the plasma membrane is mediated by a GTPase (Rab GTPase) on the vesicle membrane. The Rab GTPase interacts with a tethering protein

complex on the target membrane which forms a first connection between the vesicle and the plasma membrane (Sztul and Lupashin 2006).

Another set of membrane bound proteins which are crucial for vesicle fusion are SNARE proteins. The interaction of SNARE proteins from the vesicle membrane (v-SNARE) with plasma membrane-bound SNARE proteins (target-SNARE = t-SNARE) are essential for membrane fusion. Some tethering proteins can bind directly to SNARE proteins and may function in the spatio-temporal regulation of SNARE complex assembly before membrane fusion (Cai et al., 2007, Kummel and Heinemann 2008). The targeting of vesicles probably function on the basis of specific interactions between v-SNAREs and t-SNAREs. Several SNARE proteins could be identified in plants cells. Each compartment which is involved in vesicle trafficking contains a different set of SNARE proteins which account for the precise vesicle targeting (Jürgens 2004).

The model of the interaction between t-SNARES and v-SNARES is illustrated in Figure 3. In neurons it could be shown that the v-SNARE Synaptotagmin contains binding sites for Ca^{2+} and that the t-SNARE SNAP-25 binds to Synaptotagmin in a Ca^{2+} dependent manner (Zang et al., 2002). If this mechanism also works in plants and accounts for the Ca^{2+} triggered increase in vesicle fusion seems likely but remains unresolved.

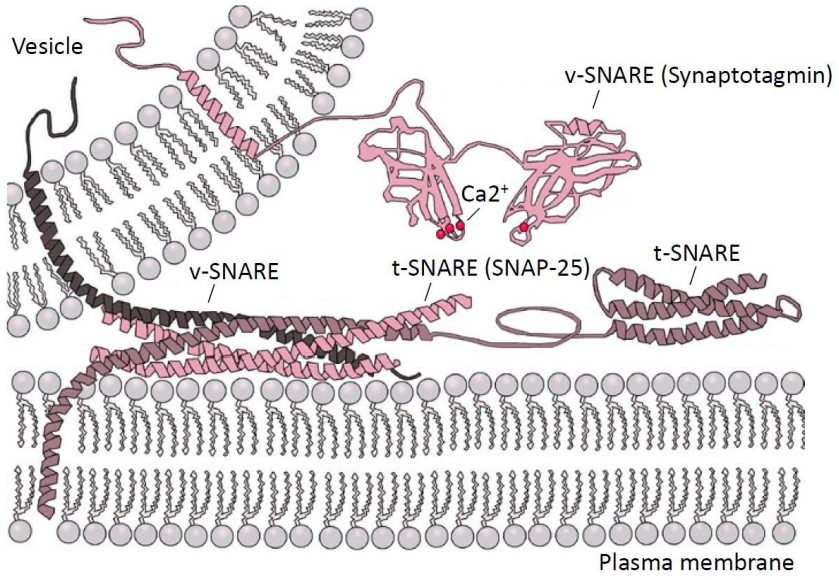

Figure 3: Interaction between v-SNARES and t-SNARES. Potential binding sides of Ca^{2+} are indicated by red dots (modified after Danko Dimchev Georgiev, M.D. 2006, available: http://en.wikipedia.org/wiki/Image:Exocytosis-machinery).

1.1.2 Endocytosis

Endocytosis describes the process of internalization of plasma membrane proteins, lipids, extracellular molecules and fluids. Endocytosis is crucial for many cellular processes such as protein transport, the recycling of membranes, and cell signalling like receptor mediated functions.

Endocytosis starts with the invagination of plasma membrane in order to surround the cargo molecules into an endocytic vesicle. After fission from the plasma membrane the vesicle sheds its coat which enables the naked vesicle to fuse with the first endosomal compartment the EE/TGN to release its content into the endocytic pathway (Gruenberg, 2001). Although there is a some evidence for receptor induced endocytosis in plant cells (Leborgne-Castel et al., 2008, Robatzek et al., 2006) no additional mechanisms which regulates endocytosis are known. This may be due to the high variability of endosomal pathways.

In plant cells the existence of endocytosis has long been a matter of debate. Even though it is now without question that endocytosis does play an important role also in plant cells, the knowledge about the stimuli and molecular mechanisms of endocytosis is still very limited.

In yeast and animal cells several mechanisms of endocytosis have been described and categorized according to their coat: clathrin–mediated, caveolae/lipid raft-mediated, clathrin-, and caveolae-independent, fluid-phase endocytosis and phagocytosis (reviewed in Doherty and McMahon, 2009).

So far in plants only clathrin-mediated endocytosis has been investigated in detail and has been shown to be involved in physiological processes such as receptor mediated endocytosis or turnover of plasma membrane transporters (Leborgne-Castel et al., 2008, Geldner et al., 2003). There are also some hints for clathrin-independent endocytosis in plants (Samay et al., 2004, Onelli et al., 2008) but information about proteins involved or the role of this process in plant physiology are missing.

1.1.3 Mechanism of Fission of Endocytic Vesicles

The first step in clathrin-mediated endocytosis is the recruitment of the adapter protein complex to the plasma membrane. Phosphoinositides play an important role in coat protein assembly by binding adapter proteins and thus creating a region just beneath the plasma membrane which is locally enriched in adaptor proteins (Holstein, 2005). Adapter proteins itself bind to both, vesicular cargo and clathrin coat proteins and play therefore a central role in the recruitment of cargo to the vesicle. The interaction of three clathrin heavy chains and three light chains forms a triskelion which induces membrane curvature and thus vesicle formation (Kirchhausen, 2000). The fission of vesicle needs additional factors like dynamin and amphiphysin. After budding the vesicle is uncoated by chaperones like auxilin and Hsc70 and is then able to fuse with endosomal compartments like the EE. In Figure 4 the process of vesicle formation and fission is illustrated.

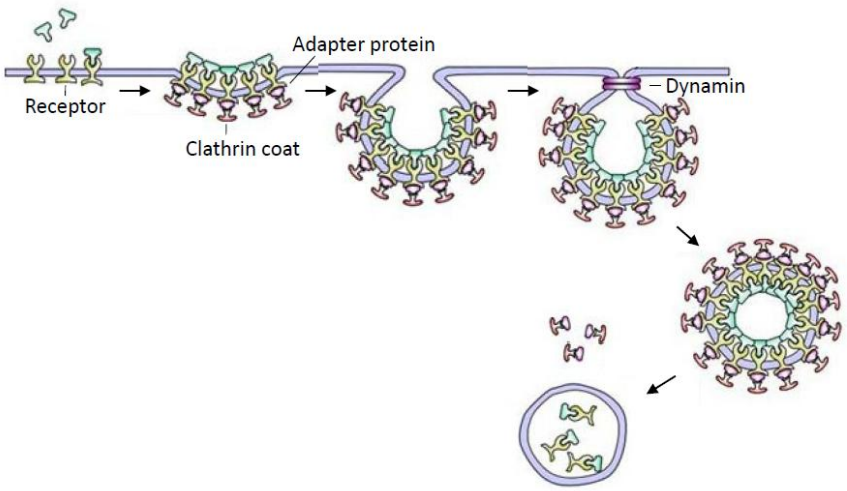

Figure 4: Endocytosis of a clathrin coated vesicle. Adapter proteins bind to the receptor and the clathrin coat. Vesicle formation by membrane curvature is induced by the assembly of additional clathrin lattice. Dynamin mediates the fission of the vesicle which fuses after coat disassembling to endosomal compartments (picture modified after Danton H. O'Day, 2006, Exocytosis and Endocytosis, http://www.utm.utoronto.ca).

In plant cells several proteins of the clathrin coat machinery like the clathrin light and heavy chain and four different adapter complexes have been identified (Holstein, 2005). Also the essential role of phosphoinositides in endocytosis has been demonstrated (König et al., 2008).

In addition, there are numerous plant homologs of dynamin and auxilinis but their molecular function in plant endocytois has still not been proven.

The increasing interest for endocytosis in plants leads to more and more knowledge about the underlying mechanisms, but still many open questions remain. Considering the many different pathways which have emerged in yeast and animal cells over the past ten years it seems very likely that additional mechanisms for endocytosis also exist in plants and are waiting to be discovered.

1.2 Application of Capacitance Measurement to study Vesicle Fusion and Fission in Plants

Measurement of membrane capacitance allows the detection of changes in the surface area and thus detection of exo- and endocytosis because biological membranes behave like electrical capacitors. The first cell capacitance measurement was reported by Neher and Marty (Neher and Marty, 1982). In bovine adrenal chromaffin cells they were able to detect significant changes in cell membrane capacitance caused by either exocytic or endocytic vesicles. These studies were mainly carried out in the so-called whole-cell configuration where the capacitance of the whole surface area is measured. In the cell-attached configuration only the membrane under the patch-clamp pipette is measured. This allows a much higher resolution but events can only be detected in a locally defined area. Six years later Lindau and Neher greatly improved the resolution of membrane capacitance measurement by the application of a sinusoidal voltage signal as excitation and the use of a lock-in amplifier to analyze the resulting current (Lindau and Neher, 1988).

After this first detection of endo- and exocytosis on the level of single vesicles, capacitance measurements were extensively used on neurotransmitter and hormone secreting cells. This contributed to a detailed understanding of the underlying processes of the kinetic of vesicle fusion and fission. The formation of fusion pores, the secretion of neurotransmitters as responses to distinct stimuli as well as the role of phosphorylation and different inhibitors have been studied using capacitance measurements (Jorgačevski et al., 2008, He et al., 2006, Ales etr al., 1999, Henke. et al., 2001).

Capacitance measurements were also successfully applied to plant cells. This contributed to important findings of the kinetic of vesicle fusion and fission, the role of Ca^{2+} on secretion in

plants and the upregulation of exocytosis as a response to hypoosmotic stress (Tester and Zorec, 1992; Homann and Tester, 1998; Homann and Thiel, 1999; Weise et al., 2000). Over the past years exo- and endocytosis in plants have also been studied extensively by different microscopy approaches.

However, the knowledge of the molecular mechanism which underlies plant exo- and endocytosis is still far behind of what is known from the animal field.

The high resolution capacitance measurement in the cell-attached configuration may help to close this gap. The big advantage of monitoring exo- and and endocytosis with capacitance measurement is the high temporal and spatial resolution. It is possible to resolve the fusion and fission of single vesicles in real time in living cells. With optimal settings the resolution is good enougsh to detect vesicles of about 60 nm in diameter. In combination with confocal microscopy the capacitance measurement provides a very promising method to obtain new insights in exo-and endocytosis in plants. However, compared to the animal field, there are only a few studies which apply capacitance measurements to investigate secretion and endocytosis in plants. A reason for the rare use of capacitance measurements in plants is the lack of a suitable model system.

1.3 Aim of the Work

One aim of this work was the establishment of tobacco BY-2 cells as a model system for cell-attached capacitance measurements. BY-2 cells are widely used as a model system for higher plants. Studies on plant cell biology, including cell division, action of phytohormones, and protein trafficking were carried out in the tobacco suspension culture cells. BY-2 cells provide a good expression system and can easily be cultivated. Also the isolation of protoplasts from intact BY-2 cells is straightforward and provides a high number of morphologically similar protoplasts.

In order to use BY-2 cells as a model system it was necessary to characterize fusion and fission on BY-2 protoplasts under non-stimulated conditions. Therefore, the first part of this work deals with the comprehensive analysis of endo- and exocytotic events detected in cell-attached membrane capacitance measurements. On the basis of these analyses further aspects of the regulation of vesicle fusion and fission were addressed and compared to control conditions.

Besides the impact of different stimuli and inhibitors one focus was on the description of clathrin-independent endocytosis. Up to now there has been no direct evidence for clathrin-independent endocytosis and its physiology relevance in plants. This gap was closed by the investigation of hexose uptake into BY-2 cells using microscopic approaches and cell-attached capacitance measurements.

The last part of this work deals with the application of cell-attached capacitance measurements on yeast. Yeast cells are a well established model system for the investigation of endo-and exocytosis but so far capacitance measurements have not been used to study vesicle fusion and fission in yeast. In this work the suitability of yeast protoplasts for cell-attached measurements was tested. In addition, endocytosis of the mating receptor was analysed by confocal microscopy and the possibility to investigate this receptor-induced endocytosis by capacitance measurements was evaluated.

1.4 References

Ales E., Lindau M., Tabares L., Poyato J. M., Valero V., Alvarez de T.G. (1999) High calcium concentrations shift the mode of exocytosis to the kiss-and-run mechanism. Nat Cell Biol, 1: 40-44.

Ambrose J.C. and Cyr R. (2008) Mitotic spindle organization by the preprophase band. Mol. Plant. 1: 950-960

Battey N.H. and Blackbourn H.D. (1993) The control of exocytosis in plant cells. New Phytologist 125: 307-338.

Cai H., Reinisch K., Ferro-Novick S. (2007) Coats, tethers, Rabs, and SNAREs work together to mediate the intracellular destination of a transport vesicle. Developmental cell 12: 671-682.

Denecke J., Botterman J., Deblaere R. (1990) Protein secretion in plant cells can occur via a default pathway. Plant cell 2: 51-59.

Doherty G.J. and McMahon H.T. (2009) Mechanisms of endocytosis. Annu Rev Biochem. 78: 857-902.

Geldner N., Anders N., Wolters H., Keicher J., Kornberger W., Muller P., Delbarre A., Ueda T., Nakano A., Jürgens G. (2003) The Arabidopsis GNOM ARF-GEF Mediates Endosomal Recycling, Auxin Transport, and Auxin-Dependent Plant Growth. Cell 112: 219-230.

Gersdorff H. von and Matthews G. (1999) Electrophysiology of synaptic vesicle cycling. Annu Rev Physiol. 61: 725-752.

Gruenberg J. (2001) The endocytic pathway: a mosaic of domains. Nat Rev Mol Cell Biol. 2: 721-730.

He L., Wu X.-S., Mohan R., Wu L.-G. (2006) Two modes of fusion pore opening revealed by cell-attached recordings at a synapse. Nature, 444: 102-105.

Henkel A. W., Kang G., Kornhuber J. (2001) A common molecular machinery for exocytosis and the kiss-and-run' mechanism in chromaffin cells is controlled by phosphorylation. J Cell Sci, 114: 4613-4620

Holstein S.E.H. (2002) Clathrin and Plant Endocytosis. Traffic 3: 614-620.

Holstein S.E.H. (2005) Molecular Dissection of the Clathrin-Endocytosis Machinery in Plants. Plant Cell Monographs 1: 83-101.

Homann U. (1998) Fusion and fission of plasma-membrane material accommodates for osmotically induced changes in the surface area of guard-cell protoplasts. Planta 206: 329-333.

Homann U. and Tester M. (1998) Patch-clamp measurements of capacitance to study exocytosis and endocytosis. Trends in Plant Science 3: 110-114.

Homann U. and Thiel G. (1999) Unitary exocytotic and endocytotic events in guard-cell protoplasts during osmotically driven volume changes. FEBS Letters 460: 495-499.

Horn M.A., Heinstein P.F., Low P.S. (1989) Receptor-Mediated Endocytosis in Plant Cells. Plant Cell 1: 1003-1009.

Jorgačevski J., Stenovec M., Kreft M., Bajić A., Rituper B., Vardjan N., Stojilkovic S., Zorec R. (2008) Hypotonicity and peptide discharge from a single vesicle. Am. J. Physiol. Cell Physiol. 295: C624–C631.

Jürgens G. (2004) Membrane trafficking in plants. Annu Rev Cell Dev Biol. 20:481-504.

Kirchhausen T. (2000) Clathrin. Annu Rev Biochem 69: 699-727.

König S., Ischebeck T., Lerche J., Stenzel I., Heilmann I. (2008) Salt-stress-induced association of phosphatidylinositol 4,5-bisphosphate with clathrin-coated vesicles in plants. Biochem J. 415: 387-399.

Kummel D. and Heinemann U. (2008) Diversity in Structure and Function of Tethering Complexes: Evidence for Different Mechanisms in Vesicular Transport Regulation. Curr Protein Pept Sci: 9(2): 197-209.

Lam S.K., Siu C.L., Hillmer S., Jang S., An G., Robinson D.G., Jiang L. (2007) Rice SCAMP1 defines clathrin-coated, trans-golgi-located tubular-vesicular structures as an early endosome in tobacco BY-2 cells. Plant Cell 19: 296-319.

Leborgne-Castel N., Lherminier, J., Der, C., Fromentin, J., Houot, V., Simon-Plas F. (2008) The plant defense elicitor cryptogein stimulates clathrin-mediated endocytosis correlated with reactive oxygen species production in bright yellow-2 tobacco cells. Plant Pphysiol. 146:1255-1266.

Lindeboom J., Mulder B.M., Vos J.W., Ketelaar T., Emons a M.C. (2008) Cellulose microfibril deposition: coordinated activity at the plant plasma membrane. J Microsc 231: 192-200.

Neher E. and Lindau M. (1988) Patch-clamp techniques for time-resolved capacitance measurements in single cells. Pflugers Arch. 411(2): 137-146.

Neher E. and Marty A. (1982) Discrete changes of cell membrane capacitance observed

under conditions of enhanced secretion in bovine adrenal chromaffin cells. Neurobiology 79: 6712-6716.

Onelli E., Prescianotto-Baschong C., Caccianiga M., Moscatelli A. (2008) Clathrin-dependent and independent endocytic pathways in tobacco protoplasts revealed by labelling with charged nanogold. J Exp Bot. 59: 3051-3068.

Pimpl P. and Denecke J. (2002) Protein-protein interactions in the secretory pathway, a growing demand for experimental approaches in vivo. Plant Mol. Biol. 50: 887–902.

Robatzek S., Chinchilla D., Boller T. (2006) Ligand-induced endocytosis of the pattern recognition receptor FLS2 in Arabidopsis. Genes and Development 20: 537-542.

Russinova E. and Vries S.D. (2005) Receptor-Mediated Endocytosis in Plants. Plant Cell Monographs 1: 103-115.

Samaj J., Baluska B., Schlicht M., Volkmann D., Menzel D. (2004) Endocytosis, Actin Cytoskeleton, and Signaling. Plant Physiol. 135: 1150–1161.

Schwake L., Henkel A.W., Riedel H.D., Stremmel W. (2002) Patch-Clamp Capacitance Measurements: New Insights into the Endocytic Uptake of Transferrin. Blood Cells, Molecules, and Diseases 29: 459-464.

Sutter J.U., Homann U., Thiel G. (2000) Ca^{2+}-stimulated exocytosis in maize coleoptile cells. Plant Cell 12: 1127-1136.

Sztul E. and Lupashin V. (2006) Role of tethering factors in secretory membrane traffic. Am J Physiol Cell Physiol. 290: C11-26.

Tester M. and Zorec R. (1992) Cytoplasmic calcium stimulates exocytosis in a plant secretory cell. Biophysical J. 63: 864-867.

Tse Y.C., Mo B., Hillmer S., Zhao M., Lo S.W., Robinson D.G., Jiang L. (2004) Identification of Multivesicular Bodies as Prevacuolar Compartments in Nicotiana tabacum BY-2 Cells. Plant Cell. 16: 672-693.

Weise R., Kreft M., Homann U., Thiel G., Zorec R. (2000) Transient and Permanent Fusion of Vesicles in Zea mays Coleoptile Protoplasts Measured in the Cell-attached Configuration. Journal of Membrane Biology 174: 15-20.

Zhang X., Kim-Miller M.J., Fukuda M., Kowalchyk J. a, Martin T.F.J. (2002) Ca^{2+}-dependent synaptotagmin binding to SNAP-25 is essential for Ca^{2+}-triggered exocytosis. Neuron 34: 599-611.

Zhang Y., Liu C-M., Emons A-M.C., Ketelaar T. (2010) The plant exocyst. J Integr Plant Biol. 52: 138-146.

Chapter 2

2 Modes of Exocytotic and Endocytotic Events in Tobacco BY-2 Protoplasts

2.1 Abstract

To analyze the kinetics and size of single exo- and endocytotic events in BY-2 protoplasts, cell-attached membrane capacitance measurements were applied. These measurements revealed different modes of fusion and fission of single vesicles. In about half of the observed exocytotic events, fusion occurred transiently, which facilitates rapid recycling of vesicles. In addition, transient sequential or multi-vesicular exocytosis observed in some recordings can contribute to an increase in efficiency of secretory product release. Microscopic analysis of the timescale of cellulose and pectin deposition in protoplasts demonstrates that rebuilding of the cell wall starts soon after isolation of protoplasts and that transient fusion events can fully account for secretion of the required soluble material. The capacitance measurements also allowed us to investigate formation of the fusion pore. It can be speculated that regulation of secretion may involve control of the length and/or size of fusion pore opening. Together, the different kinetic modes of exo- and endocytosis revealed by capacitance measurements underline the complexity of this process in plants and provide a basis for future research into the underlying mechanisms. The fact that similar fusion/fission kinetics are present in plant and animal cells suggests that many of these mechanisms are highly conserved among eukaryotes.

2.2 Introduction

Over the past years interest in the regulation of exo- and endocytosis in plant cells has increased rapidly. This is largely due to the fact that exo- and endocytosis have now been recognized as an essential part of many physiological processes in plant cells ranging from cell division to signaling and development (Murphy et al., 2005; Campanoni and Blatt, 2007; Robatzek, 2007; Lam et al., 2007). In order to understand normal function and pathological conditions of plant organisms, knowledge of the rather complex processes of vesicle fusion and fission is therefore essential.

So far, nearly all in vivo investigations of the regulation of exo- and endocytosis rely on indirect measurements of these processes via analysis of secreted proteins or uptake of plasma membrane markers. A more direct approach to characterize exo- and encoytotic events in vivo is provided by patch-clamp capacitance measurements. Capacitance measurements take advantage of the fact that exo- and endocytosis are associated with changes in plasma membrane area leading to proportional changes in the electrical membrane capacitance (Cm). The technique allows the following of exo- and endocytosis in real time in single living cells. The high-resolution capacitance measurements can be used to resolve the fusion and fission of single vesicles. In the past, patch-clamp capacitance measurements have been successfully applied to plant cells (see, e.g. Tester and Zorec, 1992; Homann and Tester, 1997; Carroll et al., 1998; Homann and Thiel, 1999; Weise et al., 2000; Thiel et al., 2009). However, in contrast to the animal field, the use of capacitance measurements in the study of exo- and endocytosis in plants is still waiting to become a widely used approach.

One reason why questions the regarding regulation of exo- and endocytosis in plants have so far only rarely been addressed by capacitance measurements is the lack of a suitable model system. To close this gap, a comprehensive characterization of single fusion and fission events in BY-2 protoplasts using membrane capacitance measurements in the cell-attached mode were carried out. BY-2 cells have widely been used in the study of plant cell biology, including cell division, action of phytohormones, and protein trafficking (Ambrose and Cyr, 2008; Hartig and Beck, 2006; Pimpl and Denecke, 2002). The cells also provide a suitable heterologous expression system to study the localization and function of proteins involved in the secretory or endocytotic pathway (Tse et al., 2004; Lam et al., 2007; Toyooka et al., 2009). However, the direct analysis of membrane turnover and especially information about the kinetics of vesicle fusion and fission are still missing. The capacitance measurements of

BY-2 protoplasts now allowed the analyses of the dynamics of exo- and endocytosis in these cells. This has led to the identification of different kinetic modes of vesicle fusion and fission, some of which have not been described in plants before. Additionally the timescale of cell wall regeneration was analyzed in BY-2 protoplasts which provide evidence for a role of transient exocytosis in secretion of cell wall material. Together, this study establishes the basis for future in vivo analysis of the regulation and physiological function of exo- and endocytosis in BY-2 protoplasts. The similarity between the kinetic modes of exo- and endocytosis observed in this study and vesicle fusion and fission described in animal cells furthermore suggests that these mechanisms are highly conserved among eukaryotes.

2.3 Results

2.3.1 Cell Wall Regeneration in BY-2 Protoplasts

One aim of our study was to establish a suitable model system for the investigation of exo- and endocytosis by patch-clamp measurements of membrane capacitance (Cm) in plants. As these measurements have to be carried out on protoplasts, one prerequisite for the use as a model system are viable protoplasts that show secretory and/or endocytotic activity.

Protoplasts are supposed to regenerate the cell wall soon after isolation. This process involves secretion of large amounts of soluble cell wall material. Analysis of cell wall regeneration would therefore allow us to gain information on both viability and secretory activity of BY-2 protoplasts. The cell wall of plant cells is build up of cellulose and non-cellulose complex glycans such as hemicellulose and pectins. To follow the rebuilding of the cell wall, the dyes ruthenium red were employed, which is a common stain for pectins, and Levacell®-Scharlach-E-3B (a synonym for Pontamine Fast Scarlet 4B), which has been shown to be a very stable fluorophore for staining of cellulose (Anderson et al., 2010).

Staining of turgid BY-2 cells by ruthenium red was most pronounced at the tip of cells and between neighboring cells (Figure 5A). This is consistent with the pectin content of the cell wall being higher in newly developing walls (i.e. tip of cells) and in the middle lamella. Levacell®-Scharlach-E-3B led to a bright fluorescent labeling of BY-2 cells with slightly less fluorescent intensity recorded between neighboring cells (Figure 5D). Immediately after isolation of protoplasts no staining by any of the two dyes could be observed (Figure 5B and Figure 5E), demonstrating that the cell wall has been removed completely during enzymatic treatment of cells.

However, already one day after isolation, some protoplasts were stained by ruthenium red (11.7% of all protoplasts) and Levacell®-Scharlach-E-3B (4.4% of all protoplasts) (Figure 5C and Figure 5F). This demonstrates that rebuilding of the cell wall is detectable within 24 h after preparation of protoplasts.

The amount of protoplasts stained by the two dyes increases with time, reaching 24.4 and 27.5%, respectively, within 4 days of protoplasts culture (Figure 5G).

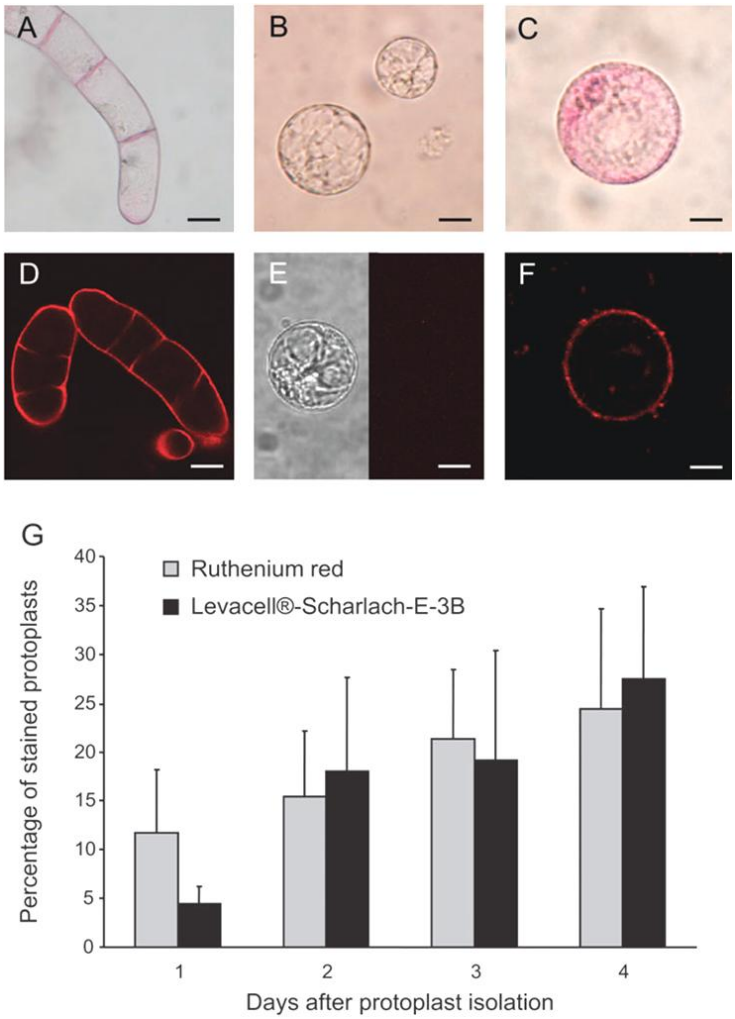

Figure 5: Cell Wall Regeneration in BY-2 Protoplasts. (A–C) Staining of pectins by ruthenium red in cells 2 days after subcultivation **(A)** and of protoplasts directly **(B)** and 1 day **(C)** after isolation. **(D–F)** Staining of cellulose by Levacell®-Scharlach-E-3B in cells 2 days after subcultivation **(D)** and in protoplasts directly **(E,** left: transmitted light image, right: fluorescent image) and 2 days **(F)** after isolation. **(G)** Time course of cell wall regeneration visualized by staining with ruthenium red and Levacell®-Scharlach-E-3B. Scale bar = 20 lm.

Considering that only larger amounts of pectin and cellulose will result in visible staining of protoplasts, the results imply that secretion of cell wall material starts soon after isolation of protoplasts. As patch-clamp experiments are usually carried out between 1 and 30 h after isolation, BY-2 protoplasts are indeed expected to start rebuilding the cell wall and thus show secretory activity during recording of Cm.

They therefore provide a promising system to analyze exo- and endocytosis via patch-clamp capacitance measurements.

2.3.2 *Permanent and Transient Exo- and Endocytotic Events in BY-2 Protoplasts*

In order to get detailed information on the kinetics and size of fusion and fission events in BY-2 cells, Cm of BY-2 protoplasts was monitored in the cell-attached mode. This allowed us to record high-resolution changes in Cm. As the membrane capacitance is proportional to the membrane area, the surface area and thus the diameter (d) of the vesicle can be determined from the vesicle capacitance (for details, see Methods).

In 64% of patches (58 cells, total recording time, 21.41 h; about 14 min per patch on average) spontaneous discrete changes in Cm were observed typically ranging between 0.25 and 10 fF. These upward and downward steps in Cm reflect exo- and endocytosis, respectively, of single vesicles of a diameter of between 100 and 630 nm. The recorded changes in Cm could be grouped into four different categories according to the different kinetics observed. Representative examples for each category are shown in Figure 6.

The first and the second groups include irreversible upward and downward steps, respectively (Figure 6A and Figure 6B). These steps represent permanent fusion (upward step) or fission (downward step) of single vesicles The events belonging to the third group are characterized by an upward step, which is shortly followed by a downward step of the same amplitude, indicating transient fusion of exocytotic vesicles (Figure 6C). The fourth group comprises a downward step shortly followed by an upward step of the same amplitude, indicating transient fission of endocytotic vesicles (Figure 6D).

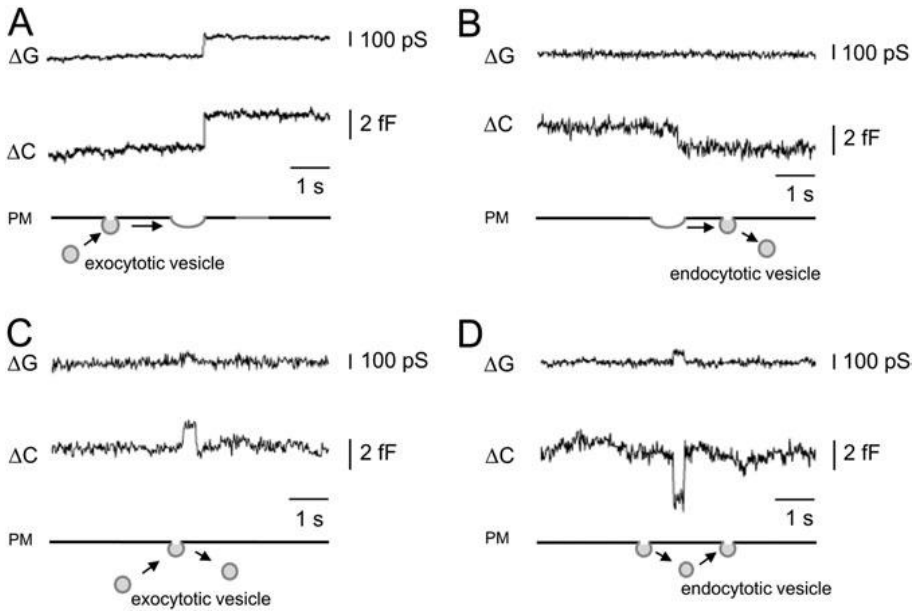

Figure 6: Representative Examples for Spontaneous Capacitance Steps Recorded in Cell-Attached Patches of BY-2 Protoplasts. Parts of a recording showing an imaginary and a real part of admittance, corresponding to changes in membrane conductance (ΔG; upper trace) and changes in membrane capacitance (ΔC; lower trace). Schematic drawings below the recorded traces illustrate the four different categories of fusion and fission events. Note that vesicles illustrated detached from the plasma membrane merely represent functionally discontinued vesicle lumen from the cell exterior and not necessarily the physical detachment. **(A)** Irreversible upward steps representing full fusion of exocytotic vesicles. **(B)** Irreversible downward steps representing full fission of endocytotic vesicles. **(C)** Reversible upward steps representing transient fusion of exocytotic vesicles. **(D)** Reversible downward steps representing transient fission of endocytotic vesicles. Note that in **(A)** the change in ΔC is reflected in a change in ΔG.

In any membrane patch either none or several discrete changes in Cm were observed. Patches of membrane with recorded capacitance events may point to hot spots of exo- and endocytotic activity in the plasma membrane of BY-2 cells. Considering that slightly more than half of the patches showed activity, the density of hot spots would be very high. Alternatively, the overall secretory and endocytotic activity may differ between protoplasts due to differences in their developmental state.

The number of permanent fusion events was not significantly different from fission events recorded in BY-2 protoplasts (122 and 101 events, respectively; Figure 7), suggesting that the surface area of protoplast is kept constant under non-stimulated conditions. Transient changes in Cm occurred about as frequently as permanent events but appeared predominantly in bursts (120 transient upward steps and 81 transient downward steps; Figure 7).

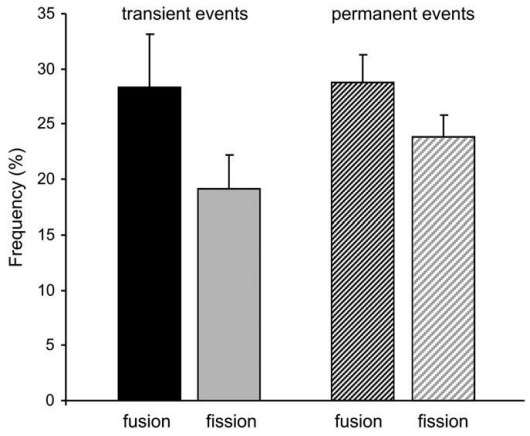

Figure 7: Number of Transient and Permanent Exo- and Endcytotic Steps. Of a total of 424 events, 120 transient fusion events (black), 81 transient fission events (gray), 122 permanent fusion events (shaded black), and 101 permanent fission events (shaded gray) were recorded. There was no significant difference (Student's t-test) between the number of transient and permanent fusion events.

In five cells fusion or fission events were observed which revealed a temporal coupling between changes in the capacitance trace and the trace representing the ohmic current. Figure 8A shows a representative example in which an increase in capacitance was associated with a downward deflection of the current trace and an increase in its noise level. The change in the current trace can therefore be interpreted as an increase in ion channel activity and most likely reflects insertion of one or more ion channels via permanent vesicle fusion. In Figure 8B, a downward deflection of the current trace is followed by a change in the current back to the baseline after 11.2 s. The changes in current are linked to an upward and downward step, respectively, of the capacitance trace.

This suggests that ion channel(s) that have been inserted by vesicle fusion are subsequently retrieved via endocytosis. Interestingly, the upward capacitance step was slightly smaller than the downward step (1.2 and 2.0 fF, respectively), implying that the exo- and endocytotic vesicles are not identical.

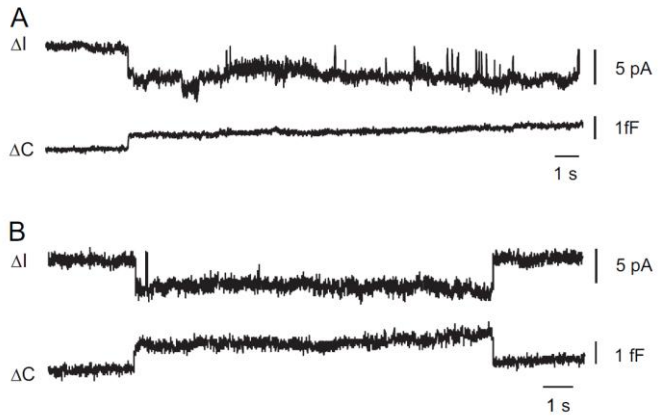

Figure 8: Fusion and Fission Events Showing Temporal Correlation between Changes in the Membrane Current and Membrane Capacitance. (A) Temporal correlation between upward step in membrane capacitance (ΔC) resulting from permanent vesicle fusion and a change in the membrane current trace (ΔI), which can be interpreted as an increase in ion channel activity. **(B)** Upward and downward steps in ΔC resulting from permanent vesicle fusion and fission, respectively, are correlated to changes in ΔI, which can be interpreted as an increase and decrease in ion channel activity.

To further analyze the transient events, the amplitude of the upward steps (on-steps) in Cm were plotted against the amplitude of the downward steps (off-steps) that followed within 1 s. Similarly, the off-steps in Cm were plotted against the amplitude of the following on-steps (Figure 9). The amplitude distributions of transient exo- and endocytotic events were best fitted with a regression line with a slope near 1, demonstrating that the on and off-steps of transient events were always of identical size.

This can, in principle, be explained by exo- and endocytosis of different vesicles of exactly the same size. However, repetitive occurrence of such a sequence of events is very unlikely. In fact, the correlation between the on- and off-steps rather supports the idea that the reversible upward and downward capacitance steps reflect the transient fusion and fission of a single vesicle.

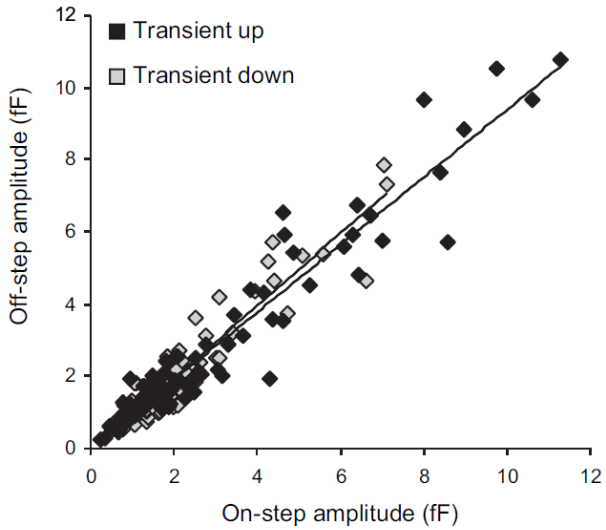

Figure 9: Correlation between Amplitudes of Upward and Downward Steps of Transient Changes in Capacitance. On-steps of transient exo- and endocytotic events (marked in black and gray, respectively) are plotted against the corresponding offsteps. The line represents the best fit of a linear regression with a slope of 0.94 for exocytotic events (correlation coefficient 0.96; n = 120) and 1.01 for endocytotic events (correlation coefficient 0.95; n = 81). Events larger than 10 pF were excluded from analysis.

Figure 10A illustrates the relative distribution of the diameter of all transiently fused exo- and endocytotic vesicles. A Student's t-test reveals that the two populations were not significantly different. The median of transient exo- and endocytotic vesicles was 303 and 251 nm, respectively. The median of permanent fusion and fission events was slightly larger (355 and 351 nm, respectively; Figure 10B). Again, the distribution of exocytotic events was not significantly different from the distribution of endocytotic events.

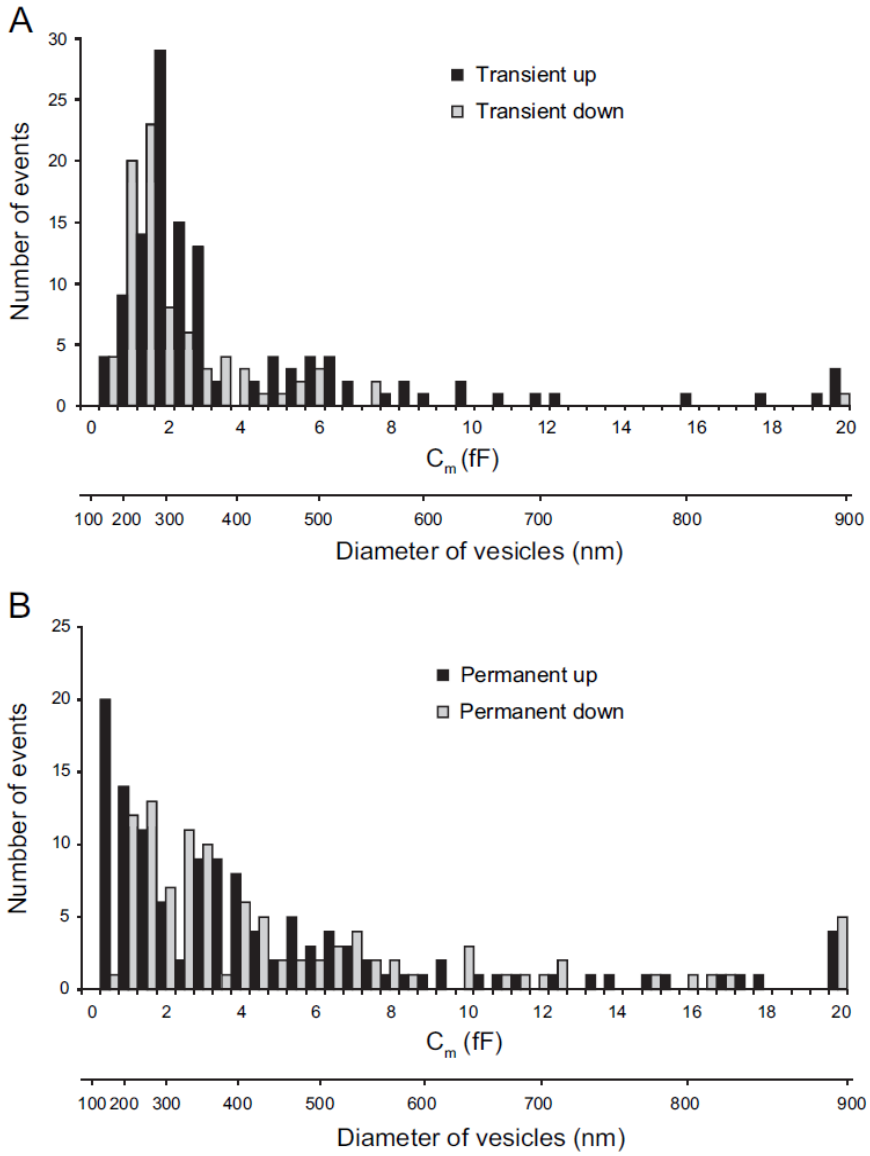

Figure 10: Distribution of Vesicle Size. (A) Size distribution of amplitudes of transient exocytotic (black, n = 120) and endocytotic (gray, n = 81) events. The plot summarizes data from 31 patches. **(B)** Size distribution amplitudes of irreversible exocytotic (black, n = 122) and endocytotic (gray, n = 101) events collected from 40 patches.

2.3.3 Kinetics of Transient Exo- and Endocytotic Events

To examine the dwell time of transient capacitance steps, the time was measured between step-wise increase and subsequent decrease in Cm of transient exocytotic events and the time

between step-wise decrease and subsequent increase in Cm of transient endocytotic events. Figure 11 shows the resulting dwell time histograms of the times at which a transient exocytotic vesicle is in contact with the membrane (black bars) or the times at which a transient endocytotic vesicle is detached from the membrane (gray bars).

The median for the transient fused state was slightly shorter than the value calculated for the transient fission state (142 and 223 ms, respectively). Some infrequent events above 1 s were excluded from analysis. A similar distribution has been described for transient fusion events recorded in maize coleoptile protoplasts (Weise et al., 2000). The maximum in the dwell time histogram demands that the reaction occurs in a preferred direction and can be described according to Colquhoun and Hawkes (1995), with the sum of two exponentials:

$$n(t) = a \bullet ((\exp(-t/\tau_1) - \exp(-t/\tau_2)) \qquad (1)$$

where τ_1 and τ_2 are the time constants and a is the number of observations multiplied by a normalizing factor. Fitting in the present case the upward and downward dwell time histograms with equation (1) yielded two time constants for the exocytotic events (τ_1 = 80 ms and τ_2 = 73 ms) and also for endocytotic events (τ_1 = 129 ms and τ_2 = 127 ms).

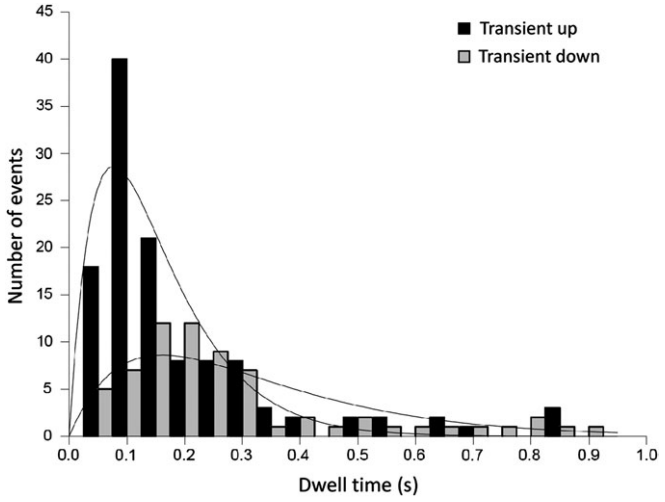

Figure 11: Dwell Time of Transient Exo- and Endocytotic Events. The dwell time of both excytotic (n = 120) and endocytotic (n = 81) events was best fitted with two exponentials (Equation 1) with time constants of s1 = 80/129 ms and s2 = 73/127 ms for the exo- and endocytotic events, respectively (correlation coefficients 0.82 and 0.79, respectively). Very long events > 1 s (three exocytotic and 11 endocytotic events) were excluded from the fit.

Further inspection of the capacitance recordings of BY-2 protoplasts also revealed flickering activity of transient exo- and endocytotic events where a sequence of several transient changes in Cm with amplitudes of approximately the same size occurred over several seconds (Figure 12A and Figure 12B). In some cases vesicles were found to undergo long periods of rhythmic opening and closing of a fusion pore (Figure 12C). Analysis of a period of rhythmic changes in Cm revealed that the 59 events analyzed have similar amplitudes of 0.74 ± 0.12 fF. The average duration of the fused and non-fused state was 52 ± 13 and 200 ± 49 ms, respectively. Periods of similar rhythmic kinetics were found in two measurements.

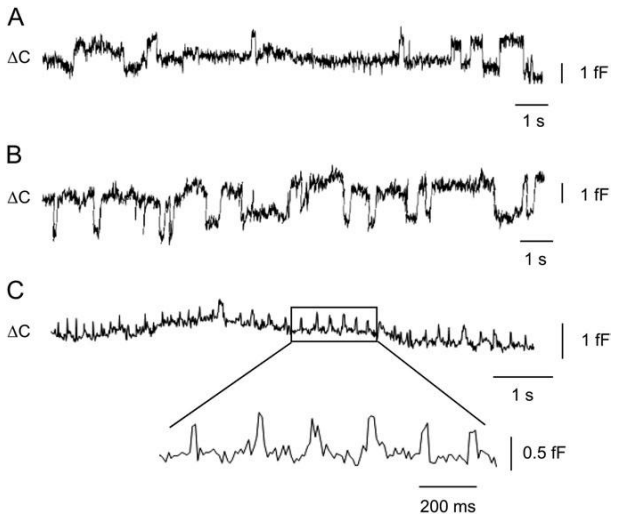

Figure 12: Flickering of Exo- and Endocytotic Events and Rhythmic Changes in Capacitance. (A) Flickering activity of transient exocytotic events. **(B)** Flickering activity of transient endocytotic events. **(C)** Rhythmic increase and decrease in membrane capacitance. Inset: amplification of the recording marked in **(C).**

2.3.4 Compound Exocytosis in BY-2 Protoplasts

In addition to successive transient opening and closing of the fusion pore of single vesicles also more complex transient fusion and fission events were observed. In five recordings changes in Cm composed of multiple amplitudes of on- and off-steps were found. Figure 13A shows a representative example of a recording with multiple-amplitude steps in Cm. These events most likely reflect so-called compound exocytosis whereby vesicles fuse with each other as well as with the plasma membrane.

In general two types of compound exocytosis could be observed. The first type is characterized by multiple upward steps that can be interpreted as sequential exocytosis. After initial fusion of a vesicle with the plasma membrane a secondary fusion event occurs, whereby a deeper-lying vesicle fuses with the already attached vesicle at the plasma membrane (Figure 13B).

The second type is composed of a single, large-amplitude upward step, which indicates compound exocytosis of vesicles fused with each other intracellularly before interacting with the plasma membrane (Figure 13C). It is unlikely that these double-amplitude on-steps represent simultaneous fusion of similarly sized vesicles, since the probability for independent fusion of two vesicles is $P<10^4$. Both types of compound exocytosis, sequential and multi-vesicular, were generally found to be transient.

Return of Cm to the baseline could either occur in a single off-step (Figure 13B) or in multiple off-steps (Figure 13C). Similarly to those described for complex fusion events, these endocytotic events most likely correspond to simultaneous retrieval of multiple vesicles from the plasma membrane (diagram in Figure 13B) or sequential endocytosis of vesicles clustering at the plasma membrane (diagram in Figure 13C).

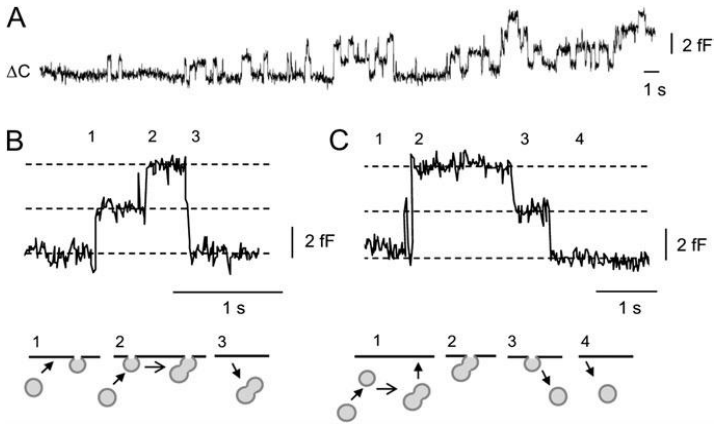

Figure 13: Complex Transient Fusion and Fission Events with Multiple Amplitudes. (A) Cell-attached recording revealing multiple-amplitude on- and off-steps. **(B)** Sequential exocytosis followed by multi-vesicular endocytosis. Recorded changes in Cm (top) and diagram of possible interpretation (bottom). **(C)** Multi-vesicular exocytosis followed by sequential endocytosis. Recorded changes in Cm (top) and diagram of possible interpretation (bottom).

2.3.5 *Fusion Pore Conductance During Exo- and Endocytotic Events*

Exocytosis is related to formation of a fusion pore that connects the vesicular lumen to the extracellular space. In the non-fused state the fusion pore conductance (Gp) is zero and increases during the fusion process when the pore dilates. Gp is therefore a measure of the size of the fusion pore (Figure 14A). In the cell-attached configuration a change in Gp is reflected in an increase in the real part (Re) of the signal. Figure 14B shows a representative example of a parallel transient change of Re and Im (imaginary part of the signal), which reflects the reversible opening of the fusion pore during transient exocytosis.

This parallel change in Im and Re did not result from incorrect phase-angle setting of the log-in amplifier, since the calibration pulse (Figure 14B, asterisk) was not projected in the Re trace. No step-wise change in the Re signal could be recorded for events in which the fusion pore conductance was high. Fast dilatation of the fusion pore prevents the measurement system from resolving the transient change in Re (Henkel et al., 2000). However, most transient exocytotic and half of the transient endocytotic events were associated with a step-wise increase in Re (74 and 48%, respectively).

From the recorded changes in Re and Im the vesicle capacitance, the fusion pore conductance, and fusion pore diameter were calculated (see Methods). Figure 14C shows the distribution of the calculated pore conductance from transient exo- and endocytotic events. The median of transient exo- and endocytotic fusion pore was 36 (range: 8–186 pS, n = 98) and 76 pS (range: 22–345 pS, n = 39), respectively.

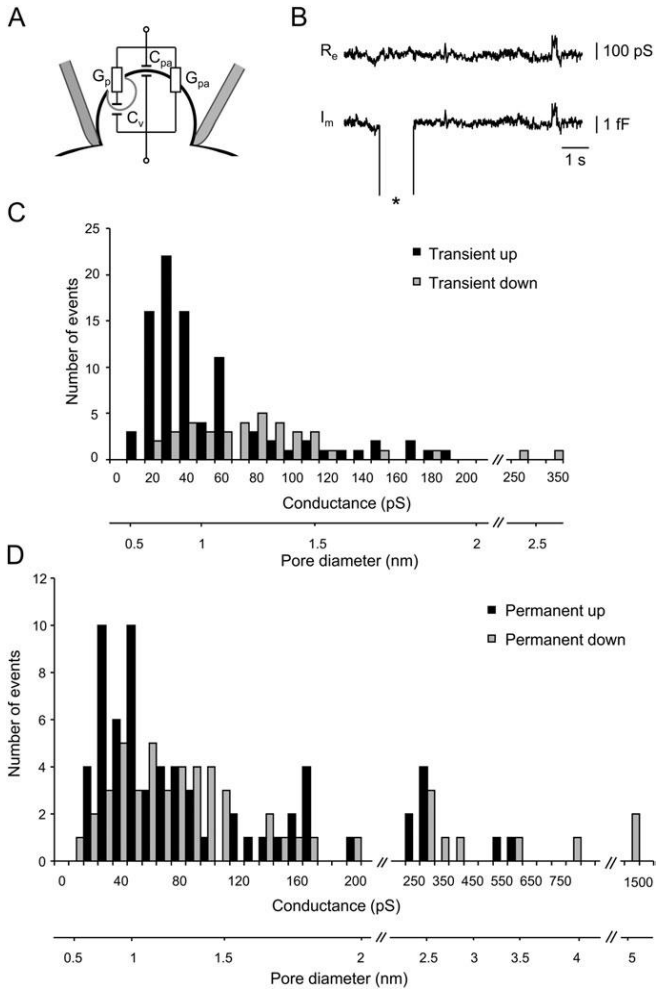

Figure 14: Distribution of Fusion Pore Size. (A) Equivalent circuit for the cell-attached configuration describing the origin of the fusion pore conductance (Gp), the vesicle capacitance (Cv), the patch conductance (Gpa), and the patch capacitance (Cpa). **(B)** Representative recording of step-wise transient changes in membrane capacitance (ΔC) associated with changes in membrane conductance (ΔG). **(C)** Distribution of fusion pore conductance calculated from transient changes in patch conductance from 89 transient exocytotic and 39 transient endocytotic events. **(D)** Distribution of fusion pore conductance calculated from permanent changes in patch conductance from 65 permanent exocytotic and 52 permanent endocytotic events.

Half of the permanent fusion and fission events were also associated with step-wise change in the Re signal (53 and 51%, respectively). The fusion pores calculated for these permanent events could be classified into two groups: small fusion pores with a conductance from 20 to 200 pS and large fusion pores with a conductance mainly between 220 and 1500 pS. The median conductance of small fusion pores was 53 pS (n = 57) for exocytotic events and 71 pS (n = 43) for endocytotic events. For the group of large exo- and endocyototic fusion pores a median conductance of about 301 and 354 pS (n = 8 and n = 9, respectively) was calculated.

2.4 Discussion

2.4.1 In BY-2 Protoplasts, Vesicles Undergo Transient and Permanent Fusion and Fission

This study aimed to the advance of the understanding of elementary properties of vesicle fusion and fission in plant cells using cell-attached membrane capacitance measurements on BY-2 protoplasts. This allowed monitoring exo- and endocytosis of single vesicles in real time. The results demonstrate that BY-2 protoplasts exhibit abundant exo- and endocytosis activity of vesicles with a median diameter of around 300 nm. From electron microscopy studies (Pope et al., 1979) or capacitance measurements (Thiel et al., 1998) on maize coleoptile protoplasts, a mean diameter for vesicles of around 100 nm has been reported. Similar small vesicles were also found in electron micrographs of Arabidopsis root hairs (average 70 nm) (Ketelaar et al., 2008). In Arabidopsis pollen tubes the average diameter of vesicles was slightly larger (182 nm, Ketelaar et al., 2008). Our results therefore suggest that most exo- and endocytotic vesicles found in BY-2 protoplasts are bigger than reported for other plant cells.

Membrane capacitance measurements have been shown to enable detection of vesicles as small as 60 nm provided that the signal-to-noise ratio is sufficiently high (Kreft and Zorec, 1997). In our measurements the background noise ranged from around 0.13 to 0.5 fF, which would allow the resolution of fusion and fission of vesicles with diameters of between 100 and 200 nm. However, it can not be excluded that capacitance changes resulting from fusion and fission of small vesicles of around 100 nm are underestimated due to the higher noise level in some recordings.

In contrast to electron microscopic studies, membrane capacitance measurements do allow not only determination of the size of vesicles, but also analysis of the kinetics of vesicle fusion and fission. The capacitance measurements on BY-2 protoplasts represented in this study demonstrate that fusion and fission of vesicles occurred either permanently or transiently. Transient exocytosis or ‘kiss-and-run’ mechanism of exocytosis has first been suggested for synaptic vesicle exocytosis (Ceccarelli et al., 1973). It has subsequently been described in numerous other mammalian cell types (for review, see Schneider, 2001) as well as in maize

coleoptile protoplasts (Weise et al., 2000). Transient exocytosis involves transient opening of the fusion pore that connects the vesicle lumen with the extracellular space.

In some cells a rhythmic opening and closing of the fusion pore that persisted for tens of seconds were observed. A similar rhythmic fusion and fission of vesicles has also been demonstrated in maize coleoptile protoplasts (Thiel et al., 2009) and animal cells (Henkel et al., 2000; Vardjan et al., 2007). To account for such an oscillating opening and closing of the fusion pore, it has been suggested that the two processes are linked by a distinct feedback system (Thiel et al., 2009).

In addition to transient exocytosis also transient endocytosis was observed in BY-2 protoplasts, as previously described in bovine chromaffin cells (Henkel et al., 2000, 2001a). One may hypothesize that transient endocytosis reflects the transition between two (or more) states of endocytosis before the energy required for full fission can be surmounted.

2.4.2 Fusion Pore Conductance as an Additional Regulatory Factor of Secretion in Plants

Permanent and transient exocytosis also differs in terms of regulation of the release rate. While the amount of soluble material released during permanent exocytosis correlates with the size of the secretory vesicles, the release rate during transient exocytosis depends on the lifetime and the size of the fusion pore.

Our results show that the majority of transient vesicles stayed attached to the plasma membrane for around 100 ms. This is similar to what has previously been described in maize coleoptile protoplasts (Weise et al., 2000) and mammalian cells (see, e.g. Ale´ s et al., 1999; Henkel et al., 2001b; Elhamdani et al., 2006; Jorgačevski et al., 2008). Studies on mammalian cells demonstrated that different factors such as Ca^{2+} (Alés et al., 1999; Elhamdani et al., 2006), phosphorylation (Henkel et al., 2001b), and hypotonicity (Jorgačevski et al., 2008) can affect the lifetime of the transient fusion event.

In these studies the time of the fusion pore and thus the time the vesicle lumen is connected to the extracellular space could change by a factor of about two in response to different treatments. This implies that modulation of the fusion pore dwell time could indeed contribute to regulating the release of secretory material. In addition, the diameter of the fusion pore also influences secretion of the vesicular content.

Our experiments represent the first quantification of the size of fusion pores in plants. For most transient as well as permanent fusion events, the calculated fusion pore conductance was below 100 pS. In addition, also larger pores were recorded with a conductance above 250 pS, which occurred mainly during permanent fusion. Differences in fusion pore conductance may represent different vesicle types, as described for large dense-core vesicles (LDCVs) and small synaptic vesicles, two classes of neurotransmitter-containing vesicles found in nerve terminals. Both vesicle types can undergo transient and permanent fusion. For transient fusion events Klyachko and Jackson (2002) reported a pore conductance of between 4 and 45 pS (average 19 pS) for microvesicles and 23–780 pS (average 213 pS) for LDCVs.

These differences in pore conductance have been postulated to contribute to differences in release kinetics of various neurotransmitters (Klyachko and Jackson, 2002). Fusion pore conductance can also vary in response to hypotonicity or depolarization (Jorgačevski et al., 2008). Thus, release of vesicle content can be controlled by both fusion pore conductance and kinetic of pore opening. In plant cells, factors that regulate secretion by influencing the dwell time of fusion and fission or the size of the fusion pore have not yet been described.

However, the fact that the different kinetic modes of exo- and endocytosis are present in both plant and animal cells suggests that similar regulatory mechanisms do exist in plant cells. It furthermore implies that the underlying mechanisms of vesicle fusion and fission are conserved among eukaryotes.

2.4.3 Possible Physiological Function of Different Kinetic Modes of Exocytosis in BY-2 Cells

The different kinetic modes of exocytosis observed in BY-2 protoplasts are most likely related to different physiological functions. Even though the present measurements do not allow a direct correlation between the observed fusion events and the underlying physiological processes, some hints on the possible role of the different exocytotic modes can be derived from a number of indirect evidences.

Most membrane proteins are subject to high turnover rates that require sustained incorporation and removal of proteins into and out of the plasma membrane via fusion and fission of vesicles with the plasma membrane. Some permanent fusion and fission events recorded in BY-2 protoplasts revealed a temporal coupling between changes in the

capacitance and current trace. The latter can be interpreted as a change in membrane conductance resulting from insertion or retrieval of ion channels. This suggests that part of the permanent exo- and endocytotic events reflect constitutive turnover of ion channels in BY-2 protoplasts. Such a turnover of ion channels is in accordance with observations in guard cells that revealed constitutive and stimulated exo- and endocytosis of the plant K^+ Channel KAT1 (Hurst et al., 2004; Meckel et al., 2004; Sutter et al., 2007).

In general, it seems likely that permanent fusion and fission observed under non-stimulating conditions serve housekeeping functions such as recycling of plasma membrane proteins. In addition to sustaining constitutive membrane turnover, protoplasts have to fulfil the remarkable task of rebuilding a new cell wall. As shown in the present study, this process is detectable within 24 h after isolation of BY-2 protoplasts. The cell wall of plant cells is build-up of cellulose and noncellulose complex glycans such as hemicellulose and pectins. These complex extracellular glycans are synthesized in large quantities in the Golgi apparatus and are transported to the plasma membrane via secretory vesicles.

Recent investigations on the secretory pathway in BY-2 cells demonstrated that clusters of secretory vesicles containing soluble secretory proteins and cell wall components are involved in secretion of cell wall material (Toyooka et al., 2009). In some cases several vesicles of these secretory vesicle cluster (SVC) were connected with each other to a region of the plasma membrane. This strongly reminds us of so-called compound fusion of multi-vesicular structures that have been observed in many different mammalian cell types (for review, see Pickett and Edwardson, 2006). Compound exocytosis recorded in BY-2 protoplasts therefore most likely represents fusion of SVCs with the plasma membrane.

The diameter of vesicles within SVCs observed in electronmicrographs of BY-2 cells was found to be 50–100 nm (Toyooka et al., 2009). This is smaller than the diameter of vesicles estimated from our capacitance measurements during compound exocytosis (around 300 nm). However, in a number of mammalian cell types showing compound exocytosis, vesicles were found to fuse with each other intracellularly before any interaction with the plasma membrane occurred (Pickett and Edwardson, 2006). The difference in vesicle diameter may therefore be explained by homotypical fusion of vesicles within the SVC, leading to formation of structures that then fuse with the plasma membrane. In contrast to targeting and fusion of single vesicles, these clusters would provide an efficient way of mass transport of secretory material to the plasma membrane, thereby facilitating secretion of cell wall material and

rebuilding a new cell wall. Compound exocytosis was generally found to be transient. It can thus be regarded as a special form of transient exocytosis.

During transient exocytosis secretory products can be released through the fusion pore, while the vesicular matrix is retained for re-use in subsequent fusion cycles. This mode of exocytosis allows faster recycling of vesicles and thereby prevents depletion of the ready-to-fuse vesicle pool under high secretory activity. For plant cells it has been speculated that the vesicular matrix does include proteins required for the maturation of secreted cell wall components and that this mode of exocytosis may thus be involved in secretion of cell wall material (Weise et al., 2000).

This hypothesis is supported by the high frequency of transient exocytotic events (about 50% of all recorded fusion events) observed in BY-2 protoplasts. To provide further evidence for the role of transient exocytotic events in secretion of cell wall material, it was estimated whether the maximum amount released by transiently fusing vesicles can account for the amount of material needed for rebuilding a new cell wall. First the volume of the cell wall was calculated from electron micrographs of intact BY-2 cells (Table 1). Assuming that around 90% of the primary cell wall is made up of secreted complex polysaccharides (Caffall and Mohnen, 2009), the maximum amount of secretory products needed for building the cell wall is about 945 μm^3. To secrete this volume, 71 380 vesicles with a diameter of 303 nm (average diameter of transiently fusing vesicles) would have to fuse with the plasma membrane and release their full content. Extrapolating the average rate at which transient exocytosis has been observed in a single membrane patch to the whole surface area of a protoplast (Table 1), revealed that it would take around 8 h to release enough secretory products to replace the whole volume of a new cell wall. In principle, transient exocytosis can therefore fully account for secretion of new cell wall material in BY-2 protoplasts. Transient exocytosis, including compound exocytosis, may therefore be the predominant mechanism for secretion of new cell wall material in BY-2 protoplasts.

Table 1: Values used for calculating the minimal time needed for rebuilding the cell wall by release of secretory material from transiently fusing vesicles only.

cell wall volume (V_{CW})	1050 μm^3
vesicle volume (V_V)	0.015 μm^3
$\frac{\text{number of transient fusion events}}{\text{hour cell surface area}}$	7657.8

2.5 Materials and Methods

2.5.1 Cell Culture and Protoplast Isolation

BY-2 cells were cultured in Linsmaier and Skoog medium (Duchefa, Haarlem Netherlands) supplemented with sucrose (30 g l^{-1}), 2,4-dichlorophenoxyacetic acid (1 mg ml^{-1}), and thiamine (1 mg ml^{-1}). Sub-culturing was performed twice a week by adding 10 ml of the cell suspension into 100 ml of new medium. Cultures were maintained in the dark, at 28°C, under rapid shaking (100 rpm).

For protoplast isolation, cells were collected 2–3 days after subcultivation. 2 ml of the cell culture suspension were incubated with 2 ml digestion medium for 3–4 h at 37°C under slow shaking. The digestion medium contained 3% Cellulase R10 (Yakult Honsha Co., Ltd, Japan), 0.2% Macerozym (Yakult Honsha Co., Ltd, Japan), 0.1% Pectolyase (Yakult Honsha Co., Ltd, Japan), 8 mM $CaCl_2$, 25 mM MES-KOH, pH 5.6, adjusted to 540 mosmol kg^{-1} with sucrose. After digestion cells were collected by centrifugation (100 g, 10 min), washed twice in wash solution (100 mM NaCl, 30 mM $CaCl_2$, 30 mM KCl, 5 mM sucrose, 20 mM MES, pH 6.5), and stored at 4°C until use.

2.5.2 Electrophysiology

Membrane capacitance (Cm) of BY-2 protoplasts was monitored with patch-clamp measurements in the cell-attached mode. Patch pipettes with a tip resistance of 4–8 MΩ were prepared from glass capillary tubing (Kimax 51; Kimax Products, Vineland, NJ, USA) and the shanks of the pipettes were coated with paraffin. Pipettes were filled with external solution (30 mM $CaCl_2$, 54 mM K-Gluconat 25 mM MES–KOH, pH 5.6 adjusted to 435 mosmol kg^{-1} with sorbitol).

Protoplasts were bathed in external solution. Measurements were performed with a dual-phase lock-in patch-clamp amplifier (SWAM IIC, Celica, Ljubljana, Slovenia). Membrane patches were clamped at –52 mV on which a sine wave (root mean square 111 mV, sine-wave frequency (f) 1.6 kHz) was applied. The phase of the lock-in amplifier was adjusted to nullify

changes in real part (Re) of the admittance signal to a manually generated 100-fF calibration pulse. The output signals were low pass filtered (10 Hz, –3 db), acquired at 100 Hz by an A/D converter (NI-DAQ, National Instruments, Austin, USA) and stored on a personal computer.
The signal in phase reflects Re and is equivalent to the patch conductance; the out-of-phase signal corresponds to the imaginary part (Im). If there is no reflection in the Re trace, Im is directly proportional to changes in Cm. For events with projections between Re and Im, the vesicle capacitance (Cv) and fusion pore conductance (Gp) were calculated from the Im and Re portion of the signal as reported previously (Lollike and Lindau, 1999): $Cv = [(Re^2 + Im^2)/Im]/ \omega$, where ω is the angular frequency ($\omega = 2\pi f$) and $Gp = (Re^2 + Im^2)/Re$. As the membrane capacitance is proportional to the membrane area, the surface area and thus the diameter (d) of the vesicle can be determined from the vesicle capacitance according to the equation $Cv = C_{spec}\pi d^2$, where C_{spec} (specific capacitance) is the capacitance per unit membrane area. C_{spec} was set to 8 mF m^{-2} a value that has previously been determined for plant protoplasts (Homann and Tester, 1998).
Fusion pore diameter was calculated according to the equation $Gp = (\pi r^2)/(p\lambda)$, where r is the radius of fusion pore, p the resistivity of saline (100 Ω cm^{-1}), and λ is the length of the fusion pore. The length of the fusion pore can be estimated from the length of a gap junction channel (15 nm), since both fusion pore and gap junction channel span two membranes (Spruce et al., 1990). Events were analyzed by using the cursor option in the software subroutine (CellAn, Celica, Slovenia) written for MATLAB (MathWorks Inc., Natik, MA, USA) with additional digital filtering as required. Values are presented as median or mean ± SEM.

2.5.3 Staining of Pectins and Cellulose

Pectin and cellulose content of BY-2 suspension cells or protoplasts was determined by staining cells with ruthenium red and Levacell®-Scharlach-E-3B, respectively. Microscopic analysis of suspension cells and preparation of protoplasts was performed 2–3 days after sub-cultivation. Ruthenium red (Merck KGaA, Darmstadt, Germany) was kept as a 6 mM stock solution in water supplemented with 0.1% (v/v) ammonia. 2 µl of staining solution was added to 50 µl protoplast suspension.
Cells were observed with a bright field microscope (Zeiss Axioskop 40, Zeiss, Jena, Germany) directly after addition of the dye. Levacell®-Scharlach-E-3B (Kemira PPC

Germany GmbH, Leverkusen, Germany) was supplied as a water-based solution from which a 0.1% (v/v) stock solution was prepared in water. For staining cellulose, 0.1–0.01% of the Levacell®-Scharlach-E-3B stock solution were added to BY-2 cells or protoplasts. Images were acquired directly after addition of the dye with a confocal laser scanning microscope (Leica TCS SP, Leica Microsystems GmbH, Heidelberg, Germany). Levacell®-Scharlach-E-3B was excited at 488 nm, emission was detected at 530–670 nm.

2.6 References

Alés E., Tabares L., Poyato J.M., Valero V., Lindau M., de Toledo G.A. (1999) High calcium concentrations shift the mode of exocytosis to the kiss-and-run mechanism. Nat. Cell Biol. 1: 40–44.

Ambrose J.C. and Cyr R. (2008) Mitotic spindle organization by the preprophase band. Mol. Plant. 1: 950–960.

Anderson C.T., Carroll A., Akhmetova L., Somerville C. (2010) Real-time imaging of cellulose reorientation during cell wall expansion in Arabidopsis roots. Plant Physiol. 152: 787–796.

Caffall K.H. and Mohnen D. (2009) The structure, function, and biosynthesis of plant cell wall pectic polysaccharides. Carbohydr. Res. 344: 1879–1900.

Campanoni P. and Blatt M.R. (2007). Membrane trafficking and polar growth in root hairs and pollen tubes. J. Exp. Bot. 58: 65–74.

Carroll A.D., Moyen C., Van Kesteren P., Tooke F., Battey N.H., Brownlee C. (1998) Ca2+, annexins, and GTP modulate exocytosis from maize root cap protoplasts. Plant Cell. 10: 1267–1276.

Ceccarelli B., Hurlbut W., Mauro A. (1973) Turnover of transmitter and synaptic vesicles at the frog neuromuscular junction. J. Cell Biol. 57: 499–524.

Colquhoun D. and Hawkes A. (1995) The principles of the stochastic interpretation of ion-channel mechanisms. In Single Channel Recording, Sakmann B. and Neher E., eds (New York: Plenum Press), pp. 397–482.

Elhamdani A., Azizi F., Artalejo C.R. (2006) Double patch clamp reveals that transient fusion (kiss-and-run) is a major mechanism of secretion in calf adrenal chromaffin cells: high calcium shifts the mechanism from kiss-and-run to complete fusion. J. Neurosci. 26: 3030–3036.

Hartig K. and Beck E. (2006) Crosstalk between auxin, cytokinins, and sugars in the plant cell cycle. Plant Biol. 8: 389–396.

Henkel A.W., Horstmann H., Henkel M.K. (2001a) Direct observation of membrane retrieval in chroman cells by capacitance measurements. FEBS Lett. 505: 414–418.

Henkel A.W., Kang, G., Kornhuber J. (2001b) A common molecular machinery for exocytosis and the ‘kiss-and-run’ mechanism in chromaffin cells is controlled by phosphorylation. J. Cell Sci. 114: 4613–4640.

Henkel A.W., Meiri H., Horstmann H., Lindau M., Almers W. (2000) Rhythmic opening and closing of vesicles during constitutive exo- and endocytosis in chromaffin cells. EMBO J. 19: 84–93.

Homann U. and Tester M. (1997) Ca2+-independent and Ca2+/GTPbinding protein-controlled exocytosis in a plant cell. Proc. Natl Acad. Sci. U S A. 94: 6565–6570.

Homann U. and Tester M. (1998) Patch-clamp measurements of capacitance to study exocytosis and endocytosis. Trends Plant Sci. 3: 110–114.

Homann U. and Thiel G. (1999) Unitary exocytotic and endocytotic events in guard-cell protoplasts during osmotically driven volume changes. FEBS Lett. 460: 495–499.

Hurst A.C., Meckel T., Tayefeh S., Thiel G., Homann U. (2004) Trafficking of the plant potassium inward rectifier KAT1 in guard cell protoplasts of Vicia faba. Plant J. 37: 391–397.

Jorgačevski J., Stenovec M., Kreft M., Bajić A., Rituper B., Vardjan N., Stojilkovic S., Zorec R. (2008) Hypotonicity and peptide discharge from a single vesicle. Am. J. Physiol. Cell Physiol. 295: C624–C631.

Ketelaar T., Galway M.E., Mulder B.M., Emons A.M.C. (2008) Rates of exocytosis and endocytosis in Arabidopsis root hairs and pollen tubes. J. Microscopy. 231: 265–273.

Klyachko V.A. and Jackson M.B. (2002) Capacitance steps and fusion pores of small and large-dense-core vesicles in nerve terminals. Nature. 418: 89–92.

Kreft M. and Zorec R. (1997) Cell-attached measurements of attofarad capacitance steps in rat melanotrophs. Eur. J. Physiol. 434: 212–214.

Lam S.K., Siu C.L., Hillmer S., Jang S., An G., Robinson D.G., Jiang L. (2007) Rice SCAMP1 defines clathrin-coated, transgolgi-located tubular-vesicular structures as an early endosome in tobacco BY-2 cells. Plant Cell. 19: 296–319.

Lollike K. and Lindau M. (1999) Membrane capacitance techniques to monitor granule exocytosis in neutrophils. J. Immunol. Methods. 232: 111–120.

Meckel T., Hurst A.C., Thiel G., Homann U. (2004) Endocytosis against high turgor: intact guard cells of Vicia faba constitutively endocytose fluorescently labelled plasma membrane and GFP-tagged K+-channel KAT1. Plant J. 39: 182–193.

Murphy A.S., Bandyopadhyay A., Holstein S.E., Peer W.A. (2005) Endocytotic cycling of PM proteins. Annu. Rev. Plant Biol. 56: 221–251.

Pickett J.A. and Edwardson J.M. (2006) Compound exocytosis: mechanisms and functional significance. Traffic. 7: 109–116.

Pimpl P. and Denecke J. (2002) Protein-protein interactions in the secretory pathway, a growing demand for experimental approaches in vivo. Plant Mol. Biol. 50: 887–902.

Pope D.G., Thorpe J.R., Al-Azzawi M.J., Hall J.L. (1979) The effect of cytochalasin B on the rate of growth and ultrastructure of wheat coleoptiles and maize. Planta. 144: 373-383.

Robatzek S. (2007) Vesicle trafficking in plant immune responses. Cell Microbiol. 9: 1–8

Schneider S.W. (2001) Kiss and run mechanism in exocytosis. J. Membrane Biol. 181: 67-76.

Spruce A., Breckenridge L., Lee A., Almers W. (1990) Properties of the fusion pore that forms during exocytosis of a mast cell secretory vesicle. Neuron. 4: 643–654.

Sutter J.U., Sieben S., Hartel A., Eisenach C., Thiel G., Blatt M.R. (2007) Abscisic acid triggers the endocytosis of the Arabidopsis KAT1 K+channel and its recycling to the plasma membrane. Current Biol. 17: 1396–1402.

Tester M. and Zorec R. (1992) Cytoplasmic calcium stimulates exocytosis in a plant secretory cell. Biophys. J. 63: 864–867.

Thiel G., Kreft M., Zorec R. (1998) Unitary exocytotic and endocytotic events in Zea mays coleoptile protoplasts. Plant J. 13: 117–120.

Thiel G., Kreft M., Zorec R. (2009) Rhythmic kinetics of single fusion and fission in a plant cell protoplast. Ann. N Y Acad. Sci. 1152: 1–6.

Toyooka K., Goto Y., Asatsuma S., Koizumi M., Mitsui T., Matsuokaa K. (2009) A mobile secretory vesicle cluster involved in mass transport from the Golgi to the plant cell exterior. Plant Cell. 21: 1212–1229.

Tse Y.C., Mo B., Hillmer S., Zhao M., Lo S.W., Robinson D.G., Jianga L. (2004) Identification of multivesicular bodies as prevacuolar compartments in Nicotiana tabacum BY-2 cells. Plant Cell. 16: 672–693.

Vardjan N., Stenovec M., Jorgačevski J., Kreft M., and Zorec R. (2007) Elementary properties of spontaneous fusion of peptidergic vesicles: fusion pore gating. J. Physiol. 585: 655–661.

Weise R., Kreft M., Zorec R., Homann U., Thiel G. (2000) Transient and permanent fusion of vesicles in Zea mays coleoptile protoplasts measured in the cell-attached configuration. J. Membrane Biol. 174: 15–20

Chapter 3

3 Insight into the Mechanism of Constitutive Exo- and Endocytosis: Role of PI-3 Kinases and Actin Cytoskeleton

3.1 Abstract

Vesicle trafficking in plants is highly regulated and modulates the kinetic of vesicle fusion and fission according to the requirements of the cell. Each step in the endocytotic and exocytotic pathway like the fusion and fission process is mediated by a complex interaction of many proteins and molecules. The application of inhibitors which interfere with specific steps in the vesicle transport accounted for important findings in function and regulation of trafficking processes. To further analyze the mechanisms of exo- and endocyotis in BY-2 cells I have applied wortmannin, a widely used inhibitor of the endocytic pathway and the cytoskeleton interfering drug cytochalasin D in cell-attached capacitance measurements and confocal microscopy studies. Treatment of cells with wortmannin did not inhibit fission of vesicles from the plasma membrane suggesting a role downstream of vesicle fission. In animal cells the temporary inhibition of cytoskeleton elongation leads to an increase in vesicle fusion. Capacitance measurements on cytochalasin D pre-treated tobacco BY-2 protoplasts reveal no enhanced vesicle fusion. In contrast, the overall probability to detect fusion and fission events was decreased.

3.2 Introduction

Vesicle trafficking pathways are likely to vary according to the requirements of the cell, its environment and stage of development. Each step in the endocytotic and exocytotic pathway is highly regulated and can be the aim of adjustments (Thiel and Battey, 1998).

The final step of exocytosis including docking to the plasma membrane, establishment of fusion pore and full or transient fusion is mediated by a complex interaction of many molecules including SNARE proteins. Also the fission of vesicles from the membrane depends on regulatory proteins like small G proteins, coat proteins and dynamins. One method to understand these complex transport systems is the use of inhibitors which interfere with specific steps of the endo-or exocytic pathway.

Wortmannin is a potent and specific inhibitor of phosphatidylinositol (PI) 3-kinases (Vanhaesebroeck et al., 1997) which play an important role in membrane trafficking processes and are probably involved in vesicle budding and fusion of vesicles with each other. In mammalian and yeast cells it could be shown that PI-3 kinase localizes to multi vesicular bodies (MVB) and endosomes (Gillooly et al., 2000). This would suggest a role for wortmannin at a later stage of the endocytic pathway. One general effect of wortmannin treatment in plant cells seems to be the formation of small vacuoles also known as wortmannin compartments. Electron microscopy studies revealed that these small vacuoles are the result of the fusion of early endosomes (EE) or trans-Golgi network (TGN) with multi vesicular bodies (MVB) which are losing their internal vesicles (Wang et al., 2009). This may in turn lead to the general disruption of the endocytic pathway.

Another tool to investigate details in the transport system is the interference with the cytoskeleton by Cytochalasin D which binds to the growing end of actin and blocks filament elongation (Pollard and Mooseker, 1981).This may than result in the disruption of all processes which are related to the function of the actin cytoskeleton like vesicular trafficking, vesicle fusion to the plasma membrane (Miller et al., 1999) and fission of vesicles from the membrane (Grebe et al., 2003).

In Drosophila synapses it could be shown that vesicles are organized in at least two different vesicle pools. The so called ready-to-release-vesicle pool contains vesicles which undergo continuous recycling. The reserve vesicle pool consists of vesicles which are retained until the ready-to-release vesicle pool needs replenishment due to extensive exocytosis (Kuromi and Kidokoro, 1998). Kuromi and Kidokoro (1998) were able to demonstrate that cells which

were pre-treated with cytochalasin D and washed before measurement, showed transfer of vesicle from the reserve vesicle pool to the ready-to-release-vesicle pool.

In Neuroendocrine cells (chromaffin cells) it could be shown that cross-linked actin filaments at the cell periphery prevent vesicle transport to the exocytotic sites at the plasma membrane (Trifaró et al., 1984). Furthermore, secretion in these cells is accompanied by a local and transient disruption of the cortical actin network (Vitale et al., 1991). This would suggest that the local removal or reorganization of cytoskeleton regulates vesicle fusion.

The existence of at least two different vesicle pools has also been suggested for plant cells (Thiel and Battey, 1998). In addition, treatment of pollen tubes with cytochalasin D implicated that the actin cytoskeleton is involved in transport of vesicles (Picton and Steer, 1981). Also in plant cells the temporary inhibition of cytoskeleton elongation may therefore have a general effect on vesicle fusion.

To further understand the role of PI-3 kinases and the cytoskeleton I have investigated the effect of wortmannin and cytochalasin D on endo- and exocytosis in tobacco BY-2 protoplasts using both confocal microscopy and membrane capacitance measurement.

3.3 Results and Discussion

3.3.1 The Effect of Wortmannin on Vesicle Fission

In recent years wortmannin has been increasingly used as a general inhibitor of endocytosis (Dhonukshe et al., 2006, Emans et al., 2002), even though it still remains unclear which step exactly in endocytois and the endocytic pathway is inhibited by the drug.

In particular, it is not known, as to whether the first step of endocytosis, the fission of vesicles from the plasma membrane is affected by wortmannin. To address this question I have applied capacitance measurements in the cell attached configuration and confocal microscopy in BY-2 protoplasts.

To visualize endocytosis by confocal microscopy BY-2 protoplasts were incubated with the plasma membrane marker FM4-64. The dye is a membrane-selective fluorescent marker which belongs to a class of amphiphilic styryl dyes (Betz et al. 1992, 1996). In water these dyes are almost non fluorescent and only in the presence of membranes the hydrophobic tail intercalates into the bilayer and the fluorescence increases dramatically. Because of their charged head group FM dyes are membrane impermeable. The dye can only be transported into the cell by endocytosis of vesicles of labelled plasma membrane material. Therefore FM dyes are widely used for tracking endocytosis in eukaryotic organisms (Gaffield and Betz, 2006), including plants (Emans et al., 2002, Meckel et al., 2004).

In Figure 15A a BY-2 protoplast which was incubated for 30 min in 10 µM FM4-64 is shown. The uptake of the dye is clearly visible by the labelling of endosomal compartments. Figure 15B shows a protoplast which was pretreated in wortmannin for 30 min. In contrast to control protoplasts almost no FM4-64 is detectable within the cell even after 30 min incubation. However, a ring-like structure appeared just beneath the plasma membrane. Similar ring-like structures labelled by FM4-64 have previously been identified as small vacuoles formed as a reaction to wortmannin treatment (Wang et al., 2009, Tse et al., 2004).

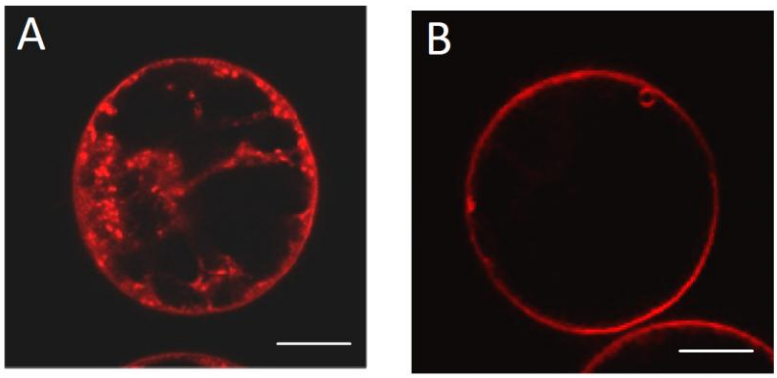

Figure 15: Labelling of the endomembrane system by FM4-64 in the absence and presence of wortmannin. (A) Clear labelling of endosomal compartments after 30 min of incubation with 10 µM FM4-64 is detectable. **(B)** After incubation with 30 µM wortmannin for 30 min almost no dye is visible in the cell and only the formation of the wortmannin compartment could be labelled with 10 µM FM4-64. Scale bar 10 µm.

The reduced internalization of FM dye points to an inhibition of endocytosis by wortmannin. However, fission of vesicles from the plasma membrane must still occur and vesicle transport must be functional at least until vesicles reach the wortmannin compartment. Otherwise the FM dye would not be detectable in the small wortmannin induces vacuole.

To get more detailed information on the effect of wortmannin on the fission of vesicles from the plasma membrane cell-attached capacitance measurements were carried out. One advantage of capacitance measurements in comparison to other methods is the possibility to resolve this very first step of endocytosis, the fision of vesicle from the plasma membrane. This makes the cell-attached capacitance measurement a potent method to study the reaction of plant cells to wortmannin on the level of single vesicles.

In Figure 16 three representative examples of capacitance measurements after 30 min wortmannin treatment are shown. Transient as well as permanent fission of vesicles could be detected. The results clearly demonstrate that vesicles are able to undergo fission even if the PI 3-kinase is blocked by the drug.

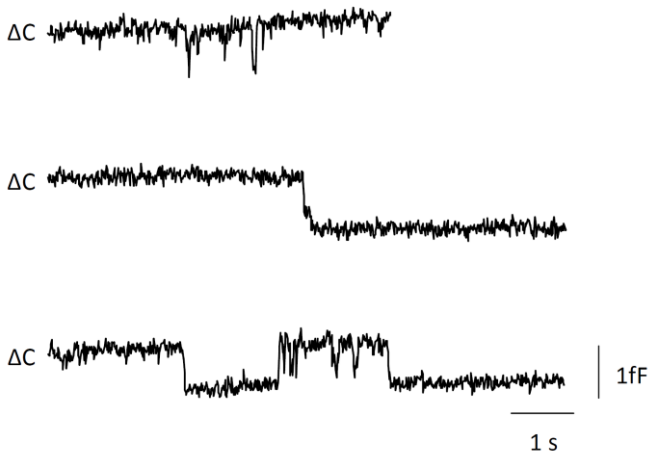

Figure 16: Permanent as well as transient fission occurs in the presence of wortmannin Representative sections from two capacitance measurements after 30 min incubation in 30 µM wortmannin

This implicates that wortmannin does not act on budding of vesicles from the plasma membrane but somewhere downstream of the endocytic pathway. This is in agreement with confocal and electron microscopy studies by Lam et al (2007) who suggested that wortmannin acts downstream of the early endosome by inhibiting the further transport of endocytic vesicles. However, the fact that the first step of endocytosis is not influenced by wortmannin should be kept in mind when using the drug as a general inhibitor of endocytosis.

3.3.2 The Effect of Cytochalasin D on Vesicle Fusion and Fission

Studies from animal cells implicate that inhibition of the actin cytoskeleton by cytochalasin D leads to a shift of vesicles from the reserve pool to the ready-to-release-pool. If such a shift does also occur in BY-2 cells one would expect an increase in vesicle fusion after treatment of cells with cytochalasin D. Such a system with increased rate in vesicle fusion and fission would provide an interesting model system for future studies on the mechanism of exo- and endocytosis.

To investigate the effect of cytochalasin D I have carried out capacitance measurements on protoplasts which were pre-treated with 10 µM cytochalasin D for 30 min and washed before measurements. In Figure 17 the percentage of measurements with and without detectable events from cytochalasin D pre-treated cells are compared with control measurements.

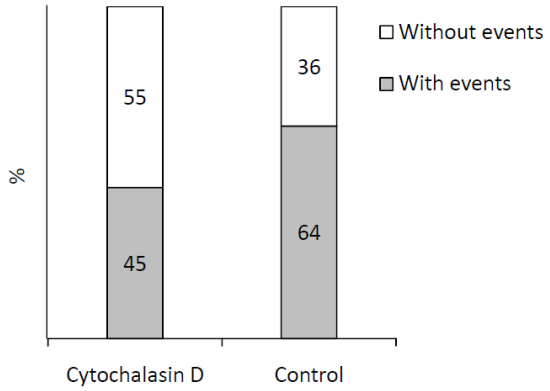

Figure 17: Comparison of measurements from control cells and cytochalasin D pre-treated cells. The percentage of measurements with and without detectable event is shown in grey and white colour, respectively. Data of cytochalasin D pre-treated cells derived from 11 measurements, data of the control from 90 measurements.

Measurements on cytochalasin D pre-treated cells revealed no increase in vesicle fusion and fission. In contrast, the percentage of measurements with detectable events was lower than in control cells. In only 45% of measurements fusion or fission of vesicles could be observed. This suggests that cytochalasin D does not increase exo– or endocytotic activity but may in contrast block fusion and fission of vesicles with the plasma membrane. However, in 2 out of 11 measurements intense transient fusion of vesicles was observed. In Figure 18 three representative sections of these measurements are shown.

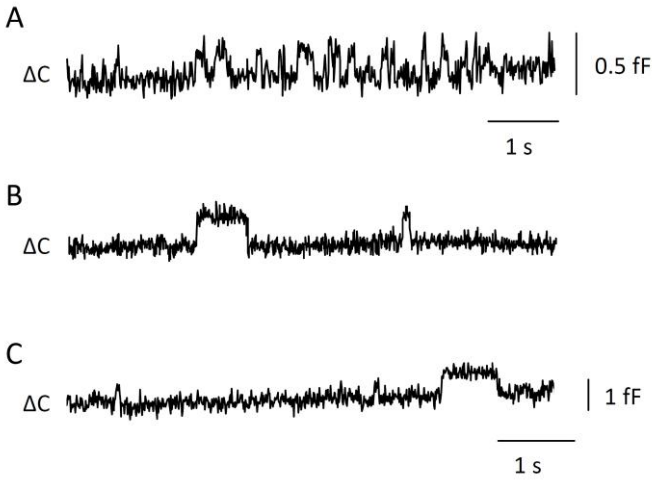

Figure 18: Section of measurement on protoplasts pre-treated with 10 µM cytochalasin D. The measurement in **(A)** shows flickering activity of an exocytotic vesicle. The two sections shown in **(C)** and **(D)** contain transient vesicle fusion.

In the measurement shown in Figure 18A an exocytotic vesicle undergoes transient flickering. In the two sections in Figure 18B and C some transient fusion events were detected. In Figure 18B different dwell times are resolved, in Figure 18C steps with different amplitudes can be seen indicating transient fusion of vesicles with different size.

The intense transient fusion of vesicles detected in two measurements may represent a shift in the relative frequency of the different kinetic modes by cytochalasin D. However, due to the limit number of measurements this hypothesis remains highly speculative.

Besides flickering and transient fusion also permanent fusion and fission were observed in cytochalasin pre-treated cells (Figure 19). This demonstrates that none of the four different kinetic modes of vesicle fusion and fission identified in control cells (see chapter XX) is blocked by the disruption of actin filaments.

Figure 19: Section of measurement on protoplasts pre-treated with 10 µM cytochalasin D.
The measurement shows fusion of a larg vesicle followed by the fission of a smaller one.

On the other hand, cytochalasin clearly reduced the percentage of cells with detectable events. Previous measurements implicated that probability to detect fusion and fission events in the cell-attached configuration may be restricted by the organization of surface area in hot spots for vesicle fusion (compare chapter 2, 2.3.2). If vesicle fusion and fission occur predominantly in hot spots, such a hot spot has to reside under the patch-clamp pipette (tip opening 1 µm in diameter) to observe the events. The fact that in cytochalasin D pre-treated protoplasts less events were detected could point to a reduction or reorganization of hot spots in these cells.

In mammalian cells actin has been suggested to play a role in the organisation of hot spots for endocytosis. In these cells clathrin-mediated endocytosis occurs only in very restricted membrane areas of about 500 - 800 nm in diameter (Gaidarov et al., 1999). These endocytic hot-spots are maintained by the actin cytoskeleton which organizes phosphoinositides which on their part bind to adapter proteins for clathrin coat assembly (Boucrot et al., 2006).

However, if the pre-treatment of cytochalasin D in tobacco BY-2 protoplasts leads to the reorganization of hot spots for vesicle fusion and fission and thus to a decreased detection of events remains to be proven. Also the lack of an adequate stimulus for the fusion of the vesicle from the ready-to-release pool could be an explanation. The fact that the treatment of cells with cytochalasin D has an impact on all cytoskeleton related mechanisms represents an additional difficulty in the interpretation of the results.

3.4 Concluding Remarks

In this chapter the inhibition of the phosphatidylinositol (PI) 3-kinases by wortmannin and the temporary disruption of actin filament elongation by cytochalasin D were studied by confocal microscopy and capacitance measurement. The inhibitory effect of wortmannin on the endocytic pathway was confirmed using FM4-64 as an endocytic marker. The internalization of the dye was almost completely repressed. Only the formation of wortmannin induced small vacuoles just beneath the plasma membrane were detected. Cell-attached capacitance measurements revealed that the fission of vesicles from the plasma membrane was not affected by wortmannin, confirming a role for wortmannin downstream of vesicle fission.

Treatment of BY-2 cells with cytoschalasin D did not lead to an enhancement of vesicle fusion and fission. This suggests that disruption of the actin cytoskeleton did not lead to a shift of vesicles to the ready-to-fuse pool or that an additional stimulus is needed to undergo fusion with the plasma membrane. The observation that the overall probability to detect fusion or fission events was decreased in cytochalasin treated cells may point to an involvement of actin in the organization of hot spot of vesicle fusion and fission in BY-2 cells.

3.5 Materials and Methods

3.5.1 Cell Culture and Protoplast Isolation

Cultivation of BY-2 cells and preparation of protoplasts were carried out as described before (Chapter 2, 2.5.1)

3.5.2 Drug Treatment

For drug treatment experiments, aliquots of wortmannin (Roth Karlsruhe, Germany) and Cytochalsin D (Sigma Hamburg, Germany) solution (stock at 1 mM in DMSO) were added to tobacco BY-2 protoplasts to a final concentration of 30 µM and 10 µM, respectively. Protoplasts were incubated in wortmannin or cytochalasin D for 30 min. Cells treated with Cytochlasin D were washed in wash solution before they were used for capacitance measurements.

3.5.3 Confocal Imaging

BY-2 protoplasts were investigated with a Leica TCS SP spectral confocal microscope (Leica Microsystems). Images were acquired with an HC PL APO CS 20 X / 0.70 objective or HCX PL APO 63×/1.2 w objective. For plasma membrane staining and monitoring of endocytosis protoplasts were incubated in 10 µM FM4-64 (Invitrogen Darmstadt, Germany). FM4-64 was excited with the 488 nm line of a 25 mW argon laser and fluorescence was detected at 630-700 nm. Images were analysed with IMAGEJ software (National Institutes of Health) and Leica Confocal Software 2.00 (LCS, Leica Microsystems).

3.5.4 Electrophysiology

Membrane capacitance measurements were carried out as described before (Bandmann et al., 2010). Protoplasts were bathed in external solution (30 mM $CaCl_2$ 54 mM K-Gluconat 25 mM MES-KOH, pH 5.6 adjusted to 435 mosmol/kg with sorbitol). Patch pipettes were filled with external solution.

Events were analysed by using the cursor option in the software subroutine CellAn Celica, Slovenia) written for MATLAB (MathWorks Inc., Natik, MA, USA). Data were stored in a database (MySQL Community Server 5.1.49, Oracle Redwood Shores USA), calculations were realized by a web-application (CAMMC, yQ-it, Darmstadt, Germany) and results were again stored in the database.

3.6 References

Bandmann V., Kreft M., Homann U. (2010) Modes of Exocytotic and Endocytotic Events in Tobacco BY-2 Protoplasts. Mol Plant 1-11.

Betz W.J., Mao F., Bewick G.S. (1992) Activity-dependent fluorescent staining and destaining of living vertebrate motor nerve terminals. The Journal of neuroscience: the official journal of the Society for Neuroscience 12: 363-75.

Betz W.J., Mao F., Bewick G.S. (1992) Activity-dependent fluorescent staining and destaining of living vertebrate motor nerve terminals. The Journal of neuroscience 12: 363-375.

Boucrot E., Saffarian S., Massol R., Kirchhausen T., Ehrlich M. (2006) Role of lipids and actin in the formation of clathrin-coated pits. Exp Cell Res. 312(20): 4036-48.

Dhonukshe P., Baluska F., Schlicht M., Hlavacka A., Samaj J., Friml J., Gadella T.W. Jr. (2006) Endocytosis of cell surface material mediates cell plate formation during plant cytokinesis. Dev Cell. 10: 137-150.

Emans N., Zimmermann S., Fischer R. (2002) Uptake of a Fluorescent Marker in Plant Cells Is Sensitive to Brefeldin A and Wortmannin. Plant Cell. 14: 71-86.

Gaffield M.A. and Betz W.J. (2006) Imaging synaptic vesicle exocytosis and endocytosis with FM dyes. Nature protocols 1: 2916-2921.

Gaidarov I., Santini F., Warren R.A., Keen J.H. (1999) Spatial control of coated-pit dynamics in living cells. Nat Cell Biol. 1: 1-7.

Gillooly D.J., Morrow I.C., Lindsay M., Gould R., Bryant N.J., Gaullier J.M., Parton R.G., Stenmark H. (2000) Localization of phosphatidylinositol 3-phosphate in yeast and mammalian cells. EMBO J. 19: 4577-4588.

Grebe M., Xu J., Möbius W., Ueda T., Nakano A., Geuze H.J., Rook M.B., Scheres B. (2003) Arabidopsis Sterol Endocytosis Involves Actin-Mediated Trafficking via ARA6-Positive Early Endosomes. Curr Biol. 13: 1378-1387.

Homann U. (1998) Fusion and fission of plasma-membrane material accommodates for osmotically induced changes in the surface area of guard-cell protoplasts. Planta 206: 329-333.

Kumari S., Mg S., Mayor S. (2010) Endocytosis unplugged: multiple ways to enter the cell. Cell Res. 20: 256-275.

Lam S.K., Tse Y.C., Robinson D.G., Jiang L. (2007) Tracking down the elusive early endosome. Trends Plant Sci 12: 497-505.

Meckel T., Gall L., Semrau S., Homann U., Thiel G. (2007) Guard cells elongate: relationship of volume and surface area during stomatal movement. Biophys J. 92: 1072-1080.

Meckel T., Hurst A.C., Thiel G., Homann U. (2004) Endocytosis against high turgor: intact guard cells of Vicia faba constitutively endocytose fluorescently labelled plasma membrane and GFP-tagged K-channel KAT1. Plant J. 39: 182-193.

Miller D.D., Ruijter N.C. A De., Bisseling T., Emons A.M.C. (1999) The role of actin in root hair morphogenesis: studies with lipochito-oligosaccharide as a growth stimulator and cytochalasin as an actin perturbing drug. The Plant J 17: 141-154.

Picton J.M. and Steer M.W. (1981) Determination of secretory vesicle production rates by dictyosomes in pollen tubes of Tradescantia using cytochalasin D. J Cell Sci. 49: 261-272.

Pollard T.D. and Mooseker M.S. (1981) Direct measurement of actin polymerization rate constants by electron microscopy of actin filaments nucleated by isolated microvillus cores. J Cell Biol. 88: 654-659.

Sandvig K., Pust S., Skotland T., Deurs B. van. (2011) Clathrin-independent endocytosis: mechanisms and function. Curr Opin Cell Biol. 23: 413-420.

Thiel G. and Battey N. (1998) Exocytosis in plants. Plant Molecular Biology 38: 111-125.

Thiel G., Rupnik M., Zorec R. (1994) Raising the cytosolic Ca^{2+} concentration increases the membrane capacitance of maize coleoptile protoplasts: Evidence for Ca^{2+} -stimulated exocytosis. Planta 49: 305-308.

Trifaró J.M., Kenigsberg R.L., Côté A., Lee R.W., Hikita H.T. (1984) Adrenal paraneurone contractile proteins and stimulus–secretion coupling. Canadian Journal of Physiology and Pharmacology 62: 493-501

Tse Y.C., Mo B., Hillmer S., Zhao M., Lo S.W., Robinson D.G., Jiang L. (2004) Identification of Multivesicular Bodies as Prevacuolar Compartments in Nicotiana tabacum BY-2 Cells. Plant Cell. 16: 672-693.

Vanhaesebroeck B., Leevers S.J., Panayotou G., Waterfield M.D. (1997) Phosohoinositide 3-kinases: aconserved family of signal transducers. Trends Biochem Sci. 22: 267-272.

Vitale M.L., Castillo A.R.D., Tchakarov L., Process S. (1991) Cortical Filamentous Actin Disassembly and Scinderin Redistribution during Chromatfin Cell Stimulation Precede Exocytosis, A Phenomenon Not Exhibited by Gelsolin. Cell 113: 1057-1067.

Wang J., Cai Y., Miao Y., Lam S.K., Jiang L. (2009) Wortmannin induces homotypic fusion of plant prevacuolar compartments. Journal of experimental botany 60: 3075-3083.

White P.J., Biskup B., Elzenga T.M., Homann U., Thiel G., Wissing F., Maathuis F.J.M. (1999) Advanced patch-clamp techniques and single-channel analysis. J Exp Bot. 50:1037-1054.

Chapter 4

4 Impact of Potential Effectors of Exo- and Endocytosis on Membrane Turnover in BY-2 Cells

4.1 Abstract

In eukaryotic cells the plasma membrane as well as the endomembrane system are highly dynamic structures. In plant cells this becomes particular apparent when looking at the incorporation or removal of membrane material during adaption of cells to different osmotic conditions and the cycling of the auxin efflux carrier PIN1. Both processes have therefore been subject of intensive studies. To gain further insight into the mechanisms underlying these processes I investigated the effect of hypoosmotic treatment and the influence of amphiphilic dyes on exo- and endocytosis in tobacco BY-2 protoplasts and in PIN1 expressing BY-2 cells. Application of confocal microscopy showed a volume increase after hypoosmotic stimulus which was clearly detectable after 20 min. This increase could not be correlated with an increase in vesicle fusion in cell-attached measurements. Only in one patch a fast and direct stimulus response was detectable. Capacitance measurements with the amphiphilic dye FM4-64 revealed no general influence on exo-and exocytosis, neither in wild type BY-2 protoplasts nor in PIN1 expressing cells.

4.2 Introduction

Plant cells are subject to different osmotic conditions. During salt stress or after freezing large changes in osmotic potential can occur. Plants also generate osmotic potentials, using the attendant cell volume changes to do work like moving leaves and regulating gas exchange. The resulting increase or decrease of volume and consequently surface area is associated with the incorporation or removal of membrane material by exo- or endocytosis respectively (Homann, 1998). This process is especially important during opening and closing of guard cells which is accompanied by a change in surface area of about 40 % (Meckel et al., 2007). However, other plant cells as well as animal and yeast are also able to adapt to different osmotic conditions by regulation of their surface area via endo- and exocytosis (Morris and Homann, 2001). To obtain more insight into the mechanisms underlying osmotic driven fusion BY-2 protoplasts were treated with hypoosmotic stimulus and studied using confocal microscopy and cell-attached capacitance measurements.

Additional to the regulation of the surface area exo- and endocytosis are important for controlling the protein as well as the lipid composition of the plasma membrane. The redistribution of plasma membrane proteins from the membrane to EE allows rapid recycling back to the plasma membrane and thus a very dynamic response to external stimuli. In plant cells it could be shown that the polar localization of the auxin efflux carrier PIN1 is maintained by the cycling of the protein (Geldner et al., 2003). The Cycling of PIN1 also accounts for a rapid change in auxin transport polarity as a reaction to changes in light and gravity (Tuvim et al., 2003). Even though it is clear now that PIN1 protein internalization occurs via clathrin coated vesicles (Dhonukshe et al., 2007), the stimulus which induces PIN1 internalization remains to be discovered. Recent studies with different FM dyes revealed that the labelling of the plasma membrane with the dye leads to an increased internalization of PIN1 proteins (Jelínková et al., 2009). Jelínková and co-workers suggested that the intercalation of the lipophilic dye in the membrane may induce a lipid phase segregation which could result in a destabilizing of proteins with specific requirements for lipid environment. To investigate if the internalization of proteins and thus induction of endocytosis is a general effect of FM dyes I carried out capacitance measurements on FM4-64 treated cells. To study the particular effect of FM dyes on the cycling of PIN1 proteins also capacitance measurements on PIN1 expressing cells with FM4-64 were realized.

4.3 Results and Discussion

4.3.1 Hypotonic Treatment of Tobacco BY-2 Protoplasts

To gain further insight into the mechanisms underlying osmotic driven fusion and fission I have studied hypoosmotically treated tobacco BY-2 protoplasts using confocal microscopy and cell-attached capacitance measurements.

To calculate the changes in surface area under hypoosmotic conditions, BY-2 protoplasts were labeled with the plasma membrane marker FM4-64 and the diameter of the protoplasts was measured by taking the distance of the two maxima of an intensity profile before and after changes in osmolarity. Figure 20A shows a protoplast in normal wash solution (left) and after the transfer to a wash solution with a 200 molmol/kg lower osmolarity. After 20 min in hypoosmotic solution the diameter of the cell increased by 5 µm (Figure 20B).

The average increase in protoplasts's diameter in response to hypotonic treatment with -100 mosomol/kg and to -200 mosmol/kg is summarized in Table 2.

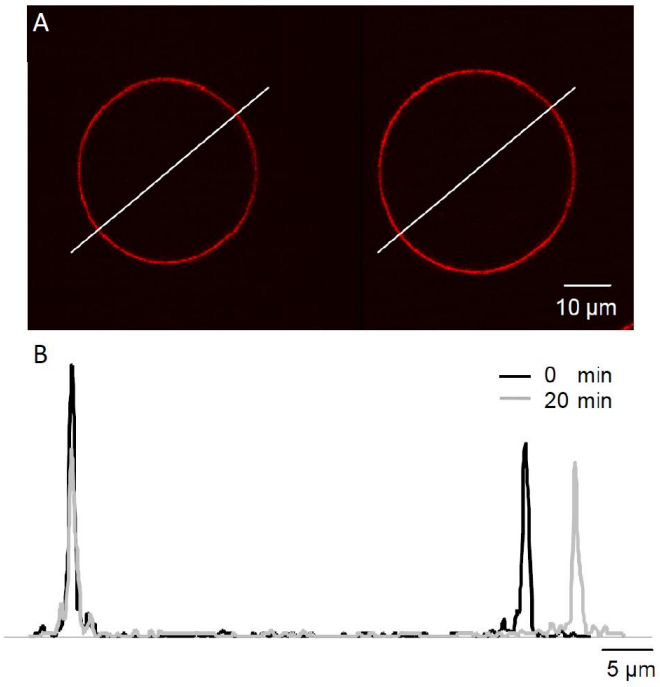

Figure 20: Increase in BY-2 protoplast diameter after transfer to hypotonic media. **(A)** BY-2 protoplasts labelled with 10 µM FM4-64 before (left) and 20 min after (right) transfer to hypotonic media. **(B)**: Intensity profile taken from the white lines indicated in **(A)**.

Table 2: Hypoosmotically induced increase in protoplast diameter. Δ (µm) represents the average change in diameter 15 min after hypoosmotic stimulus. The number of estimated vesicles which can account for the changes in surface area was calculated by assuming a vesicle diameter of 300 nm. Data were taken from 10 measurements at each condition.

Δ (mosmol/kg)	Δ (µm)	Estimated surface area changes (µm^2)	Estimated number of vesicles
0	-0.23 ± 0.13		0
-100	0.86±0.26	3.86 ± 1.56	13.65
-200	3.07±0.41	33.92 ± 7.25	119.95

On average, a stimulus of -200 mosmol/kg results in a surface area increase of 33.92 µm^2. Assuming that vesicles with a diameter of 300 nm fuse to the plasma membrane about 120 vesicles would be needed to account for this enlargement. Hypoosmotic treatment should therefore result in an increase in exocytotic activity. To further analyze the hypoosmotic effect on surface area changes I applied cell-attached membrane capacitance measurements on BY-2 protoplasts. In cell-attached capacitance measurements the exchange of bath solution by a continuous flow results in the loss of a stable measurement configuration. The hypotonic stimulus of -200 mosmol/kg was therefore applied by a second pipette which was brought in direct proximity to the measured protoplasts by a second micromanipulator. To ensure a fast efflux of the solution the tip opening of the second pipette was wider, with a resistance of 1-2 MΩ (normal patch pipette: 4-8 MΩ). By addition of ink to the pipette solution the fast efflux from the pipette was verified.

In 10 measurements single fusion and fission events were recorded after application of hypoosmotic solution. The events could again be grouped into four kinetic modes of vesicle fusion and fission as described before (Chapter 2, 3.2.3). In addition to the four different kinetic modes sections of flickering activity were recorded before and after stimulus appliance. Flickering of endocytotic vesicle (in one measurement before stimulus appliance) and flickering of exocytotic vesicle (in two measurements, one before and one after hypotonic treatment) were taken as transient fission and transient fusion events respectively. The numbers of the four different fusion and fission modes per h are summarized in Table 3.

In Figure 21 the relative frequency of the four kinetic fusion and fission modes are shown before and after the application of the stimulus.

Table 3: Summary of recorded events/h before and after hypoosmotic treatment. Frequency of events were calculated for each measurement and averaged.

	Total recording time (h)	Number of recorded events	Transient fusion/h	Permanent fusion/h	Transient fission/h	Permanent fission/h
Before stimulus	2.91	85	294.16±60.09	197.91±14.74	117.68±22.81	218.40±26.11
After stimulus	1.96	49	111.73±31.14	77.81±6.87	0.00	99.03±7.95

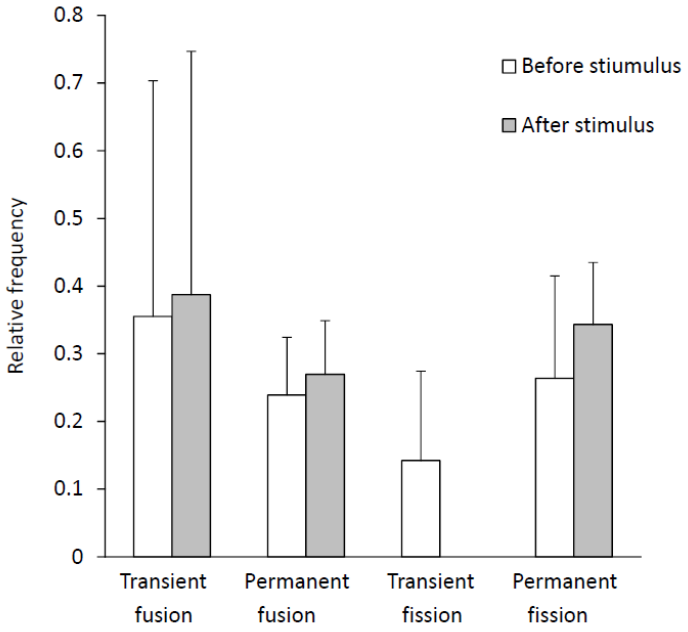

Figure 21: Frequency of fusion and fission events before and after hypoosmotic treatment. Data were taken from 22 measurements. Frequency of events were calculated for each measurement and averaged. Values represent ± SEM.

Apart from the lack of transient fission events there was no significant difference in the distribution of the four kinetic modes of vesicle fusion and fission before and after the application of a hypoosmotic stimulus. In particular, no increase in permanent fusion events which would account for an increase in surface area could be observed.

This may imply that the fusion of small vesicles below the detection limit of the capacitance measurement account for the increase in surface area. However, there is no obvious difference in the distribution of the vesicle size or the median diameter of vesicles (Figure 22) after hypotonic treatment in comparison to control conditions (Figure 22 and Table 4).

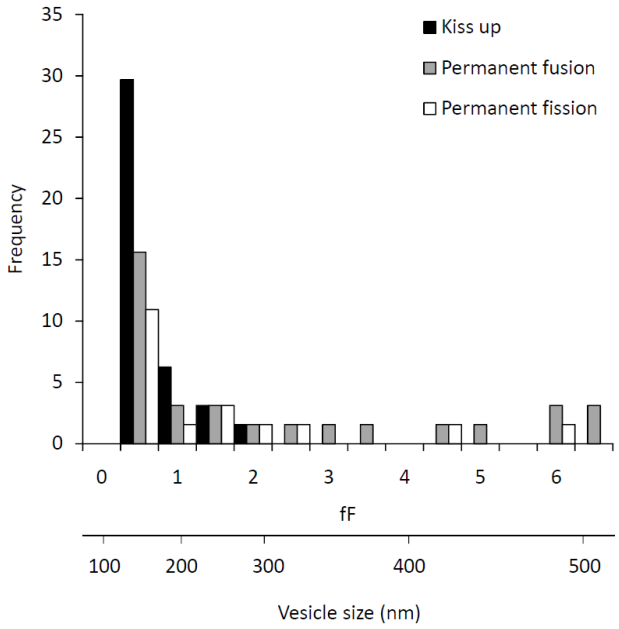

Figure 22: Distribution of vesicle size after stimulus. Size distribution of amplitudes of transient fusion (black, n = 26), permanent fusion (grey, n = 14) and permanent fission (white, n = 24), events collected from 10 patches.

Table 4: Comparison of median diameter of vesicle before and after stimulus appliance.

Median	Transient fusion	Permanent fusion	Permanent fission
Before stimulus	199.64 nm	291.14 nm	130.08 nm
After stimulus	118.18 nm	230.19 nm	191.17 nm

It therefore seems unlikely that very small vesicles account for the predicted surface area increase. Furthermore, measurements on guard cell protoplasts revealed vesicles of around 300 nm in diameter after hypoosmotic stress (Homann and Thiel, 1999).

An alternative explanation for the absence of an increase in permanent vesicle fusion as a response to the hypoosmotic stimulus arises from the concept of hot spots for vesicle fusion. If vesicle fusion occurs only in a locally restricted area of the cell surface this hot spot has to reside under the patch-clamp pipette in order to allow detection of these events. This hypothesis is supported by the measurements shown in Figure 23.

In this measurement successive upward steps resulting from permanent fusion events were detected 18 s after the hypoosmotic stimulus was applied. This implicates a very fast response to hypoosmotic condition. Such a fast response may imply the presence of a “ready-to-release vesicle pool.” The existence of such a vesicle reservoir which allows the cell to react very fast

to different environmental stimuli could be shown in maize coleoptile protoplasts. (Thiel et al., 1994).

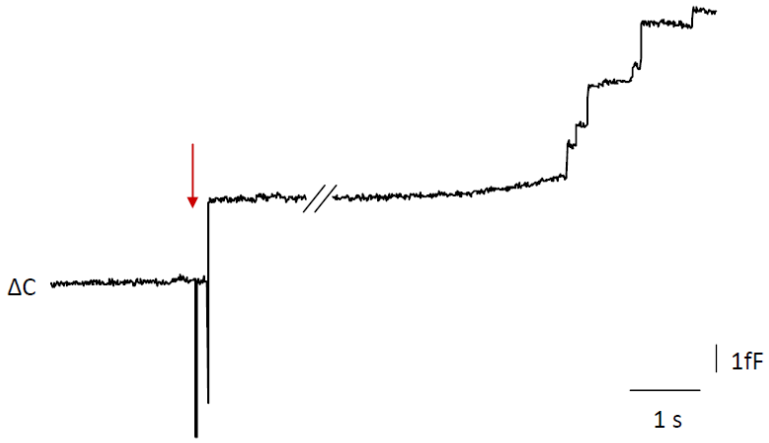

Figure 23: Permanent fusion events after hypootonic stimulus. Successive permanent fusion events were recorded 18 s after application of a hypoosmotic stimulus of 200 mosmol/kg (red arrow).

From the confocal microscopy analysis an average surface area increase of 33.92 µm^2 was estimated for a hypoosmotic stimulus of 200 mosmol/kg. From the size of the capacitance steps in Fig. 8 the diameter and thus surface area of the exocytotic vesicles can be estimated. The fusion of the six exocytotic vesicles shown in the recording did therefore result in a surface area increase of 8.07 µm^2 which accounts for 24 % of the predicted surface area increase. Assuming a protoplast diameter of 30 µm the membrane patch under the patch clamp pipette reflects only 0.12 % of the protoplasts surface area. This suggests that a large part of the vesicles which are needed for the surface area increase, fuse in a locally defined area. The results therefore support the hypothesis that vesicle fusion and fission in BY-2 cells is organized in hot spots (see also chapter 2, 3.2.3 and chapter 3, 3.2.2). Hot spot of vesicle fusion and fission have also been described in mammalian cells. In baby hamster kidney (BHK cells) cells the organization lipid domains in the plasma membrane were found to be responsible for the induction of endocytosis (Hilgemann and Fine, 2011). The observation of clathrin coated pits in mammalian cells which exist for an extended period on the plasma membrane prior to endocytosis (Rappoport et al., 2003) may also represent a form of hot spot for vesicle trafficking.

Under control conditions fusion and fission of vesicles could be recorded in slightly more than half of the patches which led to the assumption that the density of hot spots is relatively high. Also after the application of a hypoosmotic stimulus events could be detected in 10 out of 22 measurements. The fact that only in one measurement a fast increase in vesicle fusion was observed may point to another subdivision in surface area. One may speculate that the surface area increase under hypoosmotic conditions is achieved by the fusion of vesicles from a ready-to-release vesicle pool. The fusion of these vesicles may occur in a locally restricted area which is probably determined by the localization of the ready-to-release vesicle pool and is different from the hot spots of exo- and endocytosis which serves normal housekeeping functions. Therefore, the detection of stimulus response in the cell-attached configuration may be restricted by the probability to hit the area where vesicles from the ready-to-release pool fuse to the plasma membrane.

4.3.2 Capacitance Measurements on PIN1 Expressing Cells Treated with FM4-64

For cells which stably express the auxin efflux carrier PIN1-GFP (Benkova et al., 2003) it was postulated that FM dyes induce endocytosis of proteins (Jelinkova et al., 2010).

To test if the induction of endocytosis by FM dyes represents a general stimulus for protein internalization, membrane capacitance measurements with 10 µM FM4-64 in the patch pipette were carried out either on WT tobacco BY-2 protoplasts or on PIN1-GFP expressing BY-2 cells. In Figure 24 the distribution of the four fusion and fission modes recorded from WT BY-2 protoplasts are shown. Eleven measurements were carried out with FM4-64 in the pipette solution and the relative frequency of each event was calculated. In comparison to the frequency of events under control conditions, endocytosis is not enhanced by FM 4-64. The frequency of transient fission as well as permanent vesicle fission is at the same level as in control measurements. Also the frequency of permanent vesicle fusion is not affected. The only difference in comparison to control conditions is the reduction of transient vesicle fusion.

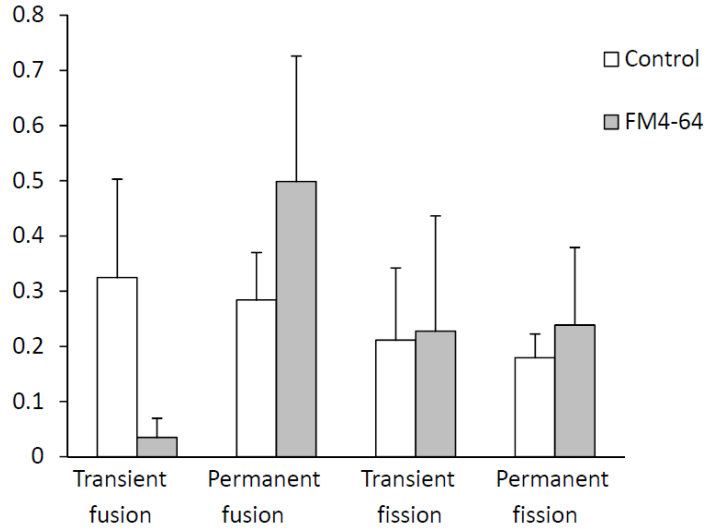

Figure 24: Frequency of fusion and fission events recorded on WT BY-2 protoplasts. Data were taken from 11 measurements. Frequency of events were calculated for each measurement and averaged. Values represent ± SEM.

Taken together these measurements revealed no effect of FM4-64 on vesicle fission. This seems to be in contrast to observations by Jelinkova and colleagues who showed the fast internalization of membrane proteins after FM 4-64 treatment.

However, the dye may only interfere specifically with the endocytosis of membrane proteins which cycle between endosomal compartments and the plasma membrane, like PIN1 proteins. The polar localization of the auxin carrier PIN1 is believed to be maintained by rapid clathrin-dependent cycling between the plasma membrane and EE (Geldner et al., 2001, Dhonukshe et al., 2007). I therefore analysed the effect of FM4-64 in cell-attched capacitance measurements on PIN1 expressing BY-2 protoplasts. In Figure 25 the frequency of events from measurements on PIN1 expressing cells with FM4-64 is compared to measurements which were carried out under control conditions.

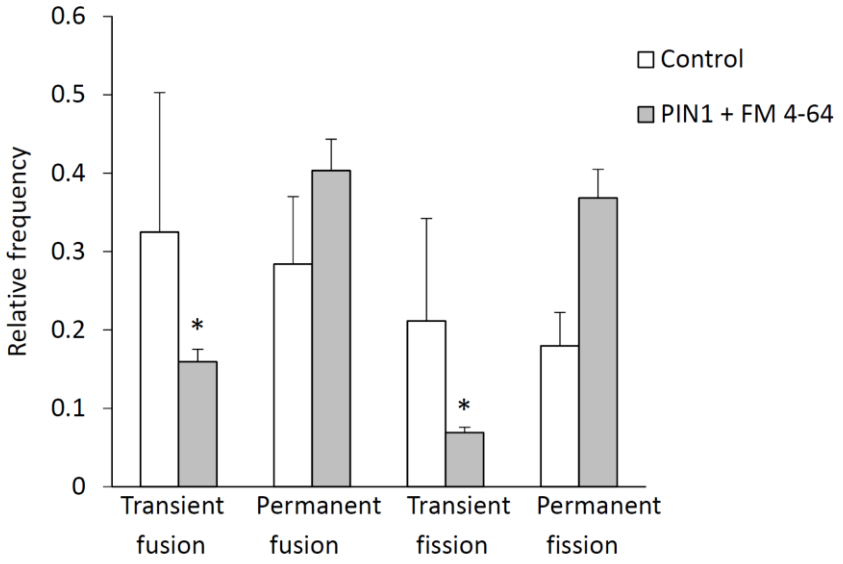

Figure 25: Frequency of fusion and fission events. Data of PIN1 + FM4-64 measurements derived from 13 measurements. Frequency of events were calculated for each measurement and averaged. Data were analyzed using a student's t-test. Significant differences are indicated by asterisk. Values represent ± SEM

In comparison to control measurements the measurements on PIN1 protoplasts showed a significant reduction in transient fusion and fission events. Permanent endocytosis is not significantly increased compared to the control measurements but the frequency of permanent endocytosis (36.83 %) and permanent exocytosis (40.32 %) is almost at the same level. The cycling of PIN1 between the membrane and endosomal compartments is still functional in BY-2 protoplasts (Dhonukshe et al., 2007). Therefore, the reduction of transient events and the equal frequency of permanent exo- and endocytosis most likely reflect the cycling of PIN1 proteins.

In contrast to Jelinkova and colleagues (Jelinkova et al., 2010) an effect of FM4-64 on the internalization of PIN1 proteins could not be confirmed in cell-attached membrane capacitance measurements.

4.4 Concluding Remarks

Hypoosmotic treatment of BY-2 protoplasts led to a volume increase which was clearly detectable after 20 min by confocal microscopy analyses. However, this increase in volume could not be correlated to an increase in vesicle fusion monitored by capacitance measurements. In only one out of 22 measurements a fast and direct stimulus response was detectable. From the short response time between stimulus application and vesicle fusion it can be deduced that vesicles are derived from a ready-to-release vesicle pool. The detection of these events in the cell-attached configuration is therefore most likely restricted by the probability to hit the area where vesicles from the ready-to-release pool fuse to the plasma membrane.

Cell-attached capacitance measurements on wild type BY-2 protoplasts and on PIN1 expressing cells did not reveal any effect of FM4-64 on endocytosis or on the internalization of PIN1 proteins. In PIN1 expressing cells the reduction of transient events and the equal frequency of permanent endo-and exocytosis most likely represent the cycling of the proteins.

4.5 Materials and Methods

4.5.1 Cell Culture and Protoplast Isolation

Wild type BY-2 cells and PIN1 expressing cells were cultured as described before (Chapter 2, 2.5.1). For the selection of PIN1 expressing cells the culture medium was supplemented with kanamycin (100 mg/l).

4.5.2 Confocal Imaging

Confocal imaging of BY-2 protoplasts was carried out as described in Chapter 3, 3.5.3.

4.5.3 Electrophysiology

Membrane capacitance measurements were carried out as described before (Bandmann et al., 2010). The signal to noise ratio was optimized in comparison to previous measurements (Bandmann et al., 2010). The background noise was reduced from 0.13-0.5 fF to 0.11-0.25 fF allowing to detect vesicles as small as 70 nm. Therefore the calculated median of vesicle diameter is smaller than in previous studies. From the vesicle capacitance C_v the surface area (A) and thus the diameter of vesicles could be calculated according to $C_v = c * A$ whereby c is the specific membrane capacitance (8 mF/m^2) determined for the plasma membrane of plant cells (White et al., 1999).

4.6 References

Bandmann V., Kreft M., Homann U. (2010) Modes of Exocytotic and Endocytotic Events in Tobacco BY-2 Protoplasts. Mol Plant 1-11.

Benková E., Michniewicz M., Sauer M., Teichmann T., Seifertová D., Jürgens G., Friml J. (2003) Local, efflux-dependent auxin gradients as a common module for plant organ formation. Cell 115: 591-602.

Dhonukshe P., Aniento F., Hwang I., Robinson D.G., Mravec J., Stierhof Y.D., Friml J. (2007) Clathrin-mediated constitutive endocytosis of PIN auxin efflux carriers in Arabidopsis. Curr. Biol. 17: 520-527.

Geldner N., Anders N., Wolters H., Keicher J., Kornberger W., Muller P., Delbarre A., Ueda T., Nakano A., Jürgens G. (2003) The Arabidopsis GNOM ARF-GEF Mediates Endosomal Recycling, Auxin Transport, and Auxin-Dependent Plant Growth. Cell 112: 219-230.

Geldner N., Friml J., Stierhof Y.D., Jürgens G., Palme K. (2001) Auxin transport inhibitors block PIN1 cycling and vesicle trafficking. Nature 413: 425-428.

Hilgemann D.W. and Fine M. (2011) Mechanistic analysis of massive endocytosis in relation to functionally defined surface membrane domains. J Gen Physiol. 2 137: 155-172.

Homann U. (1998) Fusion and fission of plasma-membrane material accommodates for osmotically induced changes in the surface area of guard-cell protoplasts. Planta 206: 329-333.

Homann U. and Thiel G. (1999) Unitary exocytotic and endocytotic events in guard-cell protoplasts during osmotically driven volume changes. FEBS Letters 460: 495-499.

Jelínková A., Malínská K., Simon S., Kleine-Vehn J., Parezová M., Pejchar P., Kubes M., Martinec J., Friml J., Zazímalová E., Petrásek J. (2010) Probing plant membranes with FM dyes: tracking, dragging or blocking? Plant J. 61: 883-892.

Jorgačevski J., Stenovec M., Kreft M., Bajic A., Rituper B., Vardjan N., Stojilkovic S., Zorec R. (2008) Hypotonicity and peptide discharge from a single vesicle. Am. J. Physiol. Cell Physiol. 295: C624–C631.

Meckel T., Gall L., Semrau S., Homann U., Thiel G. (2007) Guard cells elongate: relationship of volume and surface area during stomatal movement. Biophys J. 92: 1072-1080.

Morris C.E. and Homann U. (2001) Cell surface area regulation and membrane tension. J Membr Biol 179(2): 79-102.

Muday G.K., Peer W.A., Murphy A.S. (2003) Vesicular cycling mechanisms that control auxin transport polarity. Trends Plant Sci 8: 301-304.

Rappoport J.Z., Taha B.W., Simon S.M. (2003) Movement of plasma-membrane-associated clathrin spots along the microtubule cytoskeleton. Traffic 4: 460-467.

Thiel G., Rupnik M., Zorec R. (1994) Raising the cytosolic Ca^{2+} concentration increases the membrane capacitance of maize coleoptile protoplasts: Evidence for Ca^{2+} -stimulated exocytosis. Planta 49: 305-308.

Tuvim M.J., Adachi R., Hoffenberg S., Dickey B.F. (2001) Traffic control: Rab GTPases and the regulation of interorganellar transport. News Physiol Sci. 16: 56-61.

White P.J., Biskup B., Elzenga T.M., Homann U., Thiel G., Wissing F., Maathuis F.J.M. (1999) Advanced patch-clamp techniques and single-channel analysis. J Exp Bot. 50:1037-1054.

Chapter 5

5 Clathrin-Independent Endocytosis Contributes to Uptake of Glucose into BY-2 Protoplasts

5.1 Abstract

In eukaryotic cells several pathways for the internalization of plasma membrane proteins and extracellular cargo molecules exist. These endocytic pathways can be grouped into clathrin-dependent and clathrin-independent endocytosis. While the former one has been described to be involved in a variety of cellular processes in plants, the latter one has so far only been identified in animal and yeast cells. In this study it could be shown that the internalization of fluorescent glucose into BY-2 cells leads to an accumulation of the sugar into the compartments of the endocytic pathway. This endocytic uptake of glucose was not blocked by ikarugamycin (IKA), an inhibitor of clathrin-dependent endocytosis, suggesting a role for clathrin-independent endocytosis in glucose uptake. Investigations of fusion and fission of single vesicles by membrane capacitance measurements revealed a stimulation of endocytic activity by extracellular glucose. Glucose stimulated fission of vesicles was not affected by addition of IKA or block of clathrin coat formation by transient over-expression HUB1 (C-terminal part of the clathrin heavy chain). These data demonstrate that clathrin-independent endocytosis does exist in plant cells. Furthermore, the uptake of glucose into non-differentiated cells, such as BY-2 cells, implies that this pathway represents a common mechanism for the uptake of external nutrients. Clathrin-independent endocytosis may thus be of general importance in plant cell physiology.

5.2 Introduction

Endocytosis is essential for many cellular processes such as protein transport, membrane recycling, cell signalling, receptor functioning and uptake of external solutes. In yeast and animal cells diverse endocytic mechanisms which are needed to fulfil this wide range of physiological different requirements have emerged. Among these different pathways clathrin-dependent endocytic is best characterized. It depends on coat formation mediated by the clathrin lattice. In addition, a variety of endocytic pathways which do not involve clathrin have been described in animal cells (Mayor and Pagano, 2007). In recent years these clathrin-independent pathways have attracted increasing attention as their important role in cellular processes such as polarization, motility, regulation of signalling and normal cell growth became evident (Sandvig et al., 2011). Although there are some indications of clathrin-independent endocytosis in plants (Moscatelli et al., 2007, Onelli et al., 2008), direct evidence for such a pathway is still missing and its molecular characteristics and physiological importance are still unknown.

A candidate for a physiological process that relies on clathrin-independent endocytosis, is fluid-phase endocytosis which is involved in the uptake of assimilates (Baluska et al., 2004, Etxeberria et al., 2005) but does also occur constitutively in plant cells (Gall et al., 2010). In animal cells the uptake of external solutes, including nutrients via fluid-phase endocytosis has been associated with clathrin-independent endocytosis (Damke et al., 1995, Sandvig and Deurs, 2005, Hansen and Nichols, 2009). However, there is no information on the mechanism of fluid-phase endocytosis in plants.

To fill this gap endocytic uptake of glucose in BY-2 cells was analysed using fluorescent microscopy and membrane capacitance measurements. Uptake of a fluorescent glucose derivative into BY-2 cells was not affected by treatment of cells with ikarugamycin (IKA), a potent inhibitor of clathrin-mediated endocytosis. This points to a role of clathrin-independent endocytosis in the internalization of glucose. The results from membrane capacitance measurements revealed an upregulation of the formation of endocytic vesicles in the presence of glucose. Again, this process was not blocked by IKA or overexpression of HUB1 (C-terminal part of the clathrin heavy chain). Together the results imply that fluid-phase endocytosis can be stimulated by external nutrients and does not rely on clathrin coat formation but on clathrin-independent fission of vesicles.

5.3 Results and Discussion

5.3.1 Endocytic Uptake of Hexose in BY-2 Protoplasts

Previous studies assumed endocytic uptake of glucose and sucrose into heterotrophic cells (Etxeberria et al., 2005, Baroja-Fernandez et al., 2006, Etxeberria et al., 2005). This process can be classified as fluid-phase endocytosis and plays an important physiological role in sugar storage (Baroja-Fernandez et al., 2006). Etxeberria et al. (Etxeberria et al., 2005) suggested that immediately needed hexose for the cytosolic metabolism is transported through plasma membrane bound carriers into the cytosol while reserve hexose is transported in bulk into the vacuole by endocytosis. Endocytic uptake of hexose bypasses the cytosol and does not disrupt the highly regulated cytosolic compositions by fluctuating sucrose concentrations. A similar mechanism has also been suggested for the transport of NaCl to the vacuole under high salt conditions (Mazel et al., 2004). Uptake of nutrients and extracellular compounds via fluid-phase endocytosis is thus most likely of general physiological importance in plant cells.

However, the molecular components of this endocytic pathway have not yet been determined. To test whether BY-protoplasts provide a suitable model system for studying the mechanisms of fluid-phase endocytosis the uptake of hexose was analysed using the non-metabolizable glucose derivative 2-NBDG (2-(N-(7-nitrobenz-2-oxa-1,3-diazol-4-yl)amino)-2-deoxyglucose) in BY-2 protoplasts. 2-NBDG is a fluorescent form of deoxyglycose; its non-metabolizable nature allows to detect the dynamics of uptake and accumulation inside cells.

Uptake of 2-NBDG into BY-2 protoplasts was monitored either on protoplasts isolated from cells kept in culture medium or from cells which were incubated in a glucose free medium for at least 8 h. Under both conditions 2-NBDG accumulated inside protoplasts; there was no appreciable difference between glucose starved (Figure 26A) and normal protoplasts (Figure 26B and C).

In all cells the fluorescent signal was visible inside the cytosol in form of bright spots (Figure 26A – C). In addition, most cells also showed a diffuse distribution of 2-NBDG in the cytosol (Figure 26A and B) and inside the vacuole (Figure 26C).

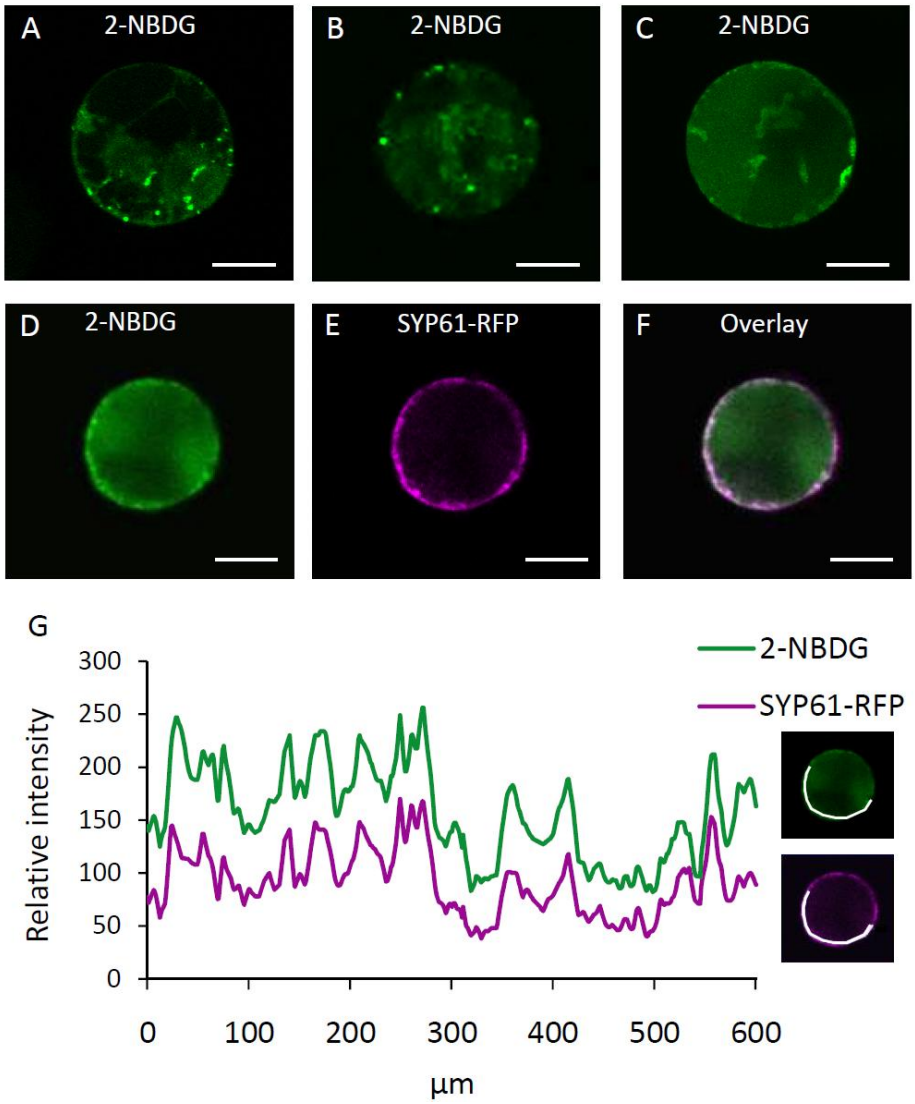

Figure 26: 2-NBDG localizes to endosomal compartments in BY-2 protoplasts (A-C): Fluorescent images of BY-2 cells 1 hour after incubation in 5 mM 2-NBDG. 2-NBDG accumulated in bright spots in the cytosol and inside the vacuole in BY-2 protoplasts from glucose starved cells **(A)** and protoplasts isolated from normal cultured cells **(B** and **C)**. **(D-F)**: 2-NBDG uptake in BY-2 cells expressing the TGN marker SYP61-RFP. 2-NBDG accumulated in bright spots in the cytosol and inside the vacuole **(D)**. SYP61-RFP was visible in small compartments in the cytosol **(E)**. The 2-NBDG signal (green) partially co-localizes with the TGN marker SYP61-RFP (magenta) **(F)**. Co-localisation is indicated by white color. **(G)**: Intensity profile of 2-NBDG (green) and SYP61-RFP (magenta) taken from the white line as indicated. Scale bars: 10 µm

The uptake of hexose but also of deoxyglucose can in principle occur either by plasma-membrane bound carriers (Büttner and Sauer, 2000, Oliveira et al., 2002) or via endocytosis (Etxeberria et al., 2005). While carrier mediated internalization of glucose leads to a distribution of glucose in the cytosol, endocytic uptake of hexose results in an accumulation

of the sugar in endocytic vesicles and compartments of the endocytic pathway. The diffuse fluorescence found in the cytosol of BY-2 cells incubated in 2-NBDG may thus result from cytosolic 2-NBDG, which has been transported across the plasma membrane via a carrier mediated mechanism. In addtion, 2-NBDG containing endocytic vesicles, which are too small to be resolved by confocal microscopy, may also contribute to the diffuse background labelling. These vesicles should follow the endocytic pathway leading to accumulation of fluorescence in endosomal compartments such as the early endosome (EE), the trans-golgi network (TGN), multivesicular bodies (MVB) and vacuoles. To determine whether the bright fluorescent spots observed in BY-2 protoplasts correspond to compartments of the endocytic pathway, protoplasts were transiently transfected with SYP61-RFP, a marker of the TGN (Cai et al., 2010). Transfected protoplasts showed numerous spots labelled by SYP61-RFP (Figure 26E). After incubation of these protoplasts in 2-NBDG a clear co-localization was found of compartments labelled by 2-NBDG and SYP61-RFP (Figure 26F). The apparent colocalization is furthermore confirmed by the correlation of the peaks of a fluorescent intensity profile (Figure 26G) taken from the white line in Figure 26G. The results of these experiments imply that internalized 2-NBDG accumulates partly in the TGN. The accumulation of 2-NBDG in compartments of the endocytic pathway confirms that endocytosis is indeed involved in the uptake of hexose into BY-2 cells. BY-2 cells thus provide a suitable model system to study the mechanisms of fluid-phase endocytosis.

5.3.2 Inhibition of Clathrin does not Affect Endocytic Uptake of Hexose

Studies on endocytosis in animal cells suggest that uptake of solutes via fluid-phase endocytosis occurs via a clathrin independent mechanism (Doherty and McMahon, 2009). To investigate the role of clathrin in the endocytic uptake of hexose into BY-2 cells ikarugamycin (IKA) was applied, a strong and specific inhibitor of clathrin-mediated endocytosis in plant and animal cells (Luo et al., 2001, Moscatelli et al., 2007, Onelli et al., 2008). First the effect of IKA on endocytosis of the plasma membrane marker FM4-64 was analysed. Previous investigations on FM4-64 demonstrated that the internalization of the dye is mainly mediated by clathrin-dependent endocytosis (Dhonukshe et al., 2007). Uptake of FM4-64 was observed in IKA treated and control BY-2 protoplasts over a period of one hour. In control protoplasts a strong labelling of the endomembrane system by FM4-64 was already visible after 10

minutes (Figure 27A, upper row). In contrast, IKA treated cells showed almost no FM4-64 uptake. Even after 60 minutes only a week FM4-64 labelling was visible inside the cell (Figure 27A, lower row).

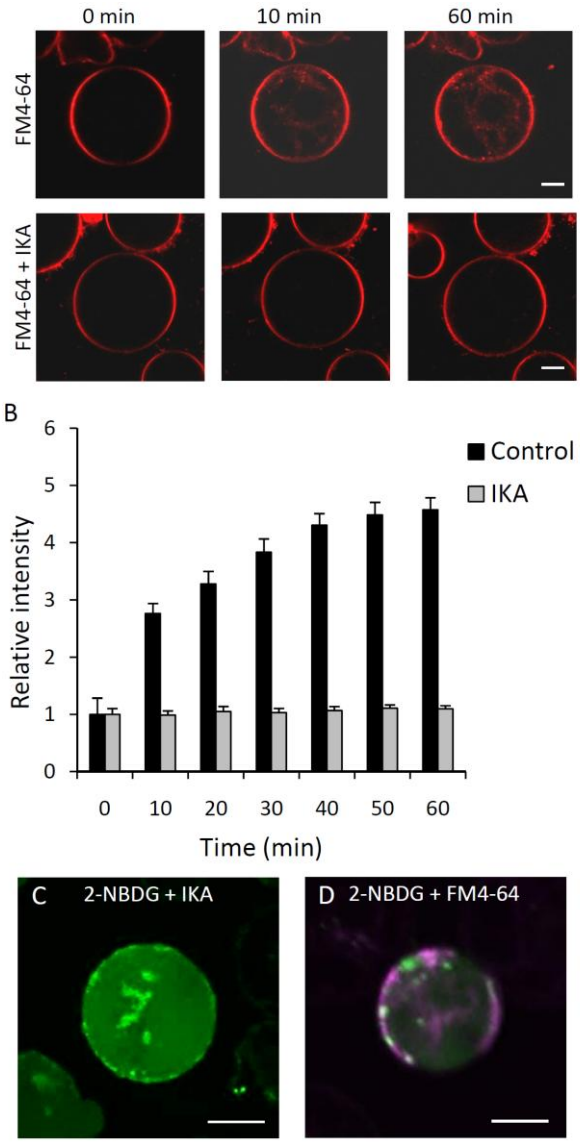

Figure 27: Inhibition of clathrin-mediated endocytosis by IKA blocks internalization of FM4-64 but not endocytic uptake of 2-NBDG. (A): Time series of BY-2 protoplasts incubated in 10 µM FM4-64. Under control conditions FM4-64 uptake was visible within 10 minutes (upper row). No FM4-64 uptake was detectable in protoplasts incubated in 10 µM IKA for 30 min before addition of the dye (lower row). **(B)**: Quantification of FM4-64 uptake. The relative fluorescence intensity is given as the ratio of intracellular fluorescence to whole-cell fluorescence. The value at time zero was set to 1. **(C)**: Protoplasts treated with 10 µM IKA for 30 min before incubation in 2-NBDG. 2-NBDG still accumulated in bright spots within the cell. **(D)**: Protoplasts incubated in 5mM 2-NBDG and 10 µM FM4-64 for 1 h. Overlay of the 2-NBDG signal (green) and FM4-64 (magenta) showed only partial co-localization. Scale bars: 10 µm.

For quantification of endocytosis the ratio of intracellular (membrane) fluorescence versus whole-cell fluorescence was estimated over time. The ratio at time zero was set to 1. A fast increase of the relative fluorescence in control protoplasts reflects rapid endocytosis of the dye (Figure 27B). In protoplasts incubated in 10 µM IKA for 30 min the relative fluorescence barely changed over time demonstrating that endocytosis of FM4-64 is strongly inhibited by IKA. Our results thus confirm the inhibitory effect of IKA on clathrin-dependent endocytosis also in BY-2 cells. Next the effect of IKA on the internalization of the glucose derivative 2-NBDG was analysed. Figure 27C shows a representative example of a BY-2 protoplast treated with IKA for 30 min before incubation in 2-NBDG. The fluorescent glucose derivative still accumulated inside the cell and in endosomal compartments. No difference was found in the uptake of 2-NBDG between IKA treated and non-treated cells demonstrating that endocytic uptake of hexose is not inhibited by IKA. In addition, co-localization of FM4-64 and 2-NBDG revealed that only a few spots were marked by both, 2-NBDG and FM4-64 (Figure 27D). This suggests that different endocytic pathways are involved in the uptake of hexose and internalization, of FM4-64. Together the results of these experiments imply that endocytic uptake of hexose into BY-2 protoplasts occurs via a clathrin-independent mechanism.

Furthermore, the accumulation of 2-NBDG in the TGN shows that clathrin-independent fluid-phase endocytosis follows at least partly the pathway described for clathrin-mediated endocytosis. This suggests that clathrin-independent and clathrin-mediated endocytosis intersect at the TGN in plant cells as they do in animal cells (Gruenberg, 2001). The TGN thus seems to operate as a sorting station also for external solutes dedicated to the vacuole which underlines the central role of the TGN in sorting of vesicle mediated transport.

5.3.3 Endocytic Events are Highly Upregulated by Glucose

To further analyze the mechanism of endocytic glucose uptake membrane capacitance measurements were performed in the cell-attached mode on BY-2 protoplasts. This technique allowed us to monitor the very first step of the endocytic pathway, the fission of vesicles from the plasma membrane, in real time. Previous measurements on BY-2 protoplasts revealed spontaneous upward and downward steps in membrane capacitance (C_m), which reflected exo- and endocytosis, respectively, of single vesicles (Hong et al., 2003). The recorded

changes in C_m could be grouped into four different categories according to their different kinetics: i) transient fusion of exocytotic vesicles, ii) transient fission of endocytotic vesicle, iii) permanent fusion and iv) permanent fission of single vesicles. Under control conditions the number of fusion events was slightly higher than the number of fission events (Table 5). In the presence of glucose the picture changed completely. With 244 mM glucose in the patch-pipette the number of fusion events and the number of transient fission events largely decreased whereas the frequency of permanent endocytic events increased fourfold (Table 5).

Table 5: Summary of recorded events, measurements +/- events gives the number of measurements with (+) and without (-) fusion or fission events. Fusion and fission events/h represent the average of the frequency of events calculated for each measurement. For control measurements calculation is based on recordings which have been published (Bandmann et al., 2010). Values are presented ± SEM.

	Total recording time (h)	measurements +/- events	Transient fusion/h	Permanent fusion/h	Transient fission/h	Permanent fission/h
Control	21.13	32/58	10.48 ± 5.75	9.17 ± 2.78	6.83 ± 4.22	5.80 ± 1.38
Glucose	3.29	9/3	3.67 ± 2.04	7.46 ± 1.76	6.50 ± 4.26	1.75 ± 0.78
IKA	5.36	14/5	2.43 ± 2.42	0.84 ± 0.57	17.81 ± 0.58	17.81 ± 6.51
Glucose+IKA	2.68	9/1	3.30 ± 2.10	2.64 ± 0.87	3.60 ± 1.86	11.54 ± 2.91
Glucose+HUB1	2.91	8/5	1.45 ± 0.93	0.92 ± 0.71	0.00	6.82 ± 2.25

This glucose-stimulated increase in permanent endocytic activity becomes even more obvious when looking at the frequency of this event normalized to the overall number of events (Figure 28). Under control condition permanent endocytic events were recorded at a relative frequency of only 18 %. With glucose the relative frequency of permanent endocytic events increased to 73 % (Figure 28).

Figure 29 shows a representative example of a capacitance measurement in the presence of glucose. Often several downward steps reflecting successive fission of single vesicles could be resolved. The capacitance measurements thus demonstrate that glucose is able to stimulate endocytic activity in BY-2 protoplasts. This process is most likely responsible for the endocytic uptake of hexose described above. It implicates the existence of an extracellular hexose sensor which is involved in the up-regulation of endocytosis. Furthermore, as glucose was only added to the pipette solution the sensing of glucose was restricted to the small area of the plasma membrane under the patch pipette (about 1 μm^2). The ability of the cell to respond to this local increase in glucose suggests that sensing of glucose and stimulation of endocytosis are locally coupled. Members of the plant sugar transporter family have been proposed to play a direct role in the signal transduction responsible for the regulation of sugar

transport (Lalonde et al., 1999). If these transporters are also involved in the regulation of endocytic sugar uptake remains to be shown.

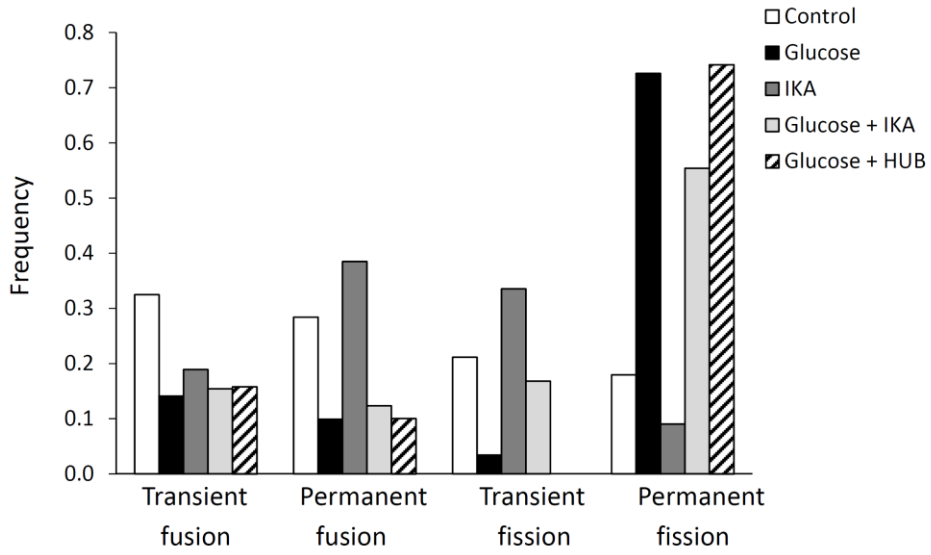

Figure 28: Permanent endocytosis is highly upregulated in the presence of glucose Relative frequency of the different kinetic modes of exo- and endocytic events given in number of events per hour recording time in relation to all events per hour (set to 100%). Measurements were carried out under different conditions as indicated beside the graph. Values are presented ± SEM.

As demonstrated above, uptake of hexose into BY-2 cells was found to be clathrin-independent. Consequently, glucose stimulated endocytosis should also not depend on clathrin coat formation. To test this hypothesis the effect of IKA on the frequency of fusion and fission events in BY-2 protoplasts in the absence and presence of glucose was analyzed. Incubation of protoplasts in IKA led to small changes in the relative frequency of both, fusion and fission events (Figure 28). The number of permanent fusion events as well as the number of transient fission events slightly increased, whereas the relative frequency of transient exocytosis and permanent endocytosis was decreased in IKA treated cells. Next it was analyzed whether stimulation of endocytosis by glucose is influenced by IKA. Figure 28 shows that addition of IKA slightly reduced the stimulatory effect of glucose. However, the relative frequency of permanent endocytic events was still three times higher compared to measurements without glucose (Figure 28). A representative capacitance trace recorded in the presence of IKA and glucose is shown in Figure 29. Again, successive downward steps reflecting fission of single vesicles could frequently be observed. This demonstrates that

inhibition of clathrin-coat formation by IKA does not prevent the stimulatory effect of glucose on endocytosis.

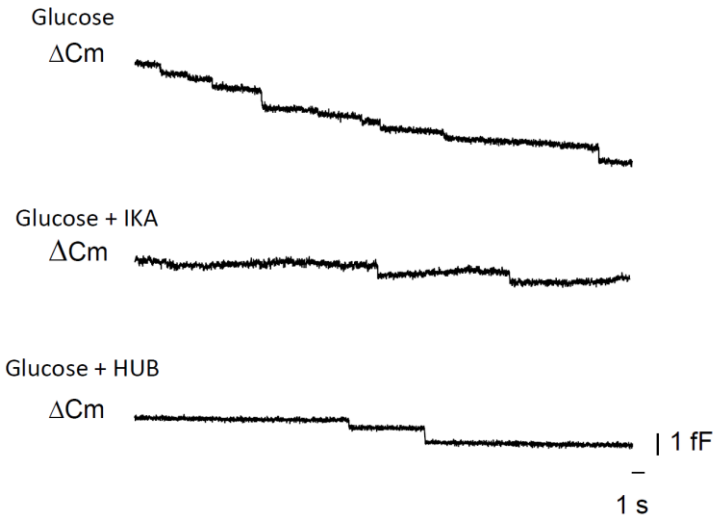

Figure 29: Representative capacitance measurements. Capacitance recordings showing successive downward deflections which correspond to permanent fission of vesicles. Measurements were carried out under different conditions as indicated at the capacitance trace.

To confirm the function of clathrin-independent vesicle formation in glucose stimulated endocytosis, capacitance measurements on BY-2 protoplasts were carried out, which transiently over-expressed the C-terminal part of clathrin heavy chain (termed HUB1) fused to GFP. HUB1 binds to and titers away the clathrin light chains making them unavailable for clathrin cage formation. It thus acts as a strong inhibitor of clathrin-dependent endocytosis (Dhonukshe et al., 2007). In HUB1-GFP transfected cells the glucose stimulated increase in the relative frequency of permanent endocytic events was not different compared to that in untransfected cells (Figure 28). The representative capacitance trace shown in Figure 29 reveals sequential downward steps resulting from endocytic events. The lack of an inhibition of glucose stimulated endocytosis by incubation in IKA or transient expression of HUB1-GFP supports the hypothesis that endocytic uptake of hexose into BY-2 protoplasts occurs via a clathrin-independent mechanism.

From the size of the capacitance steps the diameter of the vesicle could be determined (for details see Material and Methods). The distribution of the size of the endocytic vesicles recorded in the presence of glucose is presented in Figure 30. Most vesicles (88 %) had a

diameter between 80 and 220 nm (median diameter 133 nm). A similar distribution was found in cells treated with IKA or transfected with HUB1-GFP (Figure 30).

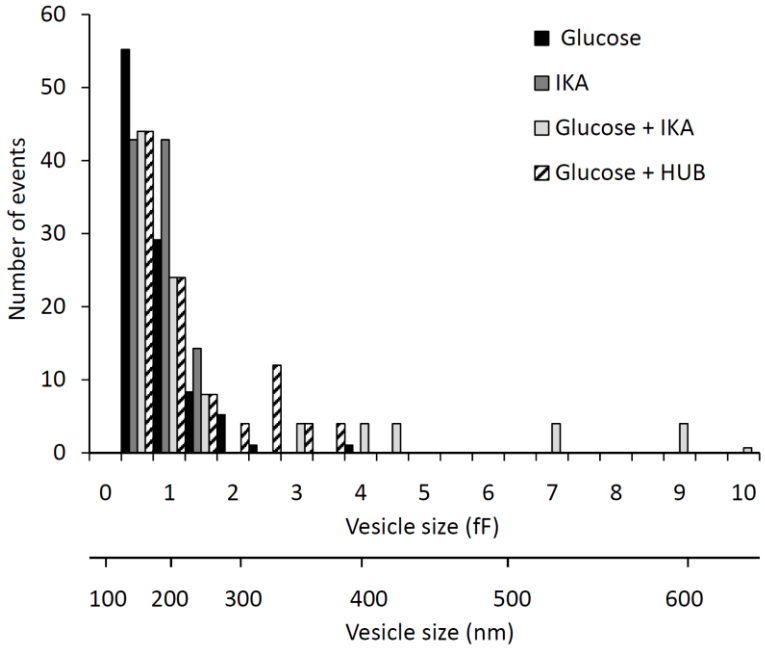

Figure 30: Distribution of endocytic vesicle size. Size distribution of permanent endocytic events. Data are derived from recordings under different conditions as indicated.

The diameter of these vesicles is in the same range as the diameter estimated for vesicles internalized by fluid-phase endocytosis in turgid guard cells (Gall et al., 2010). This suggests that the absence of turgor in protoplasts does not affect the size of endocytic vesicles. For most plant clathrin vesicles a diameter between 70 and 100 nm has been determined from electron micrographs. This is similar to the diameter of endocytic vesicles which were recorded upon block of clathrin-coat formation. Thus glucose stimulated endocytosis involves vesicles which have the size of clathrin coated vesicles but their formation does not depend on clathrin. Together the results provide the first direct demonstration of clathrin-independent endocytosis in plants.

5.4 Concluding Remarks

Endocytosis is a key feature of all eukaryotic cells and is involved in diverse cellular processes such as regulation of cell-surface expression of membrane proteins, remodelling of plasma membrane, recycling of vesicles and nutrient uptake (for review see Conner and Schmid, 2003, Murphy et al., 2005). To meet the different requirements of such processes cells possess a variety of endocytic pathways regulated by diverse molecular machineries. The best studied pathway is clathrin-mediated endocytosis. It is so far the only pathway which has been described for plant cells. The presented results uncover a clathrin-independent endocytic pathway which contributes to internalization of glucose into BY-2 cells. This also implies that the physiological important process of endocytic glucose uptake is not limited to specialized cells but rather represents a general mechanism. Endocytosed glucose was found to follow the same pathway as the cargo internalized by clathrin-mediated endocytosis. In both cases cargo accumulated at the TGN, which functions as a central sorting station. Although speculative at this stage, clathrin-independent endocytosis is likely to play an important role not only in the uptake of hexose but also of other nutrients and may be involved in various cellular processes. In animal and yeast cells an increasing number of components which take part in the clathrin-independent formation of endocytic vesicles are being identified (Kumari and Mayor, 2010). Homologs of some of these components such as dynamin are also found in plants (Hong et al., 2003) but have so far not been associated with clathrin-independent endocytosis. The future task will thus be to identify and characterize the molecular machinery that mediates clathrin-independent endocytic pathways in plants.

5.5 Materials and Methods

5.5.1 Cell Culture and Protoplast Isolation

Cultivation of BY-2 cells and preparation of protoplasts were carried out as described before (Chapter 2, 2.5.1)

5.5.2 Transfection of BY-2 Protoplasts

For PEG mediated transfection 100 µl protoplast suspension (2-5 x 10^6 protoplasts) were placed in a petri dish (35 mm). Thirty µg of plasmid DNA was diluted in distilled water to a final volume of 500 µl and added to the protoplasts. Immediately after addition of the plasmid DNA, 600 µl of PEG solution (40 % PEG 4000, 100 mM $CaCl_2$, 200 mM sucrose, pH 6) was given drop by drop to the suspension. After 15 min incubation at room temperature 1 ml of wash solution was added. To slowly readjust the osmolarity of the protoplast suspension, 1, 2 and 5 ml of wash solution were added at intervals of 15 min. Protoplasts were incubated over night at 25° C before use for capacitance measurements or microscopic analysis.

5.5.3 Drug Treatment

For drug treatment experiments, aliquots of IKA (Biomol Hamburg, Germany) solution (stock at 1 mM in DMSO) were added to tobacco BY-2 protoplasts to a final concentration of 10 µM. Protoplasts were incubated in IKA for 30 min before use for capacitance measurements or microscopic analysis.

5.5.4 Confocal Imaging

BY-2 protoplasts were investigated with a Leica TCS SP spectral confocal microscope (Leica Microsystems) either directly after protoplast isolation or approximately 24 h after transfection. Images were acquired with an HC PL APO CS 20 X / 0.70 objective or HCX PL APO 63×/1.2 w objective. 2-NBDG was kept at a stock solution of 500 mM in distilled water. Protoplasts were incubated for 1 h in 5 mM 2-NBDG and washed twice with wash solution before confocal analysis. 2-NBDG was excited with the 488 nm line of a 25 mW argon laser and fluorescence was detected at 505–580 nm. RFP was excited with the 543 nm line of a 25 mW helium/neon laser and fluorescence was detected at 560-600 nm. For plasma membrane staining and monitoring of endocytosis protoplasts were incubated in 10 µM FM4-64 (Invitrogen Darmstadt, Germany) for 10 min on ice to ensure saturation of the plasma membrane with the dye. FM 4-64 was excited with the 488 nm line of a 25 mW argon laser and fluorescence was detected at 630-700 nm. Images were analysed with IMAGEJ software (National Institutes of Health) and Leica Confocal Software 2.00 (LCS, Leica Microsystems). For analysis of the relative intracellular fluorescence, the outline of the cell was determined using the plasma membrane marker FM4-64. The area just below the outline of the protoplasts was taken as a measure of the intracellular fluorescence intensity. The relative intracellular fluorescence is given as the ratio of the intracellular fluorescence to the whole cell fluorescence. The ratio at the time point zero was set to 0.1. Values are presented mean ± SEM.

5.5.5 Electrophysiology

Membrane capacitance measurements were carried out as described before (Bandmann et al., 2010) Protoplasts were bathed in external solution (30 mM $CaCl_2$ 54 mM K-Gluconat 25 mM MES-KOH, pH 5.6 adjusted to 435 mosmol/kg with sorbitol). Patch pipettes were either filled with external solution or with external solution containing 244 mM glucose instead of sorbitol for adjustment of the osmolarity. Events were analyzed by using the cursor option in the software subroutine (CellAn Celica, Slovenia) written for MATLAB (MathWorks Inc., Natik, MA, USA). Data were stored in a database (MySQL Community Server 5.1.49, Oracle

Redwood Shores USA), calculations were realized by a web-application (CAMMC, yQ-it, Darmstadt, Germany) and results were again stored in the database.

From the vesicle capacitance C_v the surface area (A) and thus the diameter of vesicles could be calculated according to $C_v = c * A$ whereby c is the specific membrane capacitance (8 mF/m^2) determined for the plasma membrane of plant cells (White et al., 1999).

5.6 References

Baluska F., Samaj J., Hlavacka A., Kendrick-Jones J., Volkmann D. (2004) Actin-dependent fluid-phase endocytosis in inner cortex cells of maize root apices. J Exp Bot. 55: 463-473.

Bandmann V., Kreft M., Homann U. (2010) Modes of Exocytotic and Endocytotic Events in Tobacco BY-2 Protoplasts. Mol Plant 1-11.

Baroja-Fernandez E., Etxeberria E., Muñoz F.J., Morán-Zorzano M.T., Alonso-Casajús N., Gonzalez P. Pozueta-Romero J. (2006) An important pool of sucrose linked to starch biosynthesis is taken up by endocytosis in heterotrophic cells. Plant Cell Physiol. 47: 447-456.

Büttner M. and Sauer N. (2000) Monosaccharide transporters in plants: structure, function and physiology. Biochim Biophys Acta. 1465: 263-274.

Cai Y., Jia T., Lam S.K., Ding Y., Gao C., San M.W., Pimpl P., Jiang L. (2010) Multiple cytosolic and transmembrane determinants are required for the trafficking of SCAMP1 via an ER-Golgi-TGN-PM pathway. Plant J. 65: 882-896.

Conner S.D. and Schmid S.L. (2003) Regulated portals of entry into the cell. Nature 422: 37-44.

Damke H., Baba T., Bliek A.M. van der, Schmid S.L. (1995) Clathrin-independent pinocytosis is induced in cells overexpressing a temperature-sensitive mutant of dynamin. J Cell Biol. 131: 69-80.5

Dhonukshe P., Aniento F., Hwang I., Robinson D.G., Mravec J., Stierhof Y.D., Friml J. (2007) Clathrin-mediated constitutive endocytosis of PIN auxin efflux carriers. in Arabidopsis. Curr. Biol. 17: 520-527.

Etxeberria E., Baroja-Fernandez E., Muñoz F.J., Pozueta-Romero J. (2005) Sucrose-inducible endocytosis as a mechanism for nutrient uptake in heterotrophic plant cells. Plant Cell Physiol. 46: 474-841.

Etxeberria E., Gonzalez P., Alfred L., Pozueta-Romero J. (2005) Sucrose Transport into Citrus Juice Cells: Evidence for an Endocytic Transport System. The American Society for Horticultural Science 30: 269-274.

Etxeberria E., González P., Tomlinson P., Pozueta-Romero J. (2005) Existence of two parallel mechanisms for glucose uptake in heterotrophic plant cells. J Exp Bot. 56: 1905-1912.

Gall L., Stan R.C., Kress A., Hertel B., Thiel G., Meckel T. (2010) Fluorescent detection of fluid phase endocytosis allows for in vivo estimation of endocytic vesicle sizes in plant cells with sub-diffraction accuracy. Traffic 11: 548-459.

Gruenberg J. (2001) The endocytic pathway: a mosaic of domains. Nat Rev Mol Cell Biol. 2: 721-30.

Hansen C.G. and Nichols B.J. (2009) Molecular mechanisms of clathrin-independent endocytosis. *J Cell Sci.* 122: 1713-1721.

Hong Z., Bednarek S.Y., Blumwald E., Hwang I., Jurgens G., Menzel D., Osteryoung K.W., Raikhel N.V., Shinozaki K., Tsutsumi N., Verma D.P. (2003) A unified nomenclature for Arabidopsis dynamin-related large GTPases based on homology and possible functions. Plant Mol Biol. 53: 261-265.

Kumari S., Mg S., Mayor S. (2010) Endocytosis unplugged: multiple ways to enter the cell. Cell Res. 20: 256-275

Lalonde S., Boles E., Hellmann H., Barker L., Patrick J.W., Frommer W.B., Ward J.M. (1999) The dual function of sugar carriers. Transport and sugar sensing. Plant Cell. 11: 707-726.

Luo T., Fredericksen B.L., Hasumi K., Endo A. (2001) Human Immunodeficiency Virus Type 1 Nef-Induced CD4 Cell Surface Downregulation Is Inhibited by Ikarugamycin. J Virol. 75: 2488-2492

Mayor S. and Pagano R.E. (2007) Pathways of clathrin-independent endocytosis. Nature Rev Mol Cell Biol. 8: 603-612.

Mazel A., Leshem Y., Tiwari B.S., Levine A. (2004) Induction of Salt and Osmotic Stress Tolerance by Overexpression of an Intracellular Vesicle Trafficking Protein AtRab7 (AtRabG3e). Plant Physiol. 134: 118-128.

Moscatelli A., Ciampolini F., Rodighiero S., Onelli E., Cresti M., Santo N., Idilli A. (2007) Distinct endocytic pathways identified in tobacco pollen tubes using charged nanogold. J Cell Sci. 120: 3804-3819.

Murphy A.S., Bandyopadhyay A., Holstein S.E., Peer W.A. (2005) Endocytotic cycling of PM proteins. Annu. Rev. Plant Biol. 56: 221–251.

Oliveira J., Tavares R.M., Gerós H. (2002) Utilization and transport of glucose in Olea Europaea cell suspensions. Plant Cell Physiol. 43: 1510-1517.

Onelli E., Prescianotto-Baschong C., Caccianiga M., Moscatelli A. (2008) Clathrin-dependent and independent endocytic pathways in tobacco protoplasts revealed by labelling with charged nanogold. J Exp Bot. 59: 3051-3068.

Sandvig K., and Deurs B. van. (2005) Delivery into cells: lessons learned from plant and bacterial toxins. Gene Ther. 12: 865-872.

Sandvig K., Pust S., Skotland T., Deurs B. van. (2011) Clathrin-independent endocytosis: mechanisms and function. Curr Opin Cell Biol. 23: 413-420.

White P.J., Biskup B., Elzenga T.M., Homann U., Thiel G., Wissing F., Maathuis F.J.M. (1999) Advanced patch-clamp techniques and single-channel analysis. J Exp Bot. 50:1037-1054.

Chapter 6

6 Measurement of Constitutive Vesicle Fusion and Fission and Analyses of Receptor Mediated Endocytosis in Yeast

6.1 Abstract

Yeast cells are widely used as a powerful model system in the investigation of endo- and exocytosis. A wide range of methods have been used to elucidate the underlying mechanisms of vesicle transport but so far no capacitance measurements have been applied to yeast. To test if fusion and fission of single vesicles can be monitored by capacitance measurements I carried out cell-attached capacitance measurements on yeast protoplasts. These capacitance measurements revealed discrete upward and downward steps which correspond to vesicle fusion and fission. Besides different kinetic modes also fusion pore conductance was measured.

In order to evaluate whether the internalization of the mating receptor represents a suitable model to study receptor mediated endocytosis, the uptake of the mating receptor Ste2 in response to the mating factor (α) was studied with confocal microscopy. These studies revealed that α-factor induces endocytosis even in protoplasts. The system therefore provides a promising model to study the mechanisms of receptor mediated endocyotis by cell-attached capacitance measurements.

6.2 Introduction

Yeast cells are a well established and widely used model system for studying exo-and endocytosis. Fundamental findings of the mechanism of membrane fusion and exo- and endocytosis have been derived from the yeast system. By the combination of yeast genetic and an in vitro assay it was possible to isolate two proteins sec17 (or NSF) and sec18 (or SNAP) which are crucial for the intra Golgi transport (Rothman and Warren, 1994). In bovine brain extract Söller and co-workers were able to identify a receptor for the complex of NSF-SNAP (Söllner et al., 1993). Together these data provided the basis for the SNARE model of membrane fusion. Furthermore, the identification of secretory mutants in yeast confirmed the SNARE model and led to the finding of additional components like synaptobrevin and syntaxin which are fundamental for the fusion process (Aalto et al., 1993, Gerstet al., 1992). Later on homologs of the synaptic SNARE protein were found to operate in all membrane fusion processes from yeast and plants and to man (Ferro-Novick and Jahn, 1994, Pratelli et al., 2004).

After these elementary findings many additional details of vesicle trafficking were investigated in the yeast system. To test if vesicle fusion and fission in yeast can also be studied with capacitance measurements, cell-attached capacitance measurements were applied to yeast protoplasts.

In addition to the study of constitutive membrane turnover, it would be interesting to investigate the response of vesicle transport to external stimuli. In yeast cells endocytosis of the mating receptor can be stimulated by the mating factor. Therefore the localization of the mating receptor Ste2 was analyzed in α-factor treated cells by confocal microscopy to test whether capacitance measurements can be applied to study this receptor mediated endocytosis. α-factor induced internalization of membrane material was also monitored in yeast protoplasts.

6.3 Results and Discussion

6.3.1 Capacitance Measurements onYeast Protoplasts

The patch clamp technique has already been successfully applied to yeast (Bertl et al., 1995, Nakanish et al., 1993) but so far no measurements of membrane capacitance have been carried out. I therefore tested the suitability of yeast cells for capacitance measurements in the cell-attached configuration. Application of the patch-clamp technique on yeast cells requires the removal of the cell wall to ensure direct contact of the patch-clamp pipette with the plasma membrane. In Figure 31 yeast protoplasts are shown. The complete removal of the cell wall is obvious by the perfect spherical shape of the cells.

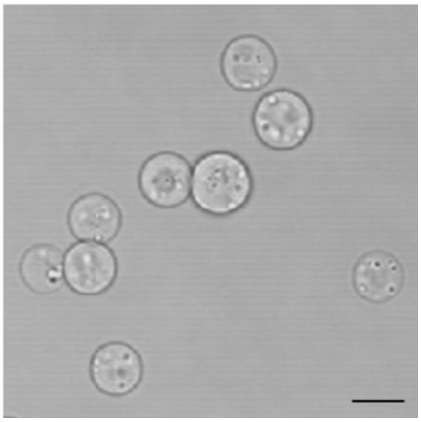

Figure 31: Yeast protoplasts. Protoplasts were isolated from Bma 64-1A cells, scale bar 5 µm.

Immediately (30 min) after isolation the protoplasts were used in patch-clamp capacitance measurements. Measurements were carried out in the cell-attached configuration. In three out of seven measurements it was possible to resolve step wise changes in the capacitance trace which corresponds to the fusion and fission of single vesicles.

In Figure 32 four sections from capacitance measurements on yeast protoplasts are shown. In Figure 32A an irreversible upward step reflects the fusion of an exocytotic vesicle. In Figure 32B a downward step indicates the fission of an endocytotic vesicle. Beside these permanent events also transient fusion and fission events could be recorded (Figure 32C and D).

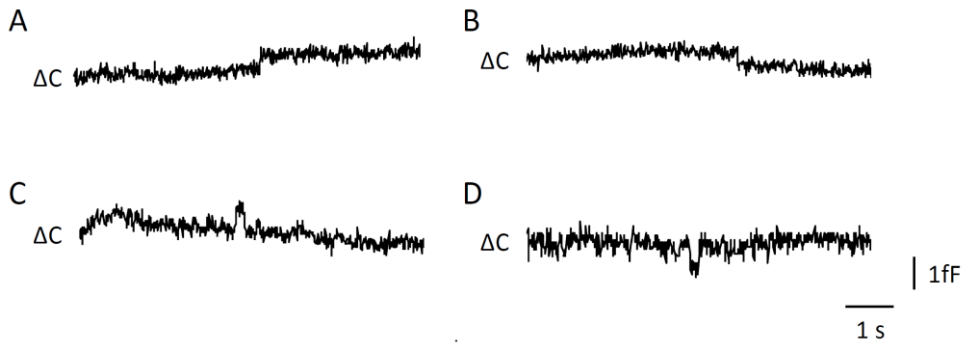

Figure 32: Four different kinetic modes of fusion and fission in yeast protoplasts. The four sections show representative examples of vesicles fusion and fission recorded in yeast protoplasts.

Recorded changes in the capacitance were in the range from 0.54 to 2.10 fF which relates to a vesicle diameter between 150 and 290 nm. During vesicle fusion and fission also fusion pore formation was detected. Almost 80% of vesicle fusion or fission events were accompanied by a measurable fusion pore which had conductances between 15 and 26 pS. These results revealed that both the vesicle diameter and the fusion pore conductance of yeast protoplasts are in the same range as those measured in BY-2 cells. Fusion or fission of vesicles did not occur in any capacitance recording on yeast protoplasts. Only in three out of seven measurements fusion or fission could be detected. Together with the observation that in these three measurements the fusion and fission activity was very high, this suggests that also in yeast protoplasts the surface area is organized in hot spots of vesicle fusion and fission. An alternative explanation would be that the protoplasts have been derived from cells in different developmental stages with different activity in vesicle trafficking.

6.3.2 Microscopic Analyzes of Receptor Mediated Endocytosis in Yeast

In addition to constitutive membrane turnover, fusion and fission of yeast cells can also be affected by external stimuli. One example is the stimulation of receptor mediated endocytosis. During mating of yeast the binding of α-factor to the receptor (Ste2) of a-factor secreting cells and conversely the binding of the a-factor to the receptor (Ste3) of α-factor secreting cells induces receptor internalization and thus a signal cascade which results in the growing of the projection. In Figure 33 the localization of Ste2-GFP in yeast cells is shown. Yeast cells were transfected with Ste2-GFP and labeled with FM4-64. In time series the distribution of the

Ste2-GFP fluorescence was analyzed under control conditions (Figure 33A) and in the presence of 10 µM α-factor (Figure 33B).

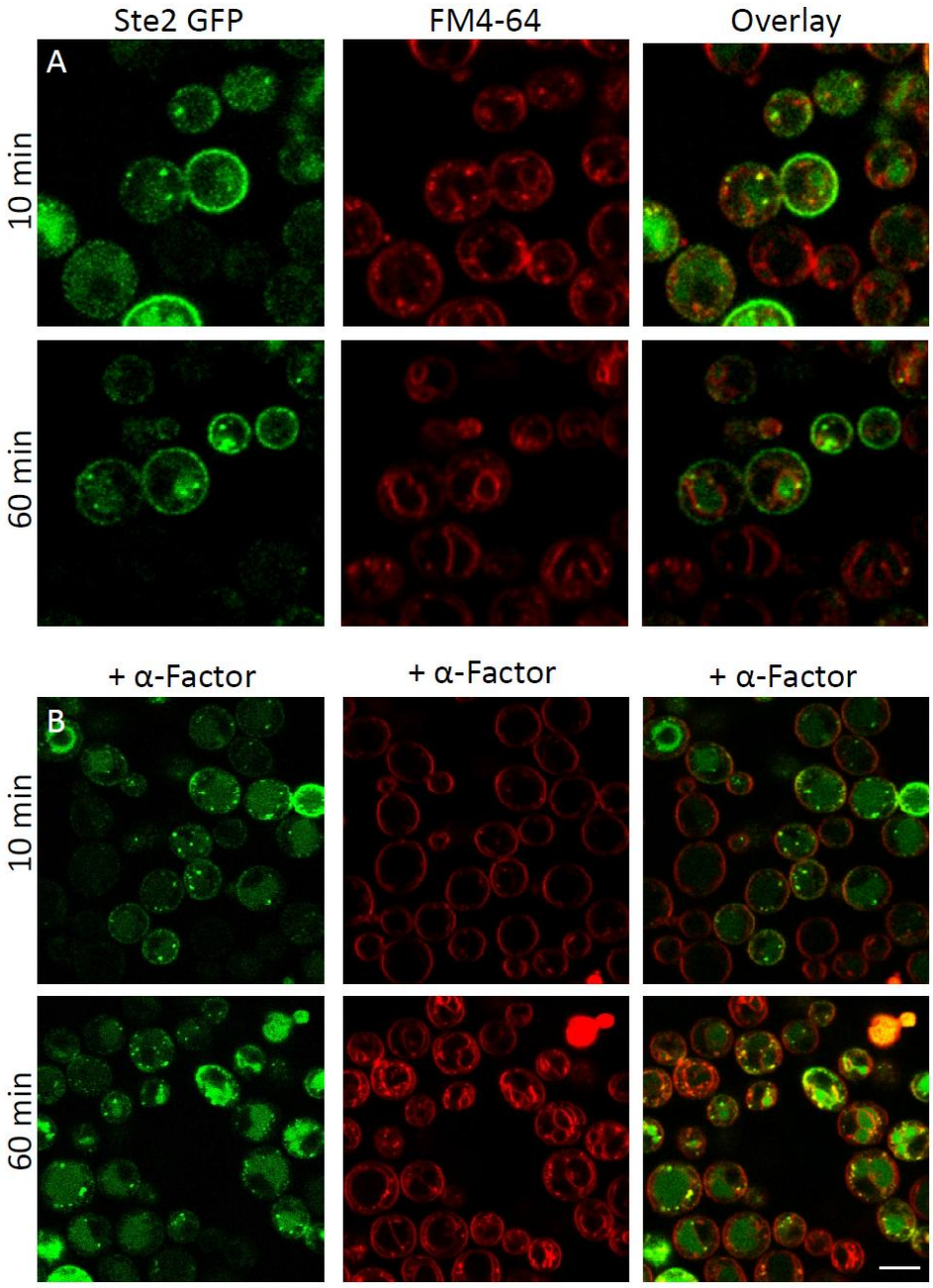

Figure 33: Localization of the receptor Ste2-GFP under control conditions and in the presence of α-factor. Bma 64-1A cells were transfected with Ste2-GFP (green) and labelled with FM4-64 (red). Distribution of the GFP and the FM4-64 signal were monitored over 1h. **(A):** Under control conditions the GFP fluorescence of the Ste2 receptor was detected in the plasma membrane and in bright spots in direct proximity to the vacuole. In addition, in some cells the vacuole shows a weak signal. **(B):** In the presence of 10 µM α-factor the receptor could be detected in the plasma membrane. In addition an accumulation in the vacuole and in bright spots is visible already after 10 min. Colocalization is shown in yellow, scale bar 5 µm.

Under control conditions the Ste2 receptor was visible in the plasma membrane and in bright spots in direct proximity to the vacuole. In addition, the vacuole showed a weak signal in some cells. Already after 10 min an uptake of FM4-64 is detectable. Besides the plasma membrane also the membrane of the vacuole and endosomal compartments are labelled. FM4-64 and the GFP signal overlap in the endosomal compartments which most likely represent pre-vacuolar compartments (PVC). After one hour the Ste2 is still visible in the plasma membrane. In the presence of 10 µM α-factor the receptor could also be detected in the plasma membrane but already after 10 min the vacuole and PVC showed a strong labelling which increased over time. In Figure 34 the percentage of cells in which the Ste2 receptor localizes to PVC is shown. Under control conditions the amount of cells with GFP fluorescence in PVC increased only slightly from 18 % to 30 % within one hour. In the presence of α-factor, the percentage of cells in which the Ste2 receptor is detectable in PVC, increased from 33 up to 68 %.

This clearly demonstrates that the the α-factor triggers the internalization of the Ste2 receptor into endosomal compartments.

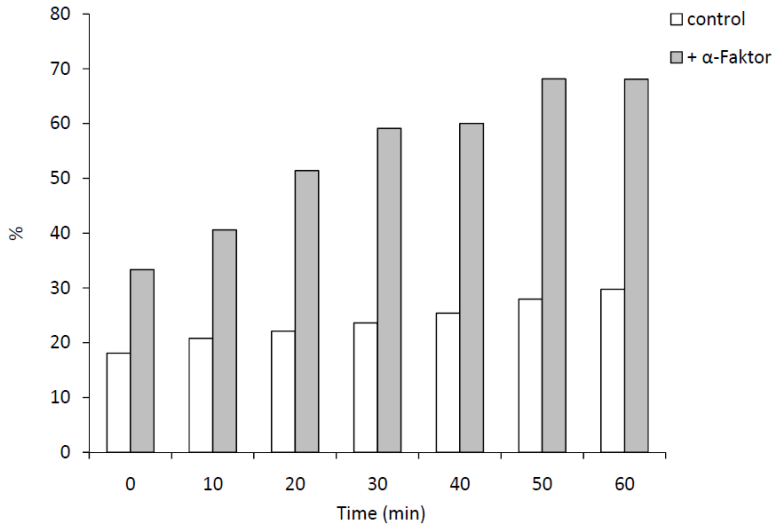

Figure 34: Percentage of cells with Ste2 receptor visible in PVCs. Percentage of cells which showed a GFP signal in PVCs were counted under control conditions and after addition of 10 µM α-factor.

In cells treated with α-factor the Ste2 receptor did not only accumulate in endosomal compartments but also an increase of GFP signal in the vacuole was visible 10 min after α-factor appliance. In Figure 35A a representative example for the localization of Ste2 receptor

is shown under control conditions (upper row) and after treatment with 10 µM α-factor (lower row). In Figure 35B the relative intensity of GFP fluorescence in the vacuole is analyzed. Under control conditions (average of 15 cells) the fluorescence remained almost constant over one hour. After adding the α-factor the fluorescence in the vacuole increased five fold (average of 20 cells).

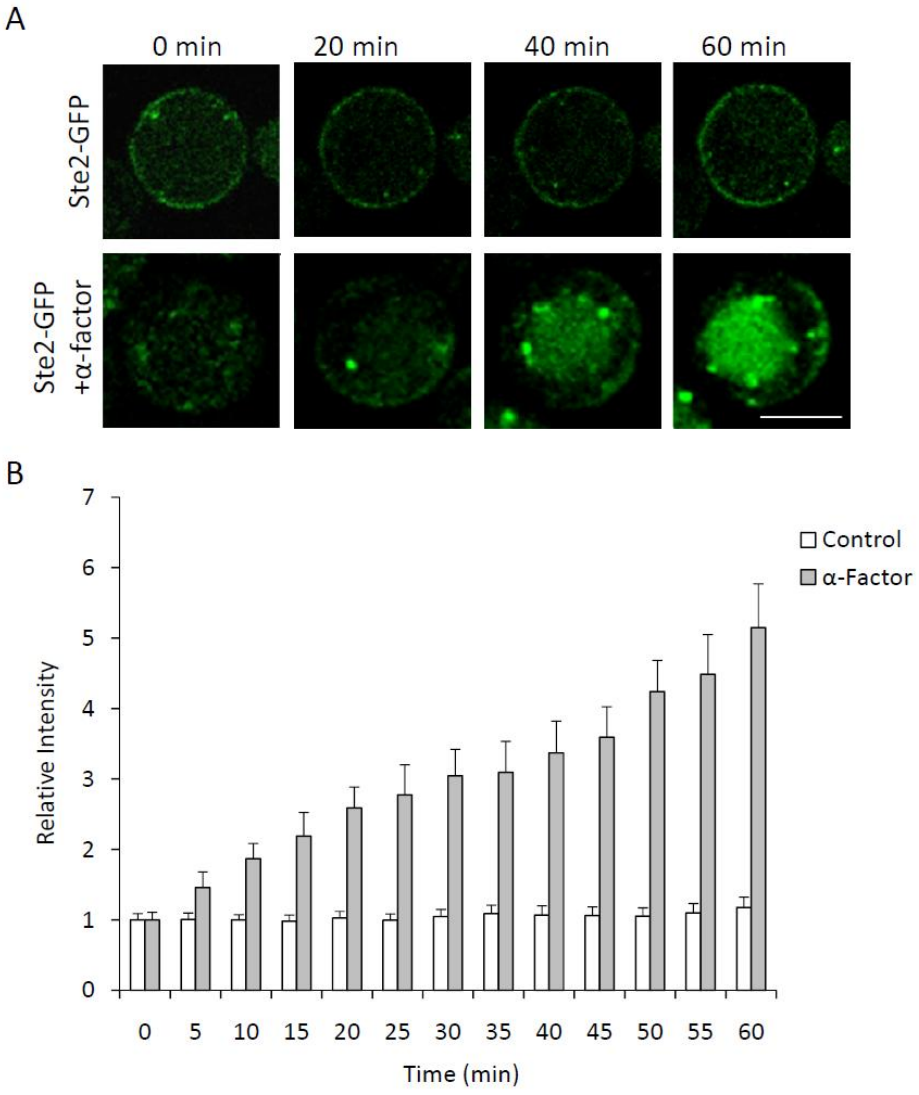

Figure 35: Ste2 receptor localizes to the vacuole after α-factor treatment. (A): Representative example of a yeast cells transfected with α-factor under control conditions (upper row) and after appliance of 10 µm α-factor (lower row). **(B):** quantification of GFP fluorescence in the vacuole of Ste2 transfected yeast cells. Values at time point zero were set to 1. Scale bar 5 µm.

Together this shows that the α-factor leads to endocytosis of the Ste2 receptor which is transported to the vacuole via PVC. The localization of Ste2 in bright spots under non-stimulated conditions most likely indicates the cycling of the Ste2 receptor between

plasma membrane and endosomal compartments.

This example of receptor induced endocytosis represents an interesting system to study receptor mediated functions and the related vesicle transport in capacitance measurements. Therefore the effect of α-factor on endocytosis was tested in yeast protoplasts. In Figure 36 the internalization of FM4-64 under control conditions and in the presence of α-factor was studied.

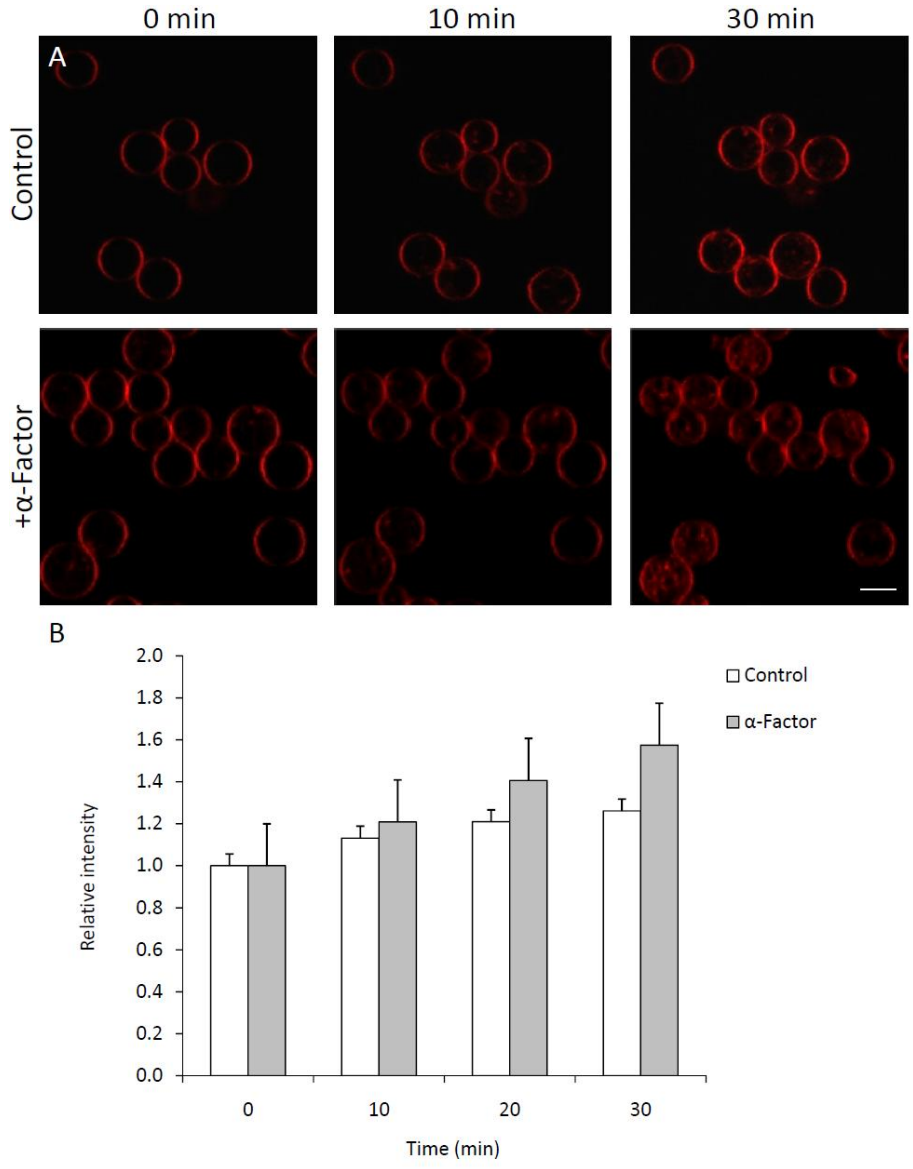

Figure 36: Internalization of FM4-64 in yeast protoplasts in the absence and presence of α-factor. (A): Time series of yeast protoplasts (isolated from BY4741 cells) incubated in 10 µM FM4-64 under control conditions (upper row) and after addition of 10 µM α-factor (lower row). **(B):** Quantification of FM4-64 uptake: The relative fluorescence intensity is given as the ratio of intracellular fluorescence to whole-cell fluorescence. The value at time zero was set to 1, data were averaged from 15 cells. Scale bar 5 µm.

In both conditions endocytosis was detectable 10 min after incubation with FM4-64 (Figure 36A). The quantification in Figure 36B shows the ratio of intracellular fluorescence to whole cell fluorescence. The increase of the ratio over time reflects the endocytosis of the dye. In protoplasts treated with α-factor the ratio increased slightly more which points to a stimulation of endocytosis in the presence of α-factor.

The observation that α-factor induces endocytosis also in yeast protoplasts supports the assumption that Ste2 is still present in protoplasts and is able to respond to α-factor application.

6.4 Concluding Remarks

Capacitance measurements in the cell attached configuration could be successfully applied to yeast protoplasts. Besides the fusion and fission of single vesicles also fusion pore conductance could be recorded. Transient and permanent fusion were measured as well as transient and permanent fission. Therefore, these measurements revealed that the four different kinetic modes of vesicle fusion and fission present in plant and animal cells are also present in yeast. In almost 80% of events open fusion pores could be detected. In comparison to the measurements in BY-2 protoplasts the vesicle size as well as the fusion pore conductance measured in yeast protoplasts were in the same range. These measurements thus confirm that the underlying mechanisms of vesicle fusion and fission are highly conserved among eukaryotes.

In addition to constitutive membrane turnover, fusion and fission of yeast cells can also be affected by external stimuli. One example is the internalization of the mating receptor Ste2 as a response to the mating factor α. In confocal microscopy studies it could be shown that the GFP tagged receptor localized to PVC and the vacuole after treatment of the cells with α-factor. Also in yeast protoplasts endocytosis is enhanced after addition of α-factor. This implies that the interaction of receptor and mating factor is still functional in protoplasts.

This receptor mediated endocytosis, triggered by the mating factor, therefore represents a promising model to study the underlying mechanisms in detail using capacitance measurements.

6.5 Materials and Methods

6.5.1 Protoplast Isolation

Protoplast isolation was mainly carried out as described in Bertl and Slayman (1990). Cells from the Bma 64-1A strain were grown overnight in YPD medium (30 ml per 125-ml Erlenmeyer flask) at 25 °C with rotary shaking of 90 rpm. Cells were harvested by centrifugation (2000 g for 5 min) after one washing step in buffer A (50 mM KH_2PO_4/40 mM 2-mercaptoethanol, adjusted to pH 7.2 with KOH) the pellet was resuspended again in 3 ml of buffer A and incubated at 30 °C for 30 min with occasional gentle shaking. For digestion of the cell wall 3 ml of buffer B [50 mM KH_2PO_4/40 mM 2-mercaptoethanol/2.4 M sorbitol with zymolyase (2 mg/ml) and glucuronidase (2 mg/ ml), adjusted to pH 7.2 with KOH)] was added and cells were incubated for another 45min at 30 °C. To stop the enzymatic digestion cells were centrifuged at 500 g for 5min and the pellet was resuspended in buffer C (200 mM KCl/10 mM $CaCl_2$/5 mM $MgCl_2$/ 5 mM Tris/Mes, pH 7.2). For measurements 20 µl protoplasts were transferred into the recording chamber which contained 180 µl external solution (165 mM KCl, 10 mM $CaCl_2$, 5 mM $MgCl_2$, 1 mM MES Tris-base adjusted to pH 6.5 with KOH).

6.5.2 Confocal Imaging

Yeast cells from Bma 64-1A-pSte2-GFP and from the BY4741 strain were investigated with a Leica TCS SP spectral confocal microscope (Leica Microsystems). Images were acquired with an HCX PL APO 100x/1,4 NA objective. For plasma membrane staining and monitoring of endocytosis protoplasts isolated from the BY4741 strain were incubated in 10 µM FM4-64 (Invitrogen Darmstadt, Germany). FM4-64 was excited with the 488 nm line of a 25 mW argon laser and fluorescence was detected at 630-700 nm. The GFP fluorescence of the Bma 64-1A-pSte2-GFP cells was excited with the 488 nm line of a 25 mW argon laser and fluorescence was detected at 505–580 nm.

α-factor was kept as a 1 mM stock and applied to the cell with a final concentration of 10 µM. Images were analysed with IMAGEJ software (National Institutes of Health) and Leica Confocal Software 2.00 (LCS, Leica Microsystems).

6.5.3 Electrophysiology

Membrane capacitance measurements were in principle carried out as described before (Bandmann et al., 2010). Patch pipettes with a tip resistance of 2-4 MΩ were prepared from glass capillary tubing (Kimax 51; Kimax Products, Vineland, NJ, USA) and the shanks of the pipettes were coated with paraffin. Pipettes were filled with external solution (165 mM KCl, 10 mM $CaCl_2$, 5 mM $MgCl_2$, 1 mM MES Tris-base adjusted to pH 6.5 with KOH). Protoplasts were bathed in external solution. Events were analysed by using the cursor option in the software subroutine CellAn Celica, Slovenia) written for MATLAB (MathWorks Inc., Natik, MA, USA). Data were stored in a database (MySQL Community Server 5.1.49, Oracle Redwood Shores USA), calculations were realized by a web-application (CAMMC, yQ-it, Darmstadt, Germany) and results were again stored in the database.

From the vesicle capacitance C_v the surface area (A) and thus the diameter of vesicles could be calculated according to $C_v = c * A$, whereby c is the specific membrane capacitance (8 mF/m^2) determined for the plasma membrane of plant cells (White et al., 1999).

6.6 References

Aalto M.K., Ronne H., Keränen S. (1993) Yeast syntaxins Sso1p and Sso2p belong to a family of related membrane proteins that function in vesicular transport. EMBO J. 12: 4095-4104.

Bandmann V., Kreft M., Homann U. (2010) Modes of Exocytotic and Endocytotic Events in Tobacco BY-2 Protoplasts. Mol Plant 1-11.

Bertl A., Andersont J.A., Slayman C.L., Gabert R.F. (1995) Use of Saccharomyces cerevisiae for patch-clamp analysis of heterologous membrane proteins: Characterization of Katl, an inward-rectifying K^+ channel from Arabidopsis thaliana, and comparison with endogeneous yeast channels and carriers. Proc. Natl. Acad. Sci. U.S.A. 92: 2701-2705.

Bertl A. and Slayman C.L. (1990) Cation-selective channels in the vacuolar membrane of Saccharomyces: Dependence on calcium, redox state, and voltage. Proc. Natl. Acad. Sci. U.S.A. 87: 7824-7828.

Gerst J.E., Rodgers L., Riggs M., Wigler M. (1992) SNC1, a yeast homolog of the synaptic vesicle-associated membrane protein/synaptobrevin gene family: genetic interactions with the RAS and CAP genes. Proc Natl Acad Sci U S A. 89: 4338-4342.

Kirkham M. and Parton R.G. (2005) Clathrin-independent endocytosis: new insights into caveolae and non-caveolar lipid raft carriers. Biochim Biophys Acta 1745: 273-286.

Nakanishi Y., Isamu Y., Masayoshi M. (2003) Patch Clamp Analysis of a H^+ Pump Heterologously Expressed in Giant Yeast Vacuoles. J Biochem. 134: 615-623.

Pratelli R., Sutter J-U., Blatt M.R. (2004) A new catch in the SNARE. Trends in Plant Science 9: 187-195

Rothman J.E. and Warren G. (1994) Implications of the SNARE hypothesis for intracellular membrane topology and dynamics. Curr Biol. 4: 220-233.

Seeger M. and Payne G.S. (1992) A role for clathrin in the sorting of vacuolar proteins in the Golgi complex of yeast. EMBO J. 11: 2811-2818.

Söllner T., Whiteheart S.W., Brunner M., Erdjument-Bromage H., Geromanos S., Tempst P., Rothman J.E. (1993) SNAP receptor implicated in vesicle targeting and fusion. Nature 362: 318-323.

Tan P.K., Davis N.G., Sprague G.F., Payne G.S. (1993) Clathrin facilitates the internalization of seven transmembrane segment receptors for mating pheromones in yeast. J Cell Biol. 123: 1707-1716.

Yeung B.G., Phan H.L., Payne G.S. (1999) Adaptor complex-independent clathrin function in yeast. Mol Biol Cell. 10: 3643-3659.

Summary

Endocytosis and Exocytosis are essential for many cellular processes such as protein transport, membrane recycling, cell signalling, secretion and uptake of external solutes. A method to directly observe endo- and exocytosis on the level of single vesicles is provided by membrane capacitance measurements. To make use of this method for the comprehensive investigation of vesicle fusion and fission in plants, tobacco BY-2 cells were established as a model system for capacitance measurements. Under non-stimulated conditions these measurements revealed spontaneous upward and downward steps in membrane capacitance reflecting vesicle fusion and fission, which could be grouped into four different categories according to their different kinetics: i) transient fusion of exocytotic vesicles, ii) transient fission of endocytotic vesicle, iii) permanent fusion and iv) permanent fission. In some recordings additional sequences of transient flickering activity and complex multi-vesicular exocytosis were observed which can contribute to an increase in efficiency of secretory product release. Comparison of microscopic analysis of the time course of cell wall rebuilding and frequency of transient exocytotic events revealed that transient vesicle fusion may account for secretion of new cell wall material.

In all capacitance measurements either none or several discrete changes in the capacitance were recorded which points to hot spots of exo- and endocytotic activity in the plasma membrane of BY-2 cells. Furthermore, analysis of fusion and fission during hypoosmotically induced swelling of protoplasts indicates that special sides for the incorporation of membrane material during surface area increase under hypoosmotic conditions may exist.

To investigate the uptake of hexose into BY-2 cells capacitance measurements were combined with fluorescent microscopy analysis. The studies demonstrate that glucose is internalized by clathrin-independent endocytosis which is induced by hexose. This is the first direct evidence for clathrin-independent fluid phase endocytosis in plants which may represent a general mechanism for the uptake of external solutes.

Membrane capacitance measurements on yeast protoplasts revealed the same kinetic groups of vesicle fusion and fission as observed on BY-2 protoplasts. This illustrates that the technique can successfully be applied on yeast protoplasts and makes yeast another promising model system to study the mechanisms of vesicle fusion and fission by capacitance recordings.

Zusammenfassung

Endocytose und Exocytose sind für viele zelluläre Prozesse wie Proteintransport, Membran-Recycling, Signalweiterleitung, Sekretion und Aufnahme von Stoffen essentiell. Eine Methode um das Fusionieren und Abschnüren einzelner Vesikel, direkt zu verfolgen, ist die Messung der Membrankapazität. Um diese Methode für eine umfassende Analyse von Exo- und Endocytose in Pflanzen zu nutzen, wurden Tabak-BY-2 Zellen als Modellsystem für die Kapazitätsmessung etabliert. Unter nicht stimulierten Bedingungen zeigten diese Messungen spontane Aufwärts- und Abwärtsschritte in der Membrankapazität, die der Fusion und der Abschnürung von Vesikeln entsprachen. Die Stufen in der Kapazität konnten entsprechend ihrer Kinetik in vier Gruppen eingeteilt werden: i) transiente Fusion von Vesikeln, ii) transientes Abschnüren von Vesikeln, iii) permanente Fusion und iv) permanentes Abschnüren. Zusätzlich wurden in manchen Messungen transientes Flickern von Vesikeln beobachten und komplexere exocytotische Schritte von mehreren Vesikeln beobachtet. Durch diese besonderen Formen der Vesikelfusion kann wahrscheinlich die Sekretionseffizienz gesteigert werden. In mikroskopischen Analysen konnte der Zeitraum ermittelt werden, in dem BY-2 Protoplasten in der Lage sind, ihre Zellwand neu zu bilden. Im gleichen Zeitraum wurde eine hohe Frequenz von transienter Vesikelfusion gemessen. Transiente Vesikelfusion könnte daher der Sekretion von neuem Zellwandmaterial dienen.

In allen Messungen wurden entweder keine oder viele Ereignisse gemessen, was darauf hindeutet, dass sich die endo- und exocytotische Aktivität in BY-2 Zellen auf spezielle *hot spots* in der Plasmamembran beschränkt. Außerdem weisen die Messungen an Protoplasten unter hypoosmotischen Bedingungen darauf hin, dass die Vesikel, die zur Oberflächenvergrößerung benötigt werden, in speziellen Bereichen mit der Plasmamembran fusionieren.

Um die Aufnahme von Hexose in BY-2 Zellen zu untersuchen, wurden fluoreszenzmikroskopische Analysen mit Membrankapazitätsmessungen kombiniert. Diese Versuche zeigten, dass Glukose über Glukose-stimulierte, Clathrin-unabhängige Endocytose aufgenommen wird. Diese Form der Clathrin-unabhängigen *fluid phase* Endocytose konnte hier zum ersten Mal in Pflanzen nachgewiesen werden. Sie stellt wahrscheinlich einen Endocytoseweg dar, der von genereller physiologischer Bedeutung ist und der Aufnahme von gelösten Stoffen aus dem extrazellulären Raum dient.

Die Durchführung von Membrankapazitätsmessungen an Hefe-Protoplasten ergaben die

gleichen vier Gruppen von Exo- und Endocytose, die auch in BY-2 Protoplasten gemessen wurden. Dies zeigt, dass die Technik der Membrankapazitätsmessung erfolgreich an Hefe-Protoplasten angewendet werden kann und macht Hefezellen damit zu einem weiteren, vielversprechenden Modellsystem, in dem Endo- und Exocytose von einzelnen Vesikeln mit Hilfe der Membrankapazitätsmessung analysiert werden kann.

Publications in this Thesis

Chapter 2:

Bandmann V, Kreft M, Homann U (2010) Modes of Exocytotic and Endocytotic Events in Tobacco BY-2 Protoplasts. *Molecular plant*: 1-11.

Chapter 5

Bandmann V and Homann U (2011) Clathrin-Independent Endocytosis Contributes to Uptake of Glucose into BY-2 Protoplasts. *submitted*

List of Abbreviations

BY-2	Nicotiana tabaccum cv. bright yellow-2
Ca^{2+}	Calcium
EE	Early endosome
ER	Endoplasmic reticulum
fF	Femto Farrad
GFP	Green fluorescent protein
h	Hour
IKA	Ikarugamycin
LE	Late endosome
min	Minute
ml	Milliliter
mM	Millimolar
MΩ	Mega Ohm
MVB	Multivesicular body
nm	Nanometer
pA	Pico ampere
PM	Plasma membrane
pS	Pico siemens
PVC	Pre-vacuolar-compartment
RFP	Red fluorescent protein
s	Second
SNARE	Soluble N-ethylmaleimide-sensitive-factor attachment receptor
TEM	Transmission electron microscop
TGN	Trans-Golgi-network
WT	Wild type
µm	Micrometer
µl	Mikroliter

Curriculum Vitae

Name	Vera Bandmann
Date of Birth	15. September 1980
Place of Birth	Groß-Umstadt, Germany

Education:

1987 - 2000	Primary and Grammar School in Darmstadt

Academic Experience

10/2001 - 11/2007	**S**tudy of biology at the TU-Darmstadt (cell biology, animal physiology and plant physiology)
2006/2007	Diploma thesis at the TU-Darmstadt, Institute of Botany supervisor PD Dr. UlrikeHomann
11/2007 - 11.2011	Ph.D. at the TU-Darmstadt, in plant cell biology supervisor PD Dr. UlrikeHomann

Publications:

- Bandmann V, Kreft M, Homann U (2010) Modes of Exocytotic and Endocytotic Events in Tobacco BY-2 Protoplasts. *Molecular Plant.* 1-11

- Bandmann V and Homann U (2011) Clathrin-Independent Endocytosis Contributes to Uptake of Glucose into BY-2 Protoplasts. submitted

Talks and Poster Presentation:

Posters:

- 31th DGZ Annual Meeting, Marburg, Germany, "Transient fusion events in plant cells"

- Exocytosis in animals fungi and plants meeting, London, Great Britten, "Membrane capacitance measurements: detection of vesicle fusion and fission in real time."

Talks:

- 11th European Plant Endomembrane Meeting, Lecce, Italy, "Measurement of single fusion and fission events in BY-2 cells"

- 22. Tagung Molekularbiologie der Pflanzen, Dabringhausen, Germany, „Exo- und Endocytose in BY-2 Zellen: die Kinetik der Vesikelfusion"

- 12th European Plant Endomembrane Meeting, Montpellier, France, "Measurement of single fusion and fission events in BY-2 cells"

- 13th European Plant Endomembrane Meeting, Marienburg, Germany, "Modes of exocytic and endocytic events in tobacco BY-2 protoplasts"

Danksagung

An dieser Stelle möchte ich mich bei allen bedanken, die auf die eine und andere Weise zum Gelingen dieser Arbeit beigetragen haben.

Mein Dank gilt vor allem **Ulrike Homann** für die wunderbare Betreuung dieser interessanten Arbeit, für die Motivation, Unterstützung, Geduld und Hilfe und besonders für den immer angenehmen und freundlichen Umgang.

Außerdem danke ich **Gerhard Thiel** für die Unterstützung, die hilfreichen Anregungen und Diskussionen und die Übernahme des Zweitgutachtens für diese Arbeit.

Besonders danken möchte ich auch **Melanie Mikosch** und **Muriel Reuff** dafür, dass ihr mich so freundlich in die AG Homann aufgenommen habt und für die tolle Arbeitsatmosphäre. Das Gefühl, dass ich einfach eine Frage in den Raum stellen kann und sie sofort von Euch beantwortet wird habe ich sehr vermisst!

Brigitte Hertel danke ich für die Hilfe und die Betreuung am Elektronenmikroskop und für Ihr offenes Ohr für alle Sorgen und Nöte.

Sivia Haase danke ich für die Hilfe im Labor und die nette Atmosphäre im Büro

Herzlich danken möchte ich der gesamten **AG Thiel**! Die tolle Arbeitsatmosphäre, die pünktlichen gemeinsamen Mittagspausen, die spannenden Kicker Turniere und alle gemeinsamen Unternehmungen haben entscheidend dazu beigetragen, dass ich die Zeit in der Arbeitsgruppe wirklich genossen habe.

Adam Bertel danke ich für die Unterstützung bei den Hefe-Fragen und **Tim Köhler** für die Durchführung der Kapazitätsmessungen an Hefe Protoplasten und der CLSM Aufnahmen von Hefe.

Besonders danken möchte ich auch meinen Eltern **Gabriele** und **Hendrik Bandmann** die mich immer unterstützt haben.

Ganz herzlich möchte ich auch meinem Freund **Tom Kehrbaum** danken, für all die Liebe und Freundschaft und für die tolle Unterstützung in stressigen Phasen.

Ehrenwörtliche Erklärung

Ich erkläre hiermit ehrenwörtlich, dass ich die vorliegende Arbeit selbständig angefertigt habe. Sämtliche aus fremden Quellen direkt oder indirekt übernommene Gedanken sind als solche kenntlich gemacht. Die Arbeit wurde bisher keiner anderen Prüfungsbehörde vorgelegt und noch nicht veröffentlicht.

Darmstadt, 15.09.2011

_____

Dipl.-Biol. Vera Bandmann